Post-Wildfire Soil Health Assessment Along Two Chronosequences of Forest Recovery, Sierra Nevada, USA

By

LAUREN LEE TIMMONS
THESIS

Submitted in partial satisfaction of the requirements for the degree of

MASTER OF SCIENCE

in

Soils and Biogeochemistry

in the

OFFICE OF GRADUATE STUDIES

of the

UNIVERSITY OF CALIFORNIA

DAVIS

Approved:

____
Anthony O'Geen, Chair

____
William Horwath

____
Sutie Xu

Committee in Charge

2025

Table of Contents

Abstract

Mixed conifer forests of California's Central Sierra Nevada mountains have historically been shaped by beneficial wildfire. However, a marked shift in forest structure occurred in the decades following the establishment of fire suppression policies. Dense understories and high fuels, in conjunction with prolonged drought and elevated temperatures associated with climate change, exacerbate the risk of catastrophic wildfire in these ecosystems. More intense, severe, and frequent catastrophic wildfires have the potential to degrade soil health and places a substantial carbon reservoir at risk of loss. The purpose of this study was: Chapter 1) evaluate soil health recovery by assessing trends in dynamic soil properties over time since catastrophic wildfire, and Chapter 2) compare soil carbon stocks and fractions in soils recovering from catastrophic wildfire with unburned soil counterparts.

In chapter 1, two chronosequences (5-, 10-, and 50+ year old burn sites) were established in the Stanislaus and Sierra National Forests reflecting high and low elevation sites, and sampled at 0-5 cm and 5-15 cm depths. Of the measured soil health indicators, the following were identified as most sensitive to change over time since wildfire: O horizon thickness, water repellency, predator:prey ratio, gram positive:gram negative bacteria (GP:GN) ratio, saturated:unsaturated (sat:unsat) PLFA ratio, Shannon diversity, pH, EC, nitrogen in the mineral associated organic matter fraction (MAOM-N), C:N ratio, C:N ratio in the mineral associated organic matter fraction (MAOM-C:N), and bulk density. Our results demonstrated that changes in soil health over time since wildfire diverged by elevation, where high elevation sites generally exhibited faster overall recovery compared to low elevation sites. Many soil health indicators of soils recovering from wildfire showed no statistical difference to unburned soils.

In chapter 2, soils recovering from wildfire (5- and 10 years since catastrophic wildfire) and unburned (50+ years of no documented burn history) were identified in the Stanislaus and Sierra National Forests reflecting high and low elevation sites. Each sample site consisted of one central soil profile excavated to approximately 1-m, and four satellite sites located 10-m in each cardinal direction from the central profile. Satellite sites were sampled at 0-5 cm and 5-15 cm depth increments, and aggregated as one depth weighted average reflecting 0-15 cm depth. A significant increase was detected in surface total carbon (TC) concentration and carbon in the mineral associated organic matter fraction (MAOM-C) at low elevation sites recovering from wildfire relative to their unburned counterparts. No significant changes were detected when considering the whole soil profile to 1-m. However, visual trends of increased high elevation subsurface (20-65 cm) median TC concentration and MAOM-C, and increased low elevation surface (0-15 cm) SOC were observed in soils recovering from wildfire. Results demonstrate SOC recovery from catastrophic wildfire is relatively rapid, and possibly due to the addition of persistent C as black carbon after fire and new C during secondary succession.

Acknowledgements

To my family: Jon Timmons, Candice Timmons, Caitlyn Timmons, and Nancy Patton. Thank you for your unwavering support, love, and belief in me. You have been my emotional rock throughout this process. I am so grateful for your interest in my project and for the countless times you let me work through challenges with you.

To my partner: Henry Cheung. Thank you for always being there for me. In difficult times, I could always count on your love, care, and encouragement. Your belief in me pushed me to do and be my best.

To my advisor and mentors: Anthony O'Geen, William Horwath, and Sutie Xu. Toby, thank you for your mentorship and guidance. I am deeply grateful to have learned from you. Will and Sutie, thank you for your support and insight as my committee members.

To the members of the California Soil Resource Lab: Jaeeun Sohng, Alyssa Flores, Seth Whiteaker, Claire Kisluik, and Heath Goertzen. Jaeeun, I aspire to be as hard working, graceful, kind, and motivated as you are. Alyssa, your intelligence, warmth, and support made our time writing and working together truly meaningful. Seth, thank you for always being willing to chat with me about coding and statistics. I always feel that I am learning something new from you. Claire, your support in the field and lab was integral to my project, and I am deeply grateful for your help. Heath, thank you for sharing your sense of humor and wit. It has been an honor to work alongside you all.

Thank you to the undergraduate students who assisted me, especially Chi Do: thank you for your dedicated, enthusiastic work and the care you put into every task.

List of Figures

List of Tables

Chapter 1: Assessment of Near Surface Soil Health Indicators During Post-Wildfire Recovery, Sierra Nevada, USA

1.1. Introduction

Fire is an integral component of western mixed coniferous forests, where frequent, low intensity fires historically shaped the structure and ecosystem function of these ecosystems. However, the effects of fire today are exacerbated by prolonged periods of drought, elevated temperatures, and dense forest understories that lead to high fuel loads. This can be attributed to anthropogenic climate change coupled with the legacy of forest management strategies focused on fire suppression (McKelvey et al., 1996; Beaty & Taylor, 2007; Collins et al., 2007; Gonzáles-Cabán, 2007; Van de Water & North, 2010; Abatzaglou & Williams, 2016). As fires increase in frequency and severity, there is a need to better understand soil health and explore the potential for recovery of productive soil properties (Turner, 2010; Seidl & Turner, 2022; Vahedifard et al., 2024). The extent to which dynamic soil properties return to pre-disturbance conditions, or equilibrate at a new ecological threshold, provides insight into the impact of wildfire on soil health (Herrick, 2001; Bestelmeyer et al., 2011; Bhaduri et al., 2022; Seidl & Turner, 2022). Soil health and its subsequent recovery of different soil types may have varying responses to wildfire. Variation in dynamic properties among soil types alters biotic and abiotic interactions, further complicating recovery trends (De Andrade Bonetti et al., 2017).

Extreme conditions associated with catastrophic wildfire rapidly degrade forest soil health by disrupting essential soil functions such as nutrient cycling, water absorption, and biological activity (Burger et al., 2010). Wildfire can produce surface temperatures that exceed 500 ºC, reaching up to 850 ºC in extreme cases. The longer these temperatures are maintained, the more damage ensues (Certini, 2005). This is characterized by soil organic matter (SOM) loss, which leads to the degradation of soil structure by reducing porosity, breaking down aggregates, and enhancing compaction, all of which limit the capacity for water infiltration and generate overland flow that displaces unanchored material (Leighton-Boyce et al., 2007). SOM combustion causes essential nutrient losses, such as nitrogen and sulfur, through volatilization. Extreme fire catalyzes indirect losses via reduced cation exchange capacity, leaching, and accelerated soil erosion. Nitrogen and phosphorus are the two most limiting soil nutrients in most forest ecosystems, the loss of which has the potential to delay post-fire recovery (Agbeshie et al., 2022). Nitrogen is readily volatilized at lower combustion temperatures (Baird et al., 1999; Caldwell et al., 2002) and lost as atmospheric emissions. A second chemical fate is nitrate loss by leaching which is accelerated by low plant uptake directly after fire (Certini 2005; Johnson, et al., 2009; Abegshie, et al., 2022). Phosphorus is not readily volatilized and remains immobile in soils through binding to iron and aluminum (Caldwell, et al., 2002; Murphy, et al., 2006; Bilyera et al., 2022). Nonetheless, nitrogen and phosphorus may be lost via erosion, as combustion of the litter layer and other organic materials can expose the mineral soil surface and produce water-repellent conditions and lead to gulley and sheet erosion (Savage, 1974; Mataix-Solera et al., 2011; Verma & Jayakumar, 2012). Moreover, extreme temperatures have been shown to degrade clay minerals, which reduces cation exchange capacity and mineral surface reactivity in general. Silica and aluminum from degraded phyllosilicate clays can function as cementing agents, forming sand sized nodules that have the effect of reducing nutrient retention (Ulery & Graham, 1993). Catastrophic wildfire also reduces soil microbial biomass and biological productivity, slowing vegetative succession trajectories (Holden et al., 2016; Ogwayo, 2023). Despite reduced soil performance in response to wildfire, a universal standard for soil function as it relates to soil health does not exist and is entirely dependent on pre-existing environmental conditions (Burger et al., 2010).

Generalizations about post-wildfire recovery trends over time are limited by the inherent heterogeneity of soils and the inconsistent nature of burn events. Literature suggests that extreme variability in post-burn recovery is largely driven by differences in soil forming factors and in burn severity (Certini, 2005; Nave et al., 2011). Wildfire behavior itself is shaped by complex interactions among landscape heterogeneity, fuel loads, and climatic conditions, which together facilitate the vertical spread of fire from the forest floor to the canopy. (Beaty & Taylor, 2008; Fang et al., 2015; Povak et al., 2018; Mansoor et al., 2022). This is becoming increasingly common with the progression of climate change, which continues to lengthen fire season (Abatzoglou & Williams, 2016; Mansoor et al., 2022). Variation in environmental conditions impacts wildfire behavior, and likely contributes to inconsistent findings across studies, introducing uncertainty about the sensitivity of soil health indicators to post-fire change.

Effects of wildfire on soil health recovery have been shown to be contradictory. For instance, soil organic carbon (SOC) is used as a burn severity metric where losses indicate degraded soil condition. However, formation pathways for different carbon fractions may be altered (positively and negatively) in response to fire-induced microbial mortality, reduction of organic inputs from the surface horizon, and formation of persistent charcoal (Kuzyakov et al., 2009; Nocentini et al., 2010; Jackson et al, 2017). Similarly, microbial communities have variable responses to wildfire. Bacterial communities exhibit rapid population growth in comparison to fungal communities in the decades following wildfire (Hart et al., 2005; Hamman et al., 2007; Bárcenas-Moreno & Bååth, 2009; Fontúrbel et al., 2012). While Vázquez et al. (1993) suggested that fungal and bacterial communities are expected to eventually return to their pre-burn conditions, Hamman et al. (2007) reported significant structural differences in microbial communities between burned and unburned sites. Despite the overall dynamic of gradual increases in microbial biomass after fire, structural and functional changes introduce a layer of uncertainty in interpreting recovery trends. Inconsistencies in interpreting trends for a variety of physical properties have also been documented after fire (Imeson et al. 1992; Certini, 2005; Hatten et al., 2005).

The purpose of this study was to evaluate dynamic soil properties relative to time since catastrophic wildfire. We compared recovery of soil properties from two wildfires (5 and 10 years since burn) relative to sites with no documented history of fire in contrasting soil types of the central Sierra Nevada mixed conifer forests. We hypothesized that soil health recovery will depend on time since wildfire, but is also influenced by elevation, which is a proxy for climate, vegetation, soil formation, and soil type. The objective of this study was to identify the dynamic soil properties most useful for wildfire recovery assessments.

1.2. Materials and methods

1.2.1. Site Description

The study area encompassed mixed montane conifer stands of the Stanislaus and Sierra National forests, located in California's central Sierra Nevada mountains. A chronosequence of time-since-catastrophic wildfire was identified to assess recovery trends of dynamic soil properties over a 5 and 10 year burn history. These conditions were compared to adjacent sites with no documented burn history termed 50+ years since fire. Study sites within the sequence were stratified by high (5,000-7,000 ft) and low (2,700-4,900 ft) elevation. Mean annual precipitation (MAP) is 800 to 1000 mm in the low elevation band and 1000 to 1,250 mm in the high elevation band. Mean annual air temperature (MAAT) is 9 ºC at high elevation sites and 11 ºC at low elevation sites (WSS, 2024). This area is characterized by hot, dry summers and cool, moist winters according to the Köppen-Geiger climate classification system (California Soil Resource Lab, n.d.). These soil landscapes have a xeric soil moisture regime. The soil temperature regime is mesic at low elevation and frigid at high elevation.

The Stanislaus and Sierra National Forests are both located on the Sierra Nevada Batholith, a geologic structure formed from the subduction of plate tectonics which melted rock material that cooled as plutons (Hill, 2006). The parent material of the study site consists of granitic colluvium, residuum, and till (WSS, 2024). Soils sampled from the high elevation band were represented by the Gerle soil series, Coarse-loamy, mixed, superactive, frigid Humic Dystroxerepts. Soils sampled from the low elevation band represented the Holland soil series, Fine-loamy, mixed, active, mesic Ultic Haploxeralfs (WSS, 2024). Sampling occurred in 2023 and 2024.

Overstory vegetation (when present) in the low elevation band is dominated by incense cedar (*Libocedrus decurrens*), ponderosa pine (*Pinus ponderosa*), white fir (*Abies concolor*), sugar pine (*Pinus lambertiana*), black oak (*Quercus kelloggii*), canyon live oak (*Quercus chrysolepis*), and leather oak (Quercus durata). At the high elevation band vegetation is similar but also includes Jeffery pine (*Pinus jeffryi*) and red fir (*Abies magnifica*) and less oak species. Understory vegetation across both elevation bands consists primarily of perennial shrubs, graminoids, and herbs (U.S. Department of Agriculture, 2023; U.S. Department of Agriculture, 2024; CalScape, 2024).

Locations representing five years since catastrophic wildfire (burn) were from within the perimeter of the Ferguson fire, ignited in the summer of 2018. Approximately 96,901 acres of land in Mariposa County were consumed across the southwestern Stanislaus and northwestern

Sierra National Forests (Reiner et al., 2018; CalFire, n.d.). Locations representing 10 years since burn were from within the perimeter of the Rim fire, ignited in the summer of 2013 and is regarded as the third largest wildfire in California history (Skalski, 2014). This fire burned about 257,314 acres in Tuolumne County, spreading across the Stanislaus National Forest and Yosemite National Park (CalFire, n.d.). Samples were also collected outside of either of the aforementioned fire perimeters in locations that have not burned in at least the past 50 years. This is denoted as the 50+ year since burn site, serving as an analog for a "no burn" control. It should be noted that all of California has burned at some point in its history, so it was deemed necessary to differentiate between the control in this study and a true "no burn" site.

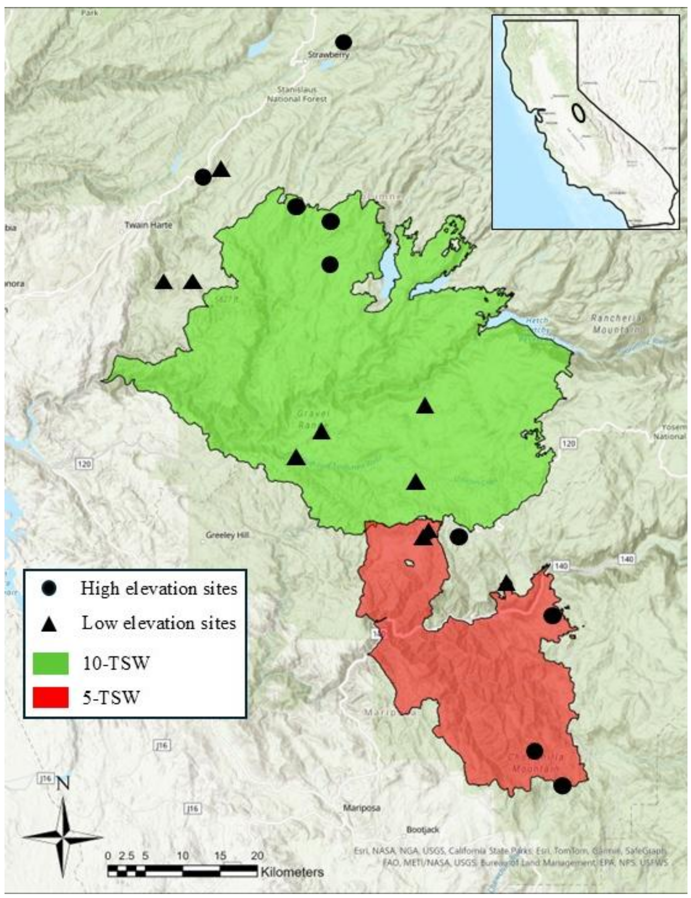

Figure 1.1. Map of study area depicting 10-TSW (green) and 5-TSW (red) sites at high (circle) and low (triangle) elevations in the Stanislaus and Sierra National Forests.

1.2.2. Soil Sampling

A total of nine sampling sites were selected in each elevation band based on burn history and granite-derived parent material resulting in 18 different locations (2 elevations x 3 times-since-burn x 3 replicate sites). Sample sites consist of one central soil profile excavation to verify the soil series and four satellite sites. Genetic horizons were identified, described, and sampled in each profile using standard soil survey techniques (Soil Survey Staff, 2012). The four satellite sites were located 10-m in each cardinal direction away from the central soil profile. Soil was collected at 0-5 cm and 5-15 cm in the satellite sites. The O horizon was also sampled if present.

Soil was sampled separately at each satellite site by hand for chemical, physical, and biological analyses. Two samples from the bulk soil were collected at each depth: one for physical and chemical analysis, and one for microbial analysis. The samples for microbial analysis were immediately stored on ice and then moved to the laboratory's cold storage at 4 ºC for no longer than one week. Bulk density cores (diameter of 7.3 cm for profile horizons and 4.8 cm for satellite sites) were collected at each genetic horizon of the central profile and at both depths in the satellite sites.

1.2.3. Field Measurements

Water repellency and litter thickness were measured in the field. Soil water repellency was done following the water drop penetration test (WDPT) (Schoeneberger et al., 2012). Five droplets of de-ionized water were dropped on the bare soil surface, and the average time it took for the water droplets to infiltrate the soil at 0 cm and 5 cm determined the hydrophobicity classification. If WDPT could not be performed in the field, a modified version from Doerr (1998) was performed in the lab. Litter thickness was determined with a measuring tape from the top of the litter layer to the mineral soil surface. If the litter layer showed development (Oi, Oe, Oa), the thickness of each horizon was recorded.

1.2.4. Laboratory Analysis

Bulk soil samples intended for physical and chemical analysis were air-dried until a stable mass was achieved then sieved through a 2 mm mesh. Fresh soil for microbial analysis was sieved through a 4 mm mesh and either stored at 4 ºC for immediate use or frozen for future use. The processed samples were measured for a variety of soil properties, including pH, electrical conductivity (EC), extractable phosphorus, particulate organic matter (POM), minerally associated organic matter (MAOM), total carbon (TC) and nitrogen (TN), and C:N ratio, litter TC and TN, and particle size analysis. Additional measurements include aggregate stability, soil color, bulk density, rock fragment volume.

Fresh soil samples sieved to 4 mm were analyzed for microbial biomass using substrate induced respiration (SIR) and phospholipid fatty acid analysis (PLFA). The method for SIR was modified from Fierer et al. (2003), in which 10 g of stored 4 ºC soil was measured into 132 mL mason jars and incubated with 25 mL of a 1.2% autolyzed yeast solution. Gas samples were collected from the headspace of jars at 0.5-, 2.5-, and 4.5-hour intervals after shaking, and analyzed for cumulative CO_2 with the Licor Model LI-6252 infrared gas analyzer. Average CO_2 concentration from these three time intervals serves as a proxy for microbial biomass, where greater rates of respiration correlate with larger microbial communities. Frozen soil saved for PLFA was freeze-dried and sent to the University of Missouri Soil Health Assessment Center for analysis with the high throughput extraction method from Buyer and Sasser (2012).

Soil pH was determined using a 1:2 slurry consisting of 10 g soil and 20 mL 0.01M $CaCl_2$, following the method described by Thomas (1998) and Soil Survey Staff (1996). Soil EC was measured in a 1:1 saturated paste 15 g soil and 15 mL deionized water. For both pH and EC, the slurry was placed on the shaker for 15 minutes and then allowed to sit for one hour prior to analysis. Extractable phosphorus was quantified with the Bray-P method, which is suitable for more acidic soils (Sims, 2000). Soil organic carbon and nitrogen concentrations were assessed in the POM and MAOM fractions. The POM and MAOM fractions were measured following the particle size fractionation procedure modified from Cotrufo et al. (2019). In this method, 5 g of soil was dispersed in 30 mL of 0.5% $Na(PO_3)_6$ by shaking for 18 hours. The slurry was then wet sieved through a 53 μm mesh to separate the fine and coarse soil fractions and oven-dried at 60 ºC. Samples were analyzed with the ECS-8024 NC Soil Special Costech elemental analyzer. This dry combustion method was also used to measure total carbon and nitrogen in the bulk soil samples. Particle size was determined with the hydrometer method (Sheldrick & Wang, 1993).

Aggregate stability was measured with the Slakes app (Soil Health Institute, 2023). Bulk density and rock fragment volume were both determined from volumetric cores.

1.2.5. Statistical Analysis

In order to identify the effects of time since wildfire (TSW) and elevation class on the numeric soil health indicators, a combination of PERMANOVA with 999 permutations and ANOVA of linear mixed effects models (LME) with the restricted maximum likelihood was used. The LMEs were utilized to predict response of soil health indicators for levels and interactions of TSW and elevation class. In order to reduce the residual error of the model, we accounted for the influence of changes in geographic space on response variables by making sample site a random effect. The focus of this study was to determine how TSW and elevation class influence the response of soil health indicators, which is reflected in the model as main effects.

LMEs were validated for goodness of fit with visual assessment of Q-Q and scale-locations plots, the Shapiro-Wilk test for normality (1965), and the Breusch-Pagan test for heteroskedasticity of residuals (1979). Log or square root transformations were performed for soil parameters that did not meet model assumptions. The following variables were log transformed: actinomycetes, arbuscular mycorrhizal fungi, gram negative bacteria, eukaryotes, other fungi, gram positive bacteria, fungi:bacteria, predator:prey, monosaturated:polysaturated PLFAs (only at 0-5 cm), EC, SIR, PLFA, TC, TN, and POM-N. Extractable P, POM-C, MAOM-C, C:N ratio, POM-C:N ratio, and MAOM-C:N ratio were square root transformed to meet the model assumptions. Soil gram negative structural ratio, pH, MAOM-N, and aggregate stability did not undergo transformations.

When model assumptions were violated and could not be amended by transformations, generalized linear mixed models (GLMM) were used instead. This was done for GP:GN ratio, saturated: unsaturated PLFAs (0-5 cm), and bulk density (0-5 cm). GLMMs were validated with the Shapiro-Wilk test for normality of residuals and Levene's test for equality of variances. This process was repeated for the listed soil health indicators at both sampling depths (0-5 cm and 5-15 cm).

*response variable ~ TSW * elevation class + (1|sample site)*

Pairwise comparisons between the control (50+ years since burn) and each TSW treatment (10 years and 5 years since burn) were performed with Dunnett's multiple comparison test to evaluate whether treatments are statistically distinguishable from the control. Significance was determined at $\alpha = 0.05$ and denoted either as n.s. (nonsignificant) or with the corresponding p-value.

All statistical analyses were performed in RStudio with the lme4, emmeans, and vegan packages.

1.3. Results and discussion

1.3.1. Field Measurements

1.3.1.1. O horizon thickness

Differences in O horizon thickness were significantly associated ($p < 0.05$) with elevation and time since wildfire (TSW), including their interaction (Fig. 1.2). At high elevation sites, recovery of O horizon thickness was 72.8% lower (mean = 2.95 cm; p = 0.0045) at 10-TSW compared to mean thickness of control sites (mean = 10.85 cm) and 72.34% lower (mean = 3 cm; p = 0.0046) at 5-TSW. In contrast, low elevation sites had much thinner O horizons (< 5 cm) and showed no significant difference in mean O horizon thickness relative to TSW. There was substantial evidence that O horizon thickness changed across the main effects of TSW ($p < 0.01$) and elevation ($p < 0.05$).

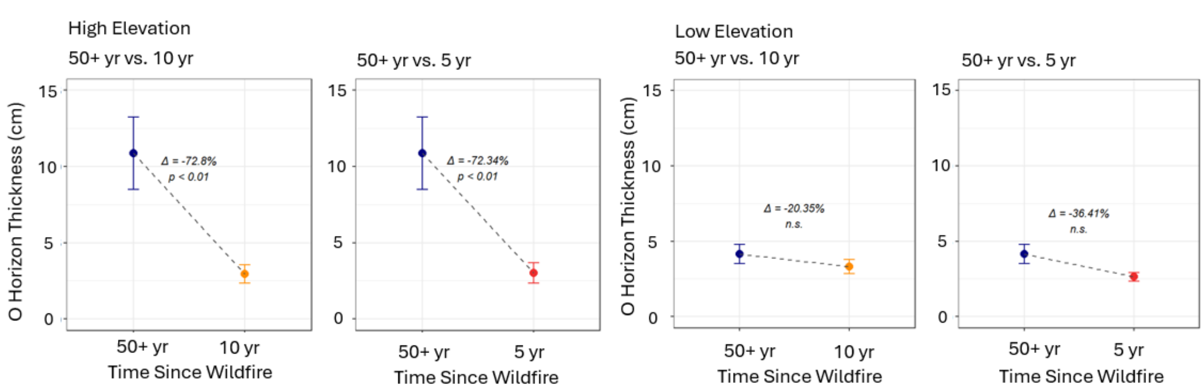

Figure 1.2. Comparison of O horizon thickness between the 50+ year (control) and 10- or 5- year since burn treatments using: a) High Elevation O horizon thickness, and b) Low Elevation O horizon thickness. Points on the plot are mean values, whiskers show standard error, and dashed lines with Δ indicate the percent-difference between means.

Fuel accumulation in the forest understory is shaped by elevation, which regulates both climate and vegetation composition. At higher elevations, cooler temperatures slow decomposition of the litter layer (Miller & Urban, 1999; Hu et al., 2025). These sites, dominated by white fir and ponderosa pine forests (van Wagtendonk et al., 2020), had a surface layer primarily composed of coniferous needles with high cellulose and lignin content, which decompose more slowly than broadleaf litter (Štursová et al., 2020; Chen et al., 2023). Conversely, low elevation forests consisted of ponderosa pine forests and black oak. Greater prevalence of black oaks and warmer climatic conditions facilitated faster decomposition of litter with reduced lignin and cellulose concentrations. This pattern is reflected in Fig. 1.2, where the O horizon thickness in high elevation control sites was greater than in low elevation control sites.

Post-wildfire recovery of the O horizon followed an elevation dependent trend. Recovery was more evident at high elevation sites, likely due to greater litter production from certain coniferous trees and slower decomposition rates which facilitated litter residue and organic matter accumulation. This may be the result of a combination of factors, including the rate of litter production under different forest types, rate of decomposition under different temperature and precipitation regimes, and differences in wildfire severity across landscapes. Conifers produce more litter than broadleaf trees, which contributes to the faster recovery of O horizons at high elevations compared to low elevations (Zajícová & Chuman, 2021). This trend was also observed by MacKenzie et al. (2004) and Hatten et al. (2005), who both reported only marginal increases in forest floor thickness over time since wildfire at similarly low elevation sites.

1.3.1.2. Water repellency

Soil water repellency varied over TSW and between elevation classes (Fig. 1.3). At high elevations, approximately 56.9% of all samples exhibited some degree of water repellency (infiltration time > 5 seconds). However, the distribution of water repellency classifications changed relative to TSW. At control sites, about 67% of surface (0–5 cm) and 25% of subsurface

(5–15 cm) samples were at least slightly water repellent. At 10-TSW, occurrence of water repellency increased in comparison to the control, with 75% of both surface and subsurface samples at least slightly water repellent. In contrast, 5-TSW occurrence of water repellency was lower than the control with 41.7% of surface and 58.3% of subsurface samples at least slightly water repellent.

At low elevations, approximately 27.8% of all samples exhibited some degree of water repellency. Similar to high elevations, the distribution of water repellency classification changed relative to TSW. At control sites, 9.1% of surface and 0% of subsurface samples were at least slightly water repellent. At 10-TSW, occurrence of water repellency increased relative to the control, with 37.5% of surface 31.2% of subsurface samples at least slightly water repellent. Similarly, water repellency at 5-TSW increased relative to the control, with 66.7% of surface and 16.7% of subsurface samples at least slightly water repellent.

High elevation sites were more water repellent than low elevation sites. Water repellency relative to time since wildfire followed different distributions at each elevation class. High elevation sites were most water repellent at 10-TSW and least water repellent at 5-TSW. In contrast, low elevation sites were most water repellent at 5-TSW and least water repellent in the control sites.

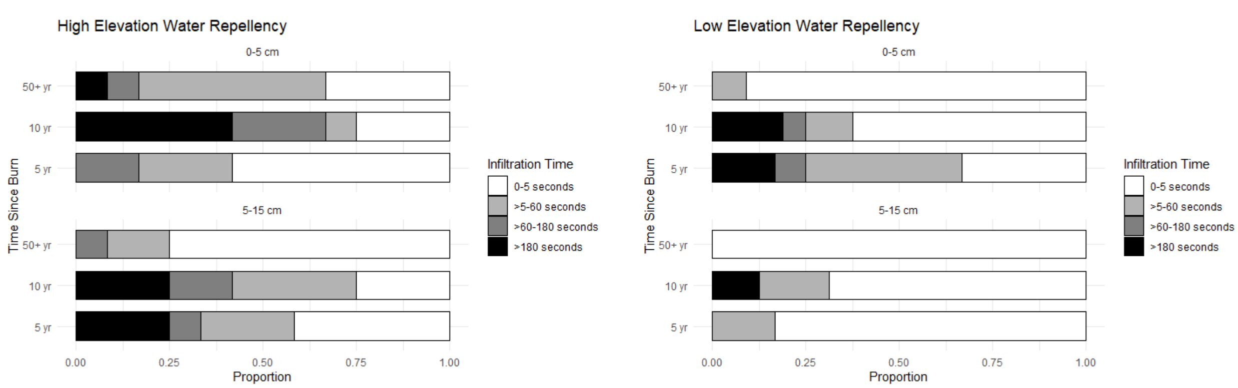

Figure 1.3. Relative abundance of water repellency classifications over TSW, across elevation classes, and between sampling depths.

At high elevations, no significant association between time since wildfire and water repellency was detected ($p = 0.0872$). Therefore, water repellency was likely driven by the quality of the litter layer rather than the effects of wildfire, or recovery occurs faster than 5 years. Wahl (2008) and Seiwa et al. (2021) reported that litter quality is negatively correlated with soil water repellency, with low quality coniferous litter containing more hydrophobic compounds than higher quality broadleaf litter (Wahl, 2008; Zhang et al., 2008; Francis et al., 2023). This may explain the enhanced hydrophobicity observed in high elevation compared to low elevation.

In contrast, there was a significant association between time since wildfire and water repellency at low elevation sites ($p = 0.038$). These sites exhibited greater water repellency with decreasing time since wildfire, indicating that repellency in these areas was driven primarily by combustion of the litter layer. Hydrophobic residues from plant material that are vaporized during fire condense to coat the soil surface as temperatures cool (Savage, 1974; Mataix-Solera et al., 2011; Verma & Jayakumar, 2012). Together, these findings indicate broad spatial variation in post-wildfire water repellency shaped by vegetation type, litter quality, and time since wildfire.

1.3.2. Biological Soil Health Indicators

1.3.2.1. Ecosystem microbial community trends

Microbial community composition of PLFA taxa differs over time since wildfire ($p < 0.01$), across elevation classes ($p < 0.01$), and with the interaction of these main effects ($p < 0.05$) (Table 1.1). However, low correlation coefficient values of each model term indicate weak associations to the multivariate relationship between main effects and PLFA taxa, as ~82% of the variation in the data remains unexplained (residual R^2). Although the association between model terms and PLFA taxa are weak, there is enough evidence of dissimilarity between groups to produce significant p-values.

Table 1.1. Permutational Analysis of Variance (PERMANOVA) by the Bray-Curtis dissimilarity method showing the main effects of TSW and elevation class, and the interaction of TSW x elevation class on PLFA taxa: arbuscular mycorrhizal fungi, gram negative bacteria, eukaryotes, other fungi, gram positive bacteria, and actinomycetes.

Model Term	df	R^2	Pseudo-F	p-value
TSW	2	0.07308	4.8148	**0.0053** **
Elevation Class	1	0.05655	7.4506	**0.0038** **
TSW x Elevation Class	2	0.05071	3.3405	**0.0258** *
Residual	108	0.81966		
Total	113	1.00000		

The table includes degrees of freedom (df), coefficient of determination (R^2), test statistic (Pseudo-F), and significance level (p-value).

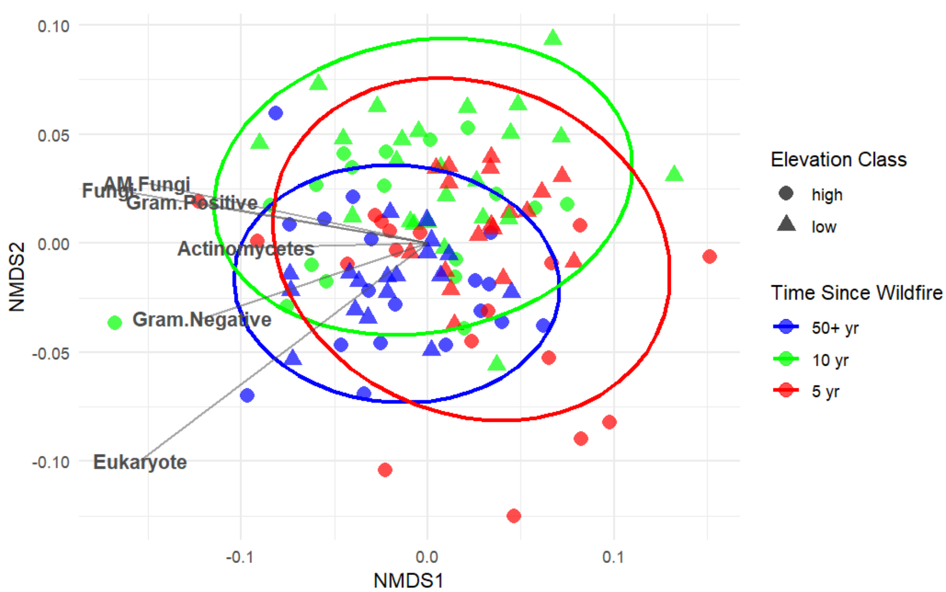

Figure 1.4. NMDS ordination of the association between PLFA taxa and time since wildfire group at 0-5 and 5-15 cm, where points closer together on the ordination are more similar than points that are farther apart. The stress value indicating overall goodness of fit of the NMDS is 0.16. NMDS was performed on arbuscular mycorrhizal fungi (R^2 = 0.37; p-value = 0.0001), gram-negative bacteria (R^2 = 0.25; p-value = 0.0001), eukaryotes (R^2 = 0.54; p-value = 0.0001), other fungi (R^2 = 0.48; p-value = 0.0001), gram-positive bacteria (R^2 = 0.26; p-value = 0.0001), and actinomycetes (R^2 = 0.15; p-value = 0.0001). Vectors in the plot demonstrate strength of the

association between individual PLFA taxa, time since wildfire ($R^2 = 0.13$; p-value = 0.0001) and elevation class ($R^2 = 0.047$; p-value = 0.0001), where longer arrows correspond to greater association. Ellipses represent groupings of each TSW group at 95% confidence.

The NMDS ordination depicts a clear clustering pattern of 50+ yr control sites, indicating a greater degree of within-group similarity of microbial community composition in “unburned” sites (Fig. 1.4). This cluster follows the eukaryote and gram negative bacteria vectors down the NMDS1 and NMDS2 axes, which is associated with greater abundance of these species. Overall, these results suggest that microbial community composition across “unburned” sites was more homogenous than recently burned sites.

The 10- and 5-TSW groups are more spread out on the NDMS plot (Fig. 1.4) than the control, indicating a greater degree of heterogeneity in community composition in recently burned sites. The 10-TSW cluster aligns with the vectors representing arbuscular mycorrhizal fungi, other fungi, and gram positive bacteria, suggesting these taxa had a stronger influence on microbial community composition at 10-TSW sites. Furthermore, samples in the 5-TSW group appear to fall opposite of the direction of the vectors, indicating lower abundance of measured PLFA taxa in these sites.

While clustering does occur in the NMDS ordination, overlap among the 95% confidence ellipses across TSW groups suggests a degree of similarity in overall forest soil microbial community composition. However, the significant PERMANOVA results (Table 1.1), coupled with the visual clustering in the ordination space (Fig. 1.4), indicate that community composition diverges in the 10- and 5-TSW sites relative to the control. Similar patterns were reported by Bárcenas-Moreno et al. (2011), Fontúrbel et al. (2012), Adkins et al. (2020), and Sáenz de Miera et al. (2020), where microbial community composition of unburned sites cluster separately from burned sites on their respective ordination plots. Conversely, burned sites were consistently more stochastic on the ordination plot. This variation in microbial community composition between burned and unburned sites has been primarily attributed to burn severity, and secondarily to vegetation (Whitman et al., 2019; Adkins et al., 2020; Sáenz de Miera et al., 2020). This highlights the disparity between burned and unburned landscapes, where unburned microbial communities remain relatively unchanged over time compared to fire affected microbial communities (Predergast-Miller et al., 2017). More recently burned sites, which in this study were dominated by nitrogen-fixing shrubs and graminoids rather than conifer stands, varied in microbial community composition across the burned landscape. These findings support an overarching trend of decreasing beta diversity of microbial communities over time since wildfire, where community structure is heterogenous across the landscape in recently burned sites and increases in similarity over time since wildfire (Wang et al., 2016; Nelson et al., 2022; Hopkins et al., 2025).

1.3.2.2. Biological soil health indicators sensitive to change over time since wildfire

Significance was detected for actinomycetes, arbuscular mycorrhizal fungi, and Shannon diversity (Table 1.2). However, post-hoc analyses of significant ANOVA results detected no statistically significant differences in actinomycetes abundance among TSW groups across elevation classes.

Table 1.2. ANOVA of mixed effects models for PLFA taxa, PLFA structural ratios, total microbial biomass, and Shannon diversity at 0-5 and 5-15 cm.

Response Variable	Model Term	0-5 cm			5-15 cm		
		df	Test Statistic	p-value	df	Test Statistic	p-value
Actinomycetes	TSW	2	1.60	0.240	2	0.977	0.403
	Elev. Class	1	0.613	0.448	1	0.431	0.523
	(TSW x Elev. Class)	2	1.39	0.283	2	3.81	**0.0499 ***
Arbuscular Mycorrhizal Fungi	TSW	2	0.997	0.396	2	1.77	0.209
	Elev. Class	1	0.333	0.574	1	0.029	0.867
	(TSW x Elev. Class)	2	0.0398	0.961	2	4.79	**0.0277 ***
Gram Negative Bacteria	TSW	2	1.41	0.280	2	1.05	0.376
	Elev. Class	1	2.95	0.110	1	3.02	0.106
	(TSW x Elev. Class)	2	0.539	0.596	2	2.75	0.101
Eukaryote	TSW	2	2.85	0.0941	2	2.93	0.0893
	Elev. Class	1	3.91	0.0697	1	2.03	0.178
	(TSW x Elev. Class)	2	0.158	0.855	2	2.94	0.0886
Fungi	TSW	2	1.20	0.332	2	1.94	0.183
	Elev. Class	1	2.61	0.130	1	0.808	0.385
	(TSW x Elev. Class)	2	0.609	0.559	2	0.788	0.475

Gram Positive Bacteria	TSW	2	0.566	0.581	2	0.973	0.404
	Elev. Class	1	0.795	0.389	1	0.745	0.404
	(TSW x Elev. Class)	2	0.240	0.790	2	3.49	0.0611
Fungi: Bacteria Ratio	TSW	2	1.43	0.277	2	3.75	0.0517
	Elev. Class	1	0.360	0.559	1	0.186	0.673
	(TSW x Elev. Class)	2	1.16	0.344	2	0.745	0.494
Predator: Prey Ratio	TSW	2	4.45	**0.0337 ***	2	4.24	**0.0382 ***
	Elev. Class	1	3.33	0.0913	1	0.238	0.634
	(TSW x Elev. Class)	2	2.90	0.0906	2	1.85	0.197
Gram$^+$: Gram$^-$ Ratio	TSW	2	18.5	**9.81e-05 *****	2	9.37	**0.00925 ****
	Elev. Class	1	12.6	**0.000387 *****	1	17.3	**3.13e-05 *****
	(TSW x Elev. Class)	2	28.9	**5.28e-07 *****	2	0.206	0.902
Saturated: Unsaturated PLFAs	TSW	2	8.38	**0.0152 ***	2	2.40	0.130
	Elev. Class	1	0.0583	0.809	1	0.251	0.625
	(TSW x Elev. Class)	2	2.03	0.363	2	5.44	**0.0192 ***
Monosaturated: Polysaturated PLFAs	TSW	2	0.704	0.513	2	1.79	0.206
	Elev. Class	1	3.31	0.0920	1	0.234	0.637
	(TSW x Elev. Class)	2	2.23	0.147	2	0.606	0.560
Gram$^-$ Metabolic stress	TSW	2	0.0039	0.996	2	0.568	0.580
	Elev. Class	1	2.28	0.155	1	1.93	0.188

	(TSW x Elev. Class)	2	1.27	0.315	2	0.925	0.421
Total PLFA	TSW	2	0.867	0.443	2	1.05	0.378
	Elev. Class	1	0.0533	0.821	1	0.222	0.646
	(TSW x Elev. Class)	2	0.183	0.835	2	0.204	0.818
SIR	TSW	2	0.974	0.404	2	0.751	0.492
	Elev. Class	1	2.43	0.143	1	5.28	**0.0390 ***
	(TSW x Elev. Class)	2	0.183	0.835	2	2.70	0.105
Shannon Diversity Index	TSW	2	6.56	**0.0377***	2	12.7	**0.00175 ****
	Elev. Class	1	0.140	0.708	1	3.32	0.0685
	(TSW x Elev. Class)	2	6.53	**0.0382 ***	2	3.51	0.173

Significant differences were detected in arbuscular mycorrhizal fungi between the subsurface 5-TSW treatment and the control at high elevation sites (Fig. S2). Abundance of arbuscular mycorrhizal fungi in the 5-TSW soil subsurface was 55.79% lower (mean = 1.07 nmol/g soil; $p = 0.0466$) than the control (mean = 2.42 nmol/g soil). No other treatment-control comparisons were statistically significant, although low elevation sites consistently showed a trend toward elevated arbuscular mycorrhizal fungi abundance in control sites relative to the 10-TSW and 5-TSW groups.

Predator:prey ratio was significantly different between TSW groups in the soil surface and subsurface at low elevation (Table 1.2; Fig. S1a). No significance was detected in high elevation sites between either the 10-TSW or 5-TSW treatments and the control. In contrast, at low elevation, predator:prey ratio was significantly lower in the 10-TSW and 5-TSW treatments compared to the control. In the soil surface, the ratio was 41.6% lower (mean = 0.0238; $p = 0.00489$) at 10-TSW sites than the control (mean = 0.0407), and the subsurface was 32.48% lower (mean = 0.0241; $p = 0.0137$) than the control. In 5-TSW sites, the surface predator:prey ratio was 34.7% lower (mean = 0.0266; $p = 0.0230$) than the control (mean = 0.0407). Significance was not detected between the 5-TSW treatment and control in the subsurface.

Gram positive:gram negative bacteria (GP:GN) ratio changed significantly in the soil surface between the high elevation 10-TSW treatment and control, and between the low elevation 5-TSW treatment and control (Table 1.2; Fig. S1b). At high elevations, the surface 10-TSW treatment was 33.7% higher (mean = 0.807; $p = 0.000000830$) than the control (mean = 0.603). Similarly, low elevation 5-TSW sites were 13.56% higher (mean = 0.791; $p = 0.04788$) than the control (mean = 0.697).

Saturated:unsaturated (sat:unsat) PLFA ratio differed between high elevation 5-TSW sites and the control (Table 1.2; Fig. S1c). In the soil surface, 5-TSW sites were 26.78% higher (mean = 1.20; $p = 0.00919$) than the control (mean = 0.950). In the subsurface, 5-TSW sites were 48.66% higher (mean = 1.66; $p = 0.0239$) than the control. All other treatment vs. control comparisons were not statistically significant.

PLFA structural ratios are commonly used as indicators of stress in the soil environment. Of the measured PLFA structural ratios, only predator:prey, GP:GN, and sat:unsat PLFA ratios provided significant evidence of stress relative to the control. The consistently elevated predator:prey ratio in control sites relative to recently burned sites, likely due to greater prey populations in unburned sites, is an indicator of healthier microbial communities and reduced environmental stress (Quist et al., 2020). Predators are key components of trophic cascades and influencers of carbon and nutrient cycling (Thakur et al., 2015; Butenko et al., 2017; Quist et al., 2020). Soil predators are generally more sensitive to disturbance than their prey, thus a useful bioindicator of soil health (Quist et al., 2020). Butenko et al. (2017) and Martin & Sprunger (2022) both detected positive correlation between elevated predator populations with carbon sequestration and nutrient mineralization, connecting this dynamic with greater soil health and ecosystem productivity. We found predator:prey ratio serves as a sensitive indicator of soil health recovery over time since wildfire, especially at low elevation. The lack of significant differences between the control and burn treatments at high elevation sites indicates either recovery occurs within the first 5 years of wildfire, or burn severity was low enough to prevent population loss. Post-wildfire recovery of the predator population may require more than a decade of succession in low elevation forests of California.

We found elevated levels of GP:GN and sat:unsat ratios in recently burned sites compared to the control, indicating a trend of stress reduction over time since wildfire. Elevated GP:GN and sat:unsat PLFA ratios are also indicators of stress in soils associated with degraded ecosystem productivity (Wixon & Balser; 2013; Fanin et al., 2019; Norris et al., 2023). GP bacteria are more resilient to environmental changes than GN bacteria due to their thicker peptidoglycan layer, utilization of more complex forms of carbon as an energy source, and ability to withstand nutrient-poor environments (Smith et al., 2008; Francis et al., 2010; Mai-Prochnow et al., 2016; Fanin et al., 2019; Hu et al., 2025). Similarly, saturated PLFAs are less sensitive to disturbance than unsaturated PLFA's due to the lack of double bonds between carbon atoms, which reduces resilience to elevated temperatures (He et al., 2023; Norris et al., 2023). At high elevations, these stress indicators were elevated relative to the control at both 10- and 5-TSW sites, suggesting environmental stress lasts more than one decade post-wildfire. At low elevation sites, stress indicators were significantly elevated at 5-TSW sites compared to the control which suggests a degree of recovery within one decade following wildfire.

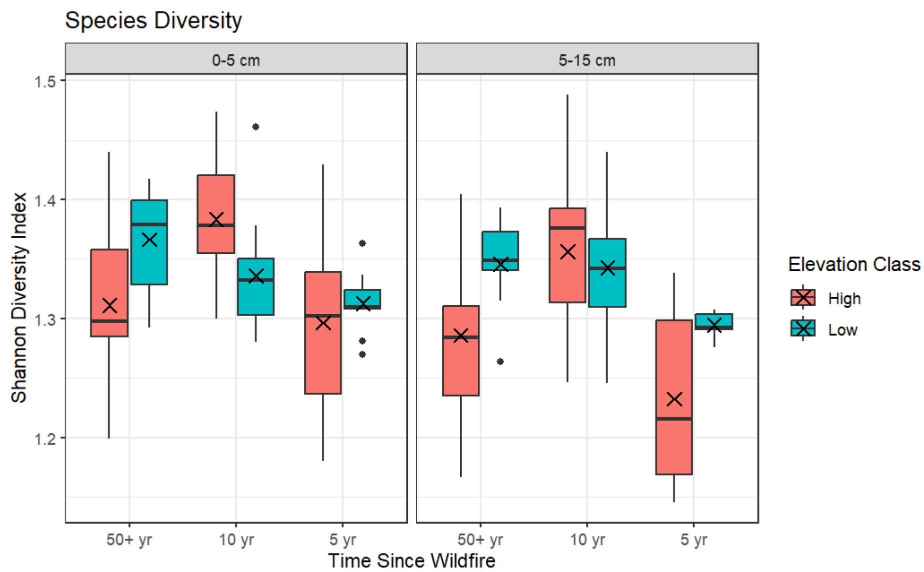

Figure 1.5. Comparison of Shannon Diversity Index over TSW, across elevation classes, and between sampling depths. Whiskers are standard maximum and minimum values, bars give median values, and "x" give mean values. Higher values correspond to greater species diversity.

Time since wildfire had a significant effect on species diversity, but trends differed by elevation (Table 1.2; Fig. 1.5). At high elevation, the linear mixed effects model detected a clear quadratic trend in Shannon diversity ($p < 0.05$), where species diversity of the 10-TSW sites was elevated relative to the control and 5-TSW. In the soil surface, the Shannon diversity index at 10-TSW was 5.49% higher (mean = 1.38; $p = 0.0295$) than the control (mean = 1.31). No significant difference was detected between the 5-TSW treatment and the control. Conversely, Shannon diversity at low elevation sites followed a linear trend where mean species diversity increased with greater time since wildfire at both sampling depths.

Catastrophic wildfire can significantly reduce Shannon diversity (Cheng et al., 2024), which limits ecosystem productivity and delays post-wildfire recovery (Rodriguez et al., 2017; Nelson et al., 2022). Similar to trends observed at our low elevation sites, Porter et al. (2023) reported the lowest diversity during early successional stages, with gradual increases over time since wildfire. Nelson et al. (2022) also found that sites afflicted by greater fire severity were consistently less diverse than unburned sites.

1.3.3. Changes in Chemical Soil Health Indicators

1.3.3.1. Overall recovery trends over time since wildfire

Soil chemical properties differed between elevation classes ($p < 0.05$) and with the interaction of TSW and elevation class ($p < 0.01$), where the soil chemical state in each TSW group depended on elevation (Table 1.3). However, the R^2 values of each model term indicate weak associations to the multivariate relationship with the main and interaction effects, as ~65% of the variation in the data remains unexplained (residual R^2). Despite these relatively weak associations, there is enough evidence of dissimilarity between groups to produce significant p-values.

Table 1.3. Permutational Analysis of Variance (PERMANOVA) by the Bray-Curtis dissimilarity method showing the main effects of TSW and elevation class, and the interaction of TSW*elevation class on soil chemical properties: pH, EC, TC, POM-C, MAOM-C, TN, POM-N, MAOM-N, C:N ratio, POM-C:N ratio, MAOM-C:N ratio, and extractable P.

Model Term	df	R^2	Pseudo-F	p-value
TSW	2	0.05621	1.3681	0.2307
Elevation Class	1	0.08870	4.3177	**0.0176 ***
TSW x Elevation Class	2	0.19766	4.8105	**0.0037 ****
Residual	32	0.65742		
Total	37	1.00000		

The table includes degrees of freedom (df), coefficient of determination (R^2), test statistic (Pseudo-F), and significance level (p-value).

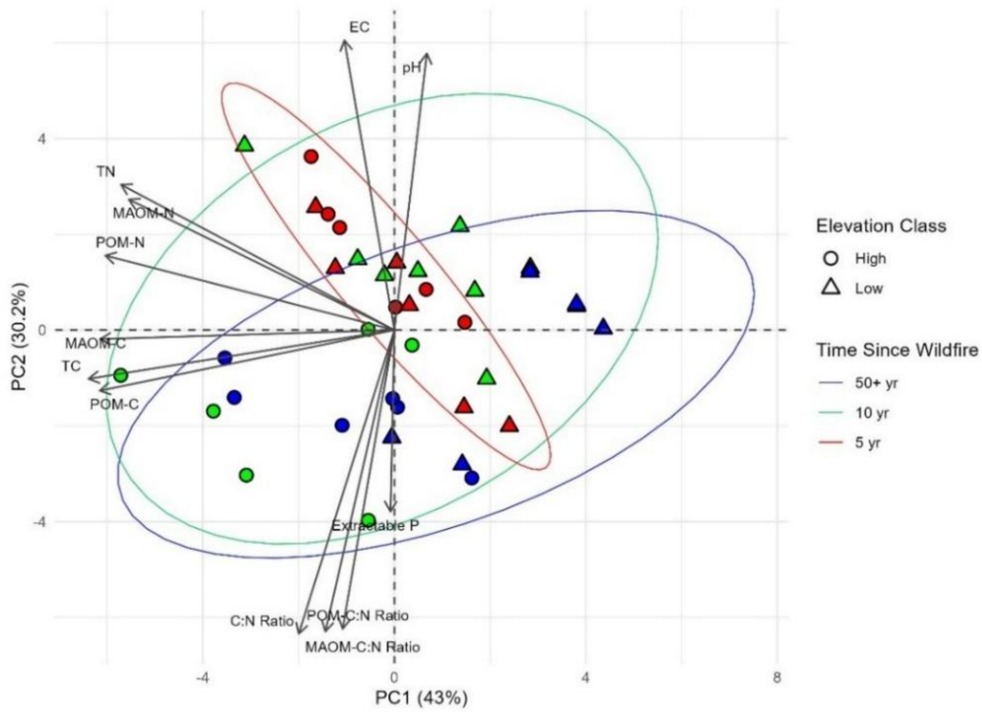

Figure 1.6. Principle component analysis (PCA) of soil chemical properties at 0-5 cm and 5-15 cm in high and low elevations, differentiated by time since wildfire. The PCA accounted for 73.2% of the total variation in the dataset (PC1 accounts for 43% of variation and PC2 accounts for 30.2% of variation). Vectors in the plot demonstrate the strength of the effects of soil chemical properties on the principle components. Ellipses represent groupings of each TSW group at 95% confidence.

PCA eigenvalues indicated that the first two principle components (PC1 and PC2) accounted for 73.2% of total variation in the dataset (Fig. 1.6). PC1 was primarily associated with soil organic matter pools of POM, MAOM, and total carbon and nitrogen, whereas PC2 was most strongly associated with reactivity and organic matter quality. Vectors show opposing trends for pH and EC compared to C:N ratios of C fractions and suggests an inverse relationship between these variables, where samples with elevated pH and EC may have lower quality SOM.

50+TSW samples were predominantly clustered by elevation class where high elevation sites are distributed below the PC1 axis and mostly to the left of the PC2 axis, while low elevation sites are mostly located above the PC1 axis and to the right of the PC2 axis (Fig. 1.6). This spatial separation suggests that chemical composition of “unburned”, mature mixed conifer forests differs by elevation. High elevation sites appear to follow the Extractable P, C:N ratio, POM-C:N ratio, MAOM-C:N ratio, POM-C, MAOM-C, and TC vectors toward the bottom left of the plot. This indicates higher values for these chemical properties and suggests that these sites were characterized by greater organic matter accumulation. Low elevation control sites follow either the Extractable P and MAOM-C:N ratio vectors, or lie opposite to the POM-C, MAOM-C, TC, POM-N, MAOM-N, and TN vectors. Although these sites were higher in Extractable P and MAOM-C:N ratio, overall SOC and nitrogen pools were lower.

Samples in the 10-TSW treatment followed a similar elevation-dependent distribution to 50+TSW. This alignment suggests that high elevation sites in the 10-TSW treatment were chemically similar to high elevation control sites, reflecting recovery of SOM pools and nutrient availability after a decade of ecological succession. In contrast to this, low elevation 10-TSW sites cluster in a way that aligns with the pH, EC, TN, POM-N, and MAOM-N vectors. The PCA demonstrates that low elevation 10-TSW were more chemically similar to the recently disturbed 5-TSW group.

Samples in the 5-TSW treatment form a tightly clustered group encompassing both high and low elevation sites, located almost entirely above the PC1 axis and to the left of the PC2 axis. Regardless of elevation, these sites align with vectors for pH, EC, TN, POM-N, and MAOM-N. The clustered distribution of both elevation classes suggests that wildfire imposes a strong homogenizing effect on soil chemical properties.

PERMANOVA (Table 1.3) and PCA (Fig. 1.6) results suggest elevation is an important factor in post-fire recovery of soil chemical properties. The distribution of soil chemical properties over time since wildfire in the PCA plot indicates divergent recovery trends based on elevation class. Wildfire initially induces a homogenizing effect, where the most recently disturbed sites are the most chemically similar across both elevation classes. After 10 years of post-wildfire recovery, high elevation sites more closely resembled the 50+ year "unburned" control, indicating that recovery time is shorter at higher elevations. In contrast to this, low elevation 10-TSW sites remain more chemically similar to 5-TSW sites, suggesting that low elevation recovery was delayed.

Other studies have detected similar post-wildfire trends, where the effects of fire severity are most pronounced immediately after disturbance. In the years following a burn event, the primary driver of soil chemical composition often shifts from fire severity to topographic factors such as elevation and slope (Kong et al., 2018; Kong et al., 2019; Dhungana et al., 2024). Warmer temperatures, optimal precipitation, and deeper soils of lower elevations in the western Sierra Nevadas generally enhances ecosystem productivity, facilitating microbial activity and biogeochemical cycling (U.S. Geological Survey, 2000; U.S. Forest Service, 2001). However, contrary to established ecological gradients, our study found that recovery of soil chemical properties was faster at high elevation sites than at low elevation sites. Accelerated recovery observed at high elevation in this study may reflect lower fire severity at those locations, potentially due to differences in vegetation type and greater soil moisture (Fang et al., 2015).

1.3.3.2. Chemical and physiochemical soil health indicators sensitive to change post-wildfire

Mixed effects models showed that in the soil surface, TSW had significant effects ($p < 0.05$) on soil pH, MAOM-N, C:N ratio, and MAOM-C:N ratio; elevation class had significant effects ($p < 0.05$) on total carbon, total nitrogen, POM-C, MAOM-C, and POM-N (Table 1.4). The interaction between TSW and elevation class (TSW x elevation class) had significant effects ($p < 0.05$) on pH, EC, POM-C, and C:N ratio. In the soil subsurface, TSW had significant effects ($p < 0.05$) on pH; elevation class had significant effects ($p < 0.05$) on total carbon, total nitrogen, POM-C, MAOM-C, POM-N, and MAOM-C:N ratio; and the interaction (TSW x elevation class) had significant effects ($p < 0.05$) on pH and EC (Table 1.4).

Table 1.4. ANOVA of mixed effects models for soil health indicators at 0-5 and 5-15 cm.

Response Variable	Model Term	0-5 cm			5-15 cm		
		df	Test Statistic	p-value	df	Test Statistic	p-value
pH	TSW	2	5.27	**0.0209 ***	2	5.09	**0.0233 ***
	Elev. Class	1	0.374	0.551	1	1.20	0.293
	(TSW x Elev. Class)	2	10.7	**0.00177****	2	8.40	**0.00455 ****
EC	TSW	2	0.168	0.847	2	0.358	0.706
	Elev. Class	1	0.975	0.341	1	3.22	0.0960
	(TSW x Elev. Class)	2	6.58	**0.0106 ***	2	9.28	**0.00314 ****
TC	TSW	2	1.02	0.388	2	1.93	0.185
	Elev. Class	1	13.5	**0.00281 ****	1	10.5	**0.00647 ****
	(TSW x Elev. Class)	2	3.10	0.0792	2	1.89	0.190
TN	TSW	2	1.81	0.203	2	3.14	0.0774
	Elev. Class	1	6.11	**0.0280 ***	1	4.99	**0.0437 ***
	(TSW x Elev. Class)	2	1.36	0.292	2	0.944	0.414
Extractable P	TSW	2	0.152	0.860	2	0.552	0.589
	Elev. Class	1	0.0883	0.771	1	0.0001	0.993
	(TSW x Elev. Class)	2	2.44	0.126	2	2.07	0.166
POM-C	TSW	2	0.823	0.461	2	1.54	0.251
	Elev. Class	1	13.9	**0.00255 ****	1	13.9	**0.00252 ****

	(TSW x Elev. Class)	2	4.27	**0.0376***	2	1.08	0.368
MAOM-C	TSW	2	2.91	0.0902	2	3.28	0.0702
	Elev. Class	1	8.32	**0.0128 ***	1	5.68	**0.0331 ***
	(TSW x Elev. Class)	2	1.45	0.269	2	1.77	0.210
POM-N	TSW	2	3.19	0.0748	2	2.62	0.110
	Elev. Class	1	10.5	**0.00647 ****	1	7.79	**0.0153 ***
	(TSW x Elev. Class)	2	3.19	0.0746	2	0.259	0.776
MAOM-N	TSW	2	5.50	**0.0186***	2	3.75	0.0520
	Elev. Class	1	4.07	0.0646	1	2.40	0.145
	(TSW x Elev. Class)	2	0.233	0.795	2	1.38	0.285
C:N	TSW	2	4.07	**0.0424***	2	1.78	0.208
	Elev. Class	1	3.31	0.0919	1	3.72	0.0758
	(TSW x Elev. Class)	2	4.49	**0.0329 ***	2	1.52	0.254
POM-C:N	TSW	2	0.294	0.750	2	0.164	0.850
	Elev. Class	1	2.46	0.141	1	2.50	0.138
	(TSW x Elev. Class)	2	2.18	0.153	2	0.830	0.458
MAOM-C:N	TSW	2	4.69	**0.0293 ***	2	1.25	0.320
	Elev. Class	1	3.55	0.0823	1	5.57	**0.0346 ***
	(TSW x Elev. Class)	2	2.194	0.151	2	1.77	0.209

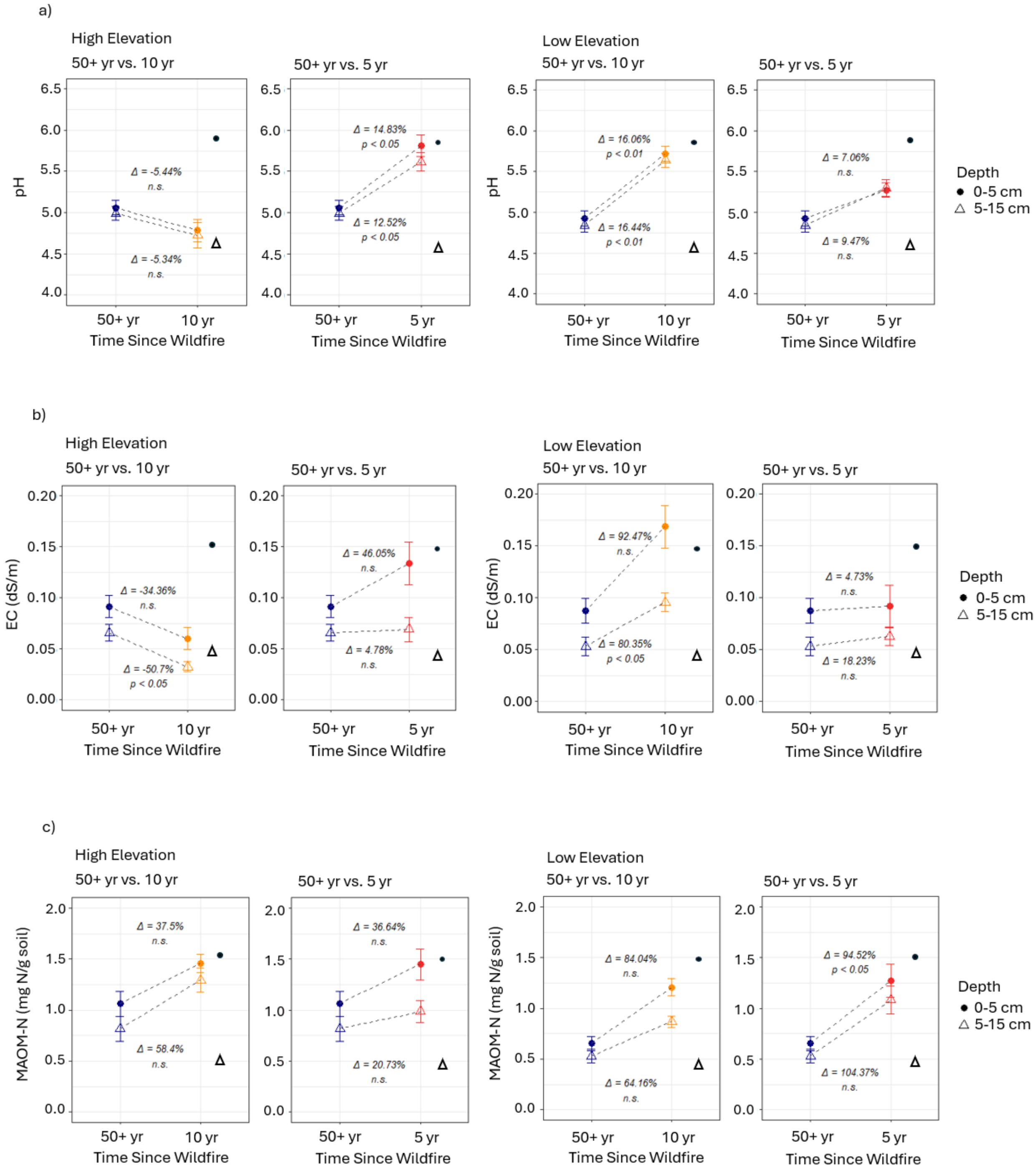

a)
High Elevation
50+ yr vs. 10 yr
50+ yr vs. 5 yr
Low Elevation
50+ yr vs. 10 yr
50+ yr vs. 5 yr
pH
Δ = -5.44%
n.s.
Δ = -5.34%
n.s.
Δ = 14.83%
p < 0.05
Δ = 12.52%
p < 0.05
Δ = 16.06%
p < 0.01
Δ = 16.44%
p < 0.01
Δ = 7.06%
n.s.
Δ = 9.47%
n.s.
50+ yr
10 yr
5 yr
Time Since Wildfire
Depth
0-5 cm
5-15 cm
b)
High Elevation
50+ yr vs. 10 yr
50+ yr vs. 5 yr
Low Elevation
50+ yr vs. 10 yr
50+ yr vs. 5 yr
EC (dS/m)
Δ = -34.36%
n.s.
Δ = -50.7%
p < 0.05
Δ = 46.05%
n.s.
Δ = 4.78%
n.s.
Δ = 92.47%
n.s.
Δ = 80.35%
p < 0.05
Δ = 4.73%
n.s.
Δ = 18.23%
n.s.
50+ yr
10 yr
5 yr
Time Since Wildfire
Depth
0-5 cm
5-15 cm
c)
High Elevation
50+ yr vs. 10 yr
50+ yr vs. 5 yr
Low Elevation
50+ yr vs. 10 yr
50+ yr vs. 5 yr
MAOM-N (mg N/g soil)
Δ = 37.5%
n.s.
Δ = 58.4%
n.s.
Δ = 36.64%
n.s.
Δ = 20.73%
n.s.
Δ = 84.04%
n.s.
Δ = 64.16%
n.s.
Δ = 94.52%
p < 0.05
Δ = 104.37%
n.s.
50+ yr
10 yr
5 yr
Time Since Wildfire
Depth
0-5 cm
5-15 cm

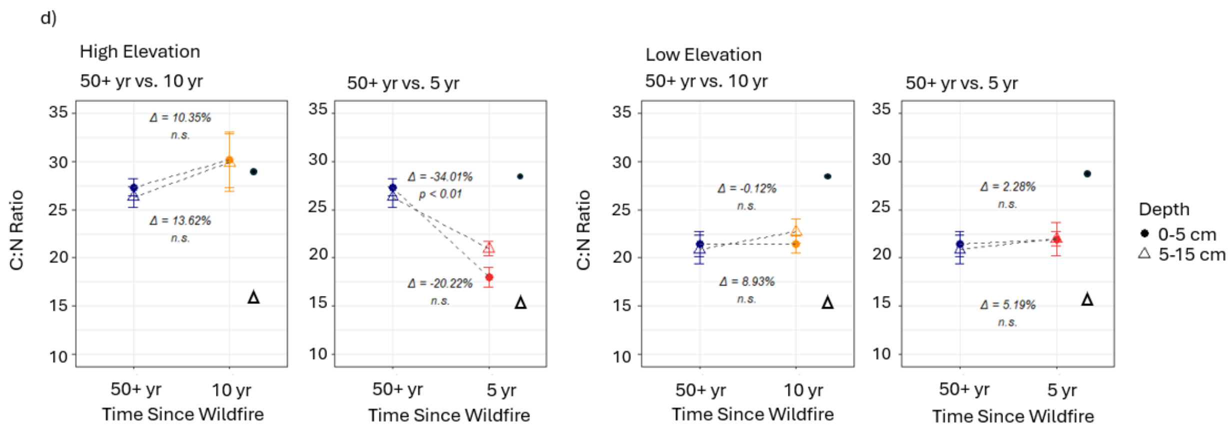

Figure 1.7. Comparison of chemical soil health indicators sensitive to change for: a) pH, b) EC, c) MAOM-N, and d) C:N ratio, significance determined by ANOVA, between the 50+ year (control) and 10- or 5- year since burn treatments at high and low elevations. Points on the plot are mean values, whiskers show standard error, and dashed lines with Δ indicate the percent-difference between means. The filled circle and clear triangle on the plot indicate the sampling depth of each percent-difference and significance value.

Surface pH was significantly associated with TSW and the interaction between TSW x elevation class ($p < 0.05$) (Table 1.4; Fig. 1.7a). At high elevation sites, no significant difference was observed in surface soils between 10-TSW and control sites. However, surface pH at 5-TSW was 14.83% higher (mean = 5.81; $p = 0.0163$) than mean surface pH of control sites (mean = 5.06). In contrast, surface pH at low elevation was elevated by 16.06% at 10-TSW (mean = 5.72; $p = 0.0066$) compared to control sites (mean = 4.93). No significant differences were detected in surface pH between 5-TSW and control sites. Subsurface soil pH (5-15 cm) followed the same trends as surface horizons.

EC was significantly associated ($p < 0.05$) with the interaction between TSW x elevation class (Table 1.4; Fig. 1.7b). Despite this, neither Tukey's HSD (see supplemental material, Table S3) nor Dunnett's post hoc tests detected significant differences in surface horizon EC among TSW treatments and the control. In contrast, subsurface EC at high elevation was 50.7% lower at 10-TSW (mean = 0.0325 dS/m; $p = 0.0247$) compared to the control (mean = 0.0659 dS/m).

Subsurface EC at low elevation was 80.35% higher at 10-TSW (mean = 16.56 dS/m; $p = 0.0297$) compared to the control (mean = 9.95 dS/m). No significant differences were detected between 5-TSW and control sites at high or low elevation.

MAOM-N differed significantly over time since wildfire in the soil surface (Table 1.4; Fig. 1.7c). At high elevation, the control and TSW treatments were statistically indistinguishable. However, MAOM-N was elevated in 5-TSW compared to the control. At low elevation, 5-TSW sites were 94.52% (mean = 1.27 mg N/g soil; $p = 0.0458$) higher than the control (mean = 0.655 mg N/g soil). Overall, soil MAOM-N was consistently higher in 5-TSW sites compared to the control across both elevation classes.

C:N ratio was statistically significant over time since wildfire ($p < 0.05$) and the interaction between time since wildfire and elevation class ($p < 0.05$) in the soil surface (Table 1.4; Fig. 1.7d). High elevation surface C:N ratio at 5-TSW sites was significantly lower by 34.01% (mean = 18.03; $p = 0.0147$) compared to the control (mean = 27.33). Similarly, high elevation surface MAOM-C:N ratio at 5-TSW sites were significantly lower by 29.81% (mean = 15.89; $p = 0.0067$) than the control (mean = 22.64).

Overall, the chemical soil health indicators most sensitive to change over time since wildfire were soil pH, EC, stabilized organic nitrogen (MAOM-N), C:N and MAOM-C:N ratios. Ephemeral increases in soil pH and EC are common after fire. Combustion of biomass supplies large pulses of base cations and soluble ions to change these properties (Chorover et al., 1994; Johnson et al., 2005). Our findings suggest pH change is short lived at high elevation and possibly longer lasting at low elevation (Fig. 1.7). EC may reveal a similar trend at low elevation. While only significant at low elevation (5-TSW), the trend of higher MAOM-N post-fire may be attributed to charred organic matter, which can lead to the formation of heterocyclic aromatic nitrogen compounds (Knicker, 2007; López-Martín et al., 2018). These compounds are considered recalcitrant compared to other nitrogen forms, effectively removing nitrogen from internal cycling processes (Bingham & Cotrufo, 2016). Our findings of elevated MAOM-N in recently burned sites align with Burgeon et al. (2021), who found pyrogenic organic matter can become sorbed onto mineral surfaces. Furthermore, López-Martín et al. (2018) reported a decrease in heterocyclic aromatic nitrogen after seven years of post-fire recovery, consistent with the decrease in MAOM-N we observed between the 10-TSW treatment and the control. We did not directly measure charcoal; it was visually identified at the burned field sites. Wildfire has been found to reduce C:N ratios immediately after fire, which then increase with recovery time (Baird et al., 1999; Hatten et al., 2005; Kong et al., 2022). This is consistent with our findings at high elevation sites, where C:N and MAOM-C:N ratios were both lower at 5-TSW compared to the control, but increased to control levels within one decade.

1.3.4. Changes in Physical Soil Health Indicators

1.3.4.1. Overall recovery trends over time since wildfire

Soil physical properties differed between elevation classes ($p < 0.001$) and the interaction of TSW and elevation class ($p < 0.05$), where the soil physical state in each TSW group depended on elevation (Table 1.5). There was evidence of a strong multivariate relationship of physical properties with the main and interaction effects, where ~50% of the variation in the data was unexplained by this model.

Table 1.5. Permutational Analysis of Variance (PERMANOVA) by the Bray-Curtis dissimilarity method showing the main effects of TSW and elevation class, and the interaction of TSW*elevation class on soil physical properties: aggregate stability, bulk density, and rock fragment volume. The table includes degrees of freedom (df), coefficient of determination (R^2), test statistic (Pseudo-F), and significance level (p-value).

Model Term	df	R^2	Pseudo-F	p-value
TSW	2	0.02634	0.8381	0.4393
Elevation Class	1	0.35552	22.6260	**0.0001 *****
TSW x Elev. Class	2	0.11533	3.6700	**0.0326 ***
Residual	32	0.50281		
Total	37	1.00000		

The table includes degrees of freedom (df), coefficient of determination (R^2), test statistic (Pseudo-F), and significance level (p-value).

1.3.4.2. Physical soil health indicators sensitive to change post-wildfire

The ANOVA results of mixed effects models in Table 1.6 indicate that aggregate stability, bulk density, and rock fragment volume were significantly different between elevation classes in both sampling depths (aggregate stability only significant in the soil surface). However, bulk density was the only physical property that changed significantly with time since wildfire. Recovery trends for bulk density varied depending on elevation class, where the control group trends toward lower values than the 10- and 5-TSW groups at high elevation, and trends toward higher values than the 10- and 5-TSW sites at low elevation. Literature suggests that there is a great deal of variation in post-burn aggregate stability and bulk density among studies. The response of bulk density to wildfire remains inconclusive, with some studies reporting increases (Mataix-Solera et al., 2011; Agbeshie et al., 2022) while others document decreases after fire (Agbeshie et al., 2022). Elevated aggregate stability was observed with increasing water repellency in some instances, where the waxy residues from volatilized compounds were shown to hold aggregates together (Mataix-Solera et al., 2011).

Table 1.6. ANOVA of mixed effects models for soil health indicators at 0-5 and 5-15 cm.

Response Variable	Model Term	0-5 cm			5-15 cm		
		df	Test Statistic	p-value	df	Test Statistic	p-value
Aggregate Stability	TSW	2	0.751	0.492	2	3.57	0.0582
	Elev. Class	1	5.28	**0.0390 ***	1	4.45	0.0549
	(TSW x Elev. Class)	2	2.70	0.105	2	0.953	0.411
Bulk Density	TSW	2	3.19	0.203	2	4.60	**0.0375***
	Elev. Class	1	8.48	**0.00359 ****	1	15.4	**0.00146 ****
	(TSW x Elev. Class)	2	8.28	**0.0159 ***	2	6.30	**0.0165 ***
Rock Fragment Volume	TSW	2	1.38	0.288	2	1.38	0.297
	Elev. Class	1	9.26	**0.00975 ****	1	4.99	**0.0434 ***
	(TSW x Elev. Class)	2	3.00	0.0873	2	2.17	0.165

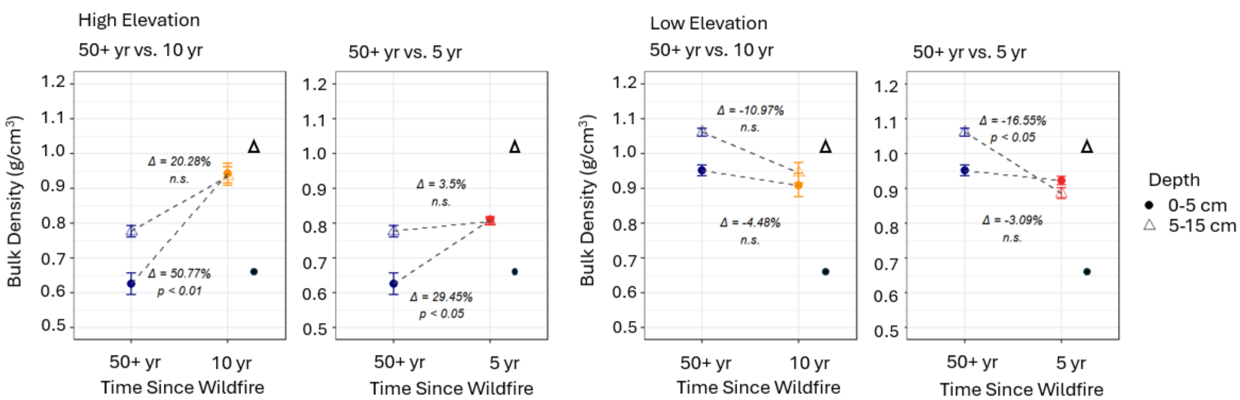

Figure 1.8. Comparison of physical soil health indicators sensitive to change between the 50+ year (control) and 10- or 5- year since burn treatments at high and low elevations. Points on the plot are mean values, whiskers show standard error, and dashed lines with Δ indicate the percent-difference between means. The filled circle and clear triangle on the plot indicate the sampling depth of each percent-difference and significance value.

The ANOVA of mixed effects models detected significance over time since wildfire for bulk density, where both surface and subsurface soils differ between TSW groups across elevation classes (Table 1.6; Fig. 1.8). At high elevation sites, surface bulk density was 50.77% higher at 10-TSW sites (mean = 0.943 g/cm^3; p = 0.00254) than the control (mean = 0.625

g/cm^3). Similarly, surface bulk density at 5-TSW sites was 29.45% higher (mean = 0.810 g/cm^3; p = 0.0202) than the control (mean = 0.625 g/cm^3). Subsurface bulk density was not significantly different. At low elevation, a significant reduction in bulk density was observed for 5-TSW by 16.55% (mean = 0.886 g/cm^3; p = 0.0133) compared to the control (mean = 1.061 g/cm^3) (Fig. 1.8). Results indicate that bulk density and its recovery trajectories differ markedly between high and low elevation. At high elevation, recent burn sites exhibited significantly higher bulk densities compared to the control. This may be the result of reduced porosity as organic matter combusts and ash fills void space, which collapses soil structure and increases compaction (Certini, 2005; Verma & Jayakumar, 2012; Agbeshie et al., 2022). Similar trends in bulk density were detected by Mataix-Solera et al. (2011), Xue et al. (2014), Wieting et al. (2017), and Kooch et al. (2024), where wildfire caused immediate and significant increases in bulk density.

Consistent with patterns observed for other soil properties in this study, bulk density appears to change more rapidly at low elevation sites. After one decade of post-wildfire recovery, bulk density was statistically indistinguishable from the control. In contrast, 10-TSW and 5-TSW sites at high elevation sites are statistically different from the control, indicating slower recovery at high elevations (Fig. 1.8). Chief et al. (2012) also detected lower bulk density in the aftermath of fire and suggested that this decrease may be attributed to fire-induced soil vapor expansion, allowing for an ephemeral increase in porosity.

1.4. Conclusion

Recovery trends in the decades following catastrophic wildfire differed by elevation, where high elevation sites appear to exhibit faster overall recovery than low elevation. After 10 years of post-wildfire recovery, high elevation burn sites more closely resembled the control than the 5-TSW treatment. In contrast, low elevation sites remained more chemically and physically similar to the 5-TSW treatment, suggesting slower recovery. Soil microbial community composition underwent structural changes in the aftermath of catastrophic wildfire, reflected by changes in Shannon diversity, beta diversity, and PLFA structural ratios over time since wildfire. Although many dynamic soil properties did not show change in response to wildfire or recovery time, several indicators were identified as sensitive to change. These included O horizon thickness, water repellency, predator:prey ratio, GP:GN ratio, sat:unsat PLFA ratio, Shannon diversity, pH, EC, MAOM-N, C:N ratio, MAOM-C:N ratio, and bulk density.

Overall, findings support our hypotheses that soil health recovery depends on time since burn and environmental factors such as elevation. However, this study was constrained by the absence of direct pre- and post-fire measurements and lack of data on fire severity. Landscapes are heterogenous, with varying topography, and microclimate, which creates inconsistency in the severity and intensity of wildfire. This presents the challenge of accurately and consistently predicting how wildfire impacts soil health. Future research should assess soil health across a broader range of environmental conditions and fire severities to improve our understanding of soil health recovery after catastrophic wildfire.

References

Abatzoglou, J. T., & Williams, A. P. (2016). Impact of anthropogenic climate change on wildfire across western US forests. *Proceedings of the National Academy of Sciences*, *113*(42), 11770–11775. https://doi.org/10.1073/pnas.1607171113

Adkins, J., Docherty, K. M., Gutknecht, J. L. M., & Miesel, J. R. (2020). How do soil microbial communities respond to fire in the intermediate term? Investigating direct and indirect effects associated with fire occurrence and burn severity. *Science of The Total Environment*, *745*, 140957. https://doi.org/10.1016/j.scitotenv.2020.140957

Agbeshie, A. A., Abugre, S., Atta-Darkwa, T., & Awuah, R. (2022). A review of the effects of forest fire on soil properties. *Journal of Forestry Research*, *33*(5), 1419–1441. https://doi.org/10.1007/s11676-022-01475-4

Bachmann, J., Horton, R., Van Der Ploeg, R. R., & Woche, S. (2000). Modified sessile drop method for assessing initial soil–water contact angle of sandy soil. *Soil Science Society of America Journal*, *64*(2), 564–567. https://doi.org/10.2136/sssaj2000.642564x

Baird, M., Zabowski, D., & Everett, R. L. (1999). Wildfire effects on carbon and nitrogen in inland coniferous forests. *Plant and Soil*, *209*(2), 233–243. https://doi.org/10.1023/A:1004602408717

Bárcenas-Moreno, G., & Bååth, E. (2009). Bacterial and fungal growth in soil heated at different temperatures to simulate a range of fire intensities. *Soil Biology and Biochemistry*, *41*(12), 2517–2526. https://doi.org/10.1016/j.soilbio.2009.09.010

Bárcenas-Moreno, G., García-Orenes, F., Mataix-Solera, J., Mataix-Beneyto, J., & Bååth, E. (2011). Soil microbial recolonisation after a fire in a Mediterranean forest. *Biology and Fertility of Soils*, *47*(3), 261–272. https://doi.org/10.1007/s00374-010-0532-2

Beaty, R. M., & Taylor, A. H. (2008). Fire history and the structure and dynamics of a mixed conifer forest landscape in the northern Sierra Nevada, Lake Tahoe Basin, California, USA. *Forest Ecology and Management*, *255*(3–4), 707–719. https://doi.org/10.1016/j.foreco.2007.09.044

Bestelmeyer, B. T., Ellison, A. M., Fraser, W. R., Gorman, K. B., Holbrook, S. J., Laney, C. M., Ohman, M. D., Peters, D. P. C., Pillsbury, F. C., Rassweiler, A., Schmitt, R. J., & Sharma, S. (2011). Analysis of abrupt transitions in ecological systems. *Ecosphere*, *2*(12), art129. https://doi.org/10.1890/ES11-00216.1

Bestelmeyer, B. T., Tugel, A. J., Peacock, G. L., Robinett, D. G., Shaver, P. L., Brown, J. R., Herrick, J. E., Sanchez, H., & Havstad, K. M. (2009). State-and-transition models for heterogeneous landscapes: A strategy for development and application. *Rangeland Ecology & Management*, *62*(1), 1–15. https://doi.org/10.2111/08-146

Bhaduri, D., Sihi, D., Bhowmik, A., Verma, B. C., Munda, S., & Dari, B. (2022). A review on effective soil health bio-indicators for ecosystem restoration and sustainability. *Frontiers in Microbiology*, *13*, 938481. https://doi.org/10.3389/fmicb.2022.938481

Bilyera, N., Hummel, C., Daudin, G., Santangeli, M., Zhang, X., Santner, J., Lippold, E., Schlüter, S., Bertrand, I., Wenzel, W., Spielvogel, S., Vetterlein, D., Razavi, B. S., & Oburger, E. (2022). Co-localised phosphorus mobilization processes in the rhizosphere of field-grown maize jointly contribute to plant nutrition. *Soil Biology and Biochemistry*, *165*, 108497. https://doi.org/10.1016/j.soilbio.2021.108497

Bingham, A. H., & Cotrufo, M. F. (2016). Organic nitrogen storage in mineral soil: Implications for policy and management. *Science of The Total Environment*, *551–552*, 116–126. https://doi.org/10.1016/j.scitotenv.2016.02.020

Burgeon, V., Fouché, J., Leifeld, J., Chenu, C., & Cornélis, J.-T. (2021). Organo-mineral associations largely contribute to the stabilization of century-old pyrogenic organic matter in cropland soils. *Geoderma*, *388*, 114841. https://doi.org/10.1016/j.geoderma.2020.114841

Burger, J. A., Gray, G., & Scott, D. A. (2010). Using soil quality indicators for monitoring sustainable forest management. *In: Page-Dumroese, Deborah; Neary, Daniel; Trettin, Carl, Tech. Eds. Scientific Background for Soil Monitoring on National Forests and Rangelands: Workshop Proceedings; April 29-30, 2008; Denver, CO. Proc. RMRS-P-59. Fort Collins, CO: U.S. Department of Agriculture, Forest Service, Rocky Mountain Research Station. p. 13-42.*, *59*, 13–42. https://research.fs.usda.gov/treesearch/35615

Butenko, K. O., Gongalsky, K. B., Korobushkin, D. I., Ekschmitt, K., & Zaitsev, A. S. (2017). Forest fires alter the trophic structure of soil nematode communities. *Soil Biology and Biochemistry*, *109*, 107–117. https://doi.org/10.1016/j.soilbio.2017.02.006

Butler, O. M., Elser, J. J., Lewis, T., Mackey, B., & Chen, C. (2018). The phosphorus-rich signature of fire in the soil–plant system: A global meta-analysis. *Ecology Letters*, *21*(3), 335–344. https://doi.org/10.1111/ele.12896

Buyer, J. S., & Sasser, M. (2012). High throughput phospholipid fatty acid analysis of soils. *Applied Soil Ecology*, *61*, 127–130. https://doi.org/10.1016/j.apsoil.2012.06.005

Caldwell, T. G., Johnson, D. W., Miller, W. W., & Qualls, R. G. (2002). Forest floor carbon and nitrogen losses due to prescription fire. *Soil Science Society of America Journal*, *66*(1), 262–267. https://doi.org/10.2136/sssaj2002.2620

California Department of Forestry and Fire Protection. (n.d.). https://www.fire.ca.gov/

California Native Plant Society. (n.d.). Calscape. https://calscape.org/

Certini, G. (2005). Effects of fire on properties of forest soils: A review. *Oecologia*, *143*(1), 1–10. https://doi.org/10.1007/s00442-004-1788-8

Chen, B., Yang, Y., Chen, L., Jiang, L., Hong, Y., Zhu, J., Liu, J., Xu, D., Kuang, K., & He, Z. (2023). Microclimate along an elevational gradient controls foliar litter cellulose and lignin degradation in a subtropical forest. *Frontiers in Forests and Global Change*, *6*, 1134598. https://doi.org/10.3389/ffgc.2023.1134598

Cheng, Z., Wu, S., Pan, H., Lu, X., Liu, Y., & Yang, L. (2024). Effect of forest fires on the alpha and beta diversity of soil bacteria in taiga forests: Proliferation of rare species as successional pioneers. *Forests*, *15*(4), 606. https://doi.org/10.3390/f15040606

Chief, K., Young, M. H., & Shafer, D. S. (2012). Changes in soil structure and hydraulic properties in a wooded-shrubland ecosystem following a prescribed fire. *Soil Science Society of America Journal*, *76*(6), 1965–1977. https://doi.org/10.2136/sssaj2011.0072

Chorover, J., Vitousek, P. M., Everson, D. A., Esperanza, A. M., & Turner, D. (1994). Solution chemistry profiles of mixed-conifer forests before and after fire. *Biogeochemistry*, *26*(2), 115–144. https://doi.org/10.1007/BF02182882

Collins, B. M., Kelly, M., Van Wagtendonk, J. W., & Stephens, S. L. (2007). Spatial patterns of large natural fires in Sierra Nevada wilderness areas. *Landscape Ecology*, *22*(4), 545–557. https://doi.org/10.1007/s10980-006-9047-5

Corwin, D. L., & Yemoto, K. (2020). Salinity: Electrical conductivity and total dissolved solids. *Soil Science Society of America Journal*, *84*(5), 1442–1461. https://doi.org/10.1002/saj2.20154

Cotrufo, M. F., Ranalli, M. G., Haddix, M. L., Six, J., & Lugato, E. (2019). Soil carbon storage informed by particulate and mineral-associated organic matter. *Nature Geoscience*, *12*(12), 989–994. https://doi.org/10.1038/s41561-019-0484-6

De Andrade Bonetti, J., Anghinoni, I., De Moraes, M. T., & Fink, J. R. (2017). Resilience of soils with different texture, mineralogy and organic matter under long-term conservation systems. *Soil and Tillage Research*, *174*, 104–112. https://doi.org/10.1016/j.still.2017.06.008

Dhungana, B. P., Chhetri, V. T., Baniya, C. B., Sharma, S. P., Ghimire, P., & Vista, S. P. (2024). Post-fire effects on soil properties in high altitude mixed-conifer forest of nepal. *Trees, Forests and People*, *17*, 100633. https://doi.org/10.1016/j.tfp.2024.100633

Doerr, S. H. (1998). On standardizing the ‘Water Drop Penetration Time’ and the ‘Molarity of an Ethanol Droplet’ techniques to classify soil hydrophobicity: A case study using medium textured soils. *Earth Surface Processes and Landforms*, *23*(7), 663–668. https://doi.org/10.1002/(SICI)1096-9837(199807)23:7<663::AID-ESP909>3.0.CO;2-6

Duncan, B. W., Schmalzer, P. A., Breininger, D. R., & Stolen, E. D. (2015). Comparing fuels reduction and patch mosaic fire regimes for reducing fire spread potential: A spatial modeling approach. *Ecological Modelling*, *314*, 90–99. https://doi.org/10.1016/j.ecolmodel.2015.07.013

Eckert, D. & Sims, J. T. “Recommended Soil pH and Lime Requirement Tests,” In: J. T. Sims and A. Wolfe, Eds., Recommended Soil Testing Procedures for the Northeastern United States.

Northeast Regional Bulletin 493, Agricultural Experiment Station, University of Delaware, Newark, pp. 11-16

Eilers, K. G., Debenport, S., Anderson, S., & Fierer, N. (2012). Digging deeper to find unique microbial communities: The strong effect of depth on the structure of bacterial and archaeal communities in soil. *Soil Biology and Biochemistry*, *50*, 58–65. https://doi.org/10.1016/j.soilbio.2012.03.011

Fang, L., Yang, J., Zu, J., Li, G., & Zhang, J. (2015). Quantifying influences and relative importance of fire weather, topography, and vegetation on fire size and fire severity in a Chinese boreal forest landscape. *Forest Ecology and Management*, *356*, 2–12. https://doi.org/10.1016/j.foreco.2015.01.011

Fanin, N., Kardol, P., Farrell, M., Nilsson, M.-C., Gundale, M. J., & Wardle, D. A. (2019). The ratio of Gram-positive to Gram-negative bacterial PLFA markers as an indicator of carbon availability in organic soils. *Soil Biology and Biochemistry*, *128*, 111–114. https://doi.org/10.1016/j.soilbio.2018.10.010

Fierer, N., Schimel, J. P., & Holden, P. A. (2003). Variations in microbial community composition through two soil depth profiles. *Soil Biology and Biochemistry*, *35*(1), 167–176. https://doi.org/10.1016/S0038-0717(02)00251-1

Fontúrbel, M. T., Barreiro, A., Vega, J. A., Martín, A., Jiménez, E., Carballas, T., Fernández, C., & Díaz-Raviña, M. (2012). Effects of an experimental fire and post-fire stabilization treatments on soil microbial communities. *Geoderma*, *191*, 51–60. https://doi.org/10.1016/j.geoderma.2012.01.037

Francis, I., Holsters, M., & Vereecke, D. (2010). The Gram-positive side of plant–microbe interactions. *Environmental Microbiology*, *12*(1), 1–12. https://doi.org/10.1111/j.1462-2920.2009.01989.x

Francis, J. R., Wuddivira, M. N., & Farrick, K. K. (2023). Reforesting degraded hillslopes with exotic pines in Trinidad and Tobago: Infiltration, repellency and implications for runoff and recharge. *Journal of Hydrology*, *622*, 129650. https://doi.org/10.1016/j.jhydrol.2023.129650

González-Cabán, A. (2007). *Wildland Fire Management Policy and Fire Management Economic Efficiency in the USDA Forest Service*. IV International Wildland Fire Conference, Seville, Spain. https://www.researchgate.net/profile/Armando-Gonzalez-Caban/publication/228846487_Wildland_Fire_Management_Policy_and_Fire_Management_Economic_Efficiency_in_the_USDA_Forest_Service/links/0c9605203c53439190000000/Wildland-Fire-Management-Policy-and-Fire-Management-Economic-Efficiency-in-the-USDA-Forest-Service.pdf

Hamman, S. T., Burke, I. C., & Stromberger, M. E. (2007). Relationships between microbial community structure and soil environmental conditions in a recently burned system. *Soil Biology and Biochemistry*, *39*(7), 1703–1711. https://doi.org/10.1016/j.soilbio.2007.01.018

Hart, S. C., DeLuca, T. H., Newman, G. S., MacKenzie, M. D., & Boyle, S. I. (2005). Post-fire vegetative dynamics as drivers of microbial community structure and function in forest soils. *Forest Ecology and Management*, *220*(1–3), 166–184. https://doi.org/10.1016/j.foreco.2005.08.012

Hatten, J., Zabowski, D., Scherer, G., & Dolan, E. (2005). A comparison of soil properties after contemporary wildfire and fire suppression. *Forest Ecology and Management*, *220*(1–3), 227–241. https://doi.org/10.1016/j.foreco.2005.08.014

He, J., Tan, X., Nie, Y., Ma, L., Zhou, W., & Shen, W. (2023). Enhancement of saturated fatty acid content in soil microbial membranes across natural and experimental warming gradients. *Soil Biology and Biochemistry*, *176*, 108866. https://doi.org/10.1016/j.soilbio.2022.108866

Herrick, J. E., Whitford, W. G., De Soyza, A. G., Van Zee, J. W., Havstad, K. M., Seybold, C. A., & Walton, M. (2001). Field soil aggregate stability kit for soil quality and rangeland health evaluations. *CATENA*, *44*(1), 27–35. https://doi.org/10.1016/S0341-8162(00)00173-9

Hill, M. (2006). 6. Great is granite. In *Geology of the Sierra Nevada* (pp. 177–210). University of California Press. https://www.degruyterbrill.com/document/doi/10.1525/9780520936942-009/html

Holden, S. R., Rogers, B. M., Treseder, K. K., & Randerson, J. T. (2016). Fire severity influences the response of soil microbes to a boreal forest fire. *Environmental Research Letters*, *11*(3), 035004. https://doi.org/10.1088/1748-9326/11/3/035004

Hopkins, J. R., Bennett, A. E., & McKenna, T. P. (2025). Fire frequency driven increases in burn heterogeneity promote microbial beta diversity: A test of the pyrodiversity-biodiversity hypothesis. *Molecular Ecology*, *34*(10), e17756. https://doi.org/10.1111/mec.17756

Hu, G., Huo, C., Hu, C., Zhong, C., Chen, S., Xu, C., & Zhang, Z. (2025). Elevational patterns of hydrological properties of forest litter layers in Daming Mountain, southern China. *Global Ecology and Conservation*, *58*, e03510. https://doi.org/10.1016/j.gecco.2025.e03510

Hu, M., Feng, J., Shi, Y., Shao, P., Chen, Z., Zhou, Z., & Wang, J. (2025). Plant above-ground biomass drives the recovery of soil microbial communities in a subtropical-temperate transition zone following forest wildfire. *Applied Soil Ecology*, *209*, 106057. https://doi.org/10.1016/j.apsoil.2025.106057

Imeson, A. C., Verstraten, J. M., Van Mulligen, E. J., & Sevink, J. (1992). The effects of fire and water repellency on infiltration and runoff under Mediterranean type forest. *CATENA*, *19*(3–4), 345–361. https://doi.org/10.1016/0341-8162(92)90008-Y

Intrusive, uplift and erosional history of the northern sierra nevada batholith | structural geology and tectonics. (n.d.). Retrieved July 9, 2025, from https://tectonics.stanford.edu/intrusive-uplift-and-erosional-history-northern-sierra-nevada-batholith

Jackson, R. B., Lajtha, K., Crow, S. E., Hugelius, G., Kramer, M. G., & Piñeiro, G. (2017). The ecology of soil carbon: Pools, vulnerabilities, and biotic and abiotic controls. *Annual Review of Ecology, Evolution, and Systematics*, *48*(1), 419–445. https://doi.org/10.1146/annurev-ecolsys-112414-054234

Johnson, C. K., Doran, J. W., Duke, H. R., Wienhold, B. J., Eskridge, K. M., & Shanahan, J. F. (2001). Field-scale electrical conductivity mapping for delineating soil condition. *Soil Science Society of America Journal*, *65*(6), 1829–1837. https://doi.org/10.2136/sssaj2001.1829

Johnson, D. W., Glass, D. W., Murphy, J. D., Stein, C. M., & Miller, W. W. (2010). Nutrient hot spots in some sierra Nevada forest soils. *Biogeochemistry*, *101*(1–3), 93–103. https://doi.org/10.1007/s10533-010-9423-8

Johnson, D. W., Murphy, J. F., Susfalk, R. B., Caldwell, T. G., Miller, W. W., Walker, R. F., & Powers, R. F. (2005). The effects of wildfire, salvage logging, and post-fire N-fixation on the nutrient budgets of a Sierran forest. *Forest Ecology and Management*, *220*(1–3), 155–165. https://doi.org/10.1016/j.foreco.2005.08.011

Knicker, H. (2007). How does fire affect the nature and stability of soil organic nitrogen and carbon? A review. *Biogeochemistry*, *85*(1), 91–118. https://doi.org/10.1007/s10533-007-9104-4

Kong, J., Yang, J., & Bai, E. (2018). Long-term effects of wildfire on available soil nutrient composition and stoichiometry in a Chinese boreal forest. *Science of The Total Environment*, *642*, 1353–1361. https://doi.org/10.1016/j.scitotenv.2018.06.154

Kong, J., Yang, J., & Cai, W. (2019). Topography controls post-fire changes in soil properties in a Chinese boreal forest. *Science of The Total Environment*, *651*, 2662–2670. https://doi.org/10.1016/j.scitotenv.2018.10.164

Kong, J., Xiang, X., & Yang, J. (2022). Wildfire alters the linkage between total and available soil C:N:P ratios and the stoichiometric effects on fine root growth in a Chinese boreal larch forest. *Plant and Soil*, *471*(1–2), 211–225. https://doi.org/10.1007/s11104-021-05215-1

Kooch, Y., Nouraei, A., Wu, D., Francaviglia, R., & Frouz, J. (2024). The effect of fire disturbance on the dynamics of soil physical, chemical, and biological properties over time in a semi-arid region. *Applied Soil Ecology*, *202*, 105568. https://doi.org/10.1016/j.apsoil.2024.105568

Kuzyakov, Y., Subbotina, I., Chen, H., Bogomolova, I., & Xu, X. (2009). Black carbon decomposition and incorporation into soil microbial biomass estimated by 14C labeling. *Soil Biology and Biochemistry*, *41*(2), 210–219. https://doi.org/10.1016/j.soilbio.2008.10.016

Leelamanie, D. A. L., Karube, J., & Yoshida, A. (2008). Characterizing water repellency indices: Contact angle and water drop penetration time of hydrophobized sand. *Soil Science and Plant Nutrition*, *54*(2), 179–187. https://doi.org/10.1111/j.1747-0765.2007.00232.x

Leighton-Boyce, G., Doerr, S. H., Shakesby, R. A., & Walsh, R. P. D. (2007). Quantifying the impact of soil water repellency on overland flow generation and erosion: A new approach using rainfall simulation and wetting agent on *in situ* soil. *Hydrological Processes*, *21*(17), 2337–2345. https://doi.org/10.1002/hyp.6744

López-Martín, M., González-Vila, F. J., & Knicker, H. (2018). Distribution of black carbon and black nitrogen in physical soil fractions from soils seven years after an intense forest fire and their role as C sink. *Science of The Total Environment*, *637–638*, 1187–1196. https://doi.org/10.1016/j.scitotenv.2018.05.084

MacKenzie, M. D., DeLuca, T. H., & Sala, A. (2004). Forest structure and organic horizon analysis along a fire chronosequence in the low elevation forests of western Montana. *Forest Ecology and Management*, *203*(1–3), 331–343. https://doi.org/10.1016/j.foreco.2004.08.003

Mai-Prochnow, A., Clauson, M., Hong, J., & Murphy, A. B. (2016). Gram positive and Gram negative bacteria differ in their sensitivity to cold plasma. *Scientific Reports*, *6*(1), 38610. https://doi.org/10.1038/srep38610

Mansoor, S., Farooq, I., Kachroo, M. M., Mahmoud, A. E. D., Fawzy, M., Popescu, S. M., Alyemeni, M. N., Sonne, C., Rinklebe, J., & Ahmad, P. (2022). Elevation in wildfire frequencies with respect to the climate change. *Journal of Environmental Management*, *301*, 113769. https://doi.org/10.1016/j.jenvman.2021.113769

Martin, T., & Sprunger, C. D. (2022). Soil food web structure and function in annual row-crop systems: How can nematode communities infer soil health? *Applied Soil Ecology*, *178*, 104553. https://doi.org/10.1016/j.apsoil.2022.104553

Mataix-Solera, J., Cerdà, A., Arcenegui, V., Jordán, A., & Zavala, L. M. (2011). Fire effects on soil aggregation: A review. *Earth-Science Reviews*, *109*(1–2), 44–60. https://doi.org/10.1016/j.earscirev.2011.08.002

McCool, K. D., Holub, S. M., Gao, S., Morrissette, B. A., Blunn, J. E., Gallo, A. C., & Hatten, J. A. (2023). Quantifying impacts of forest fire on soil carbon in a young, intensively managed tree farm in the western Oregon Cascades. *Soil Science Society of America Journal*, *87*(6), 1458–1473. https://doi.org/10.1002/saj2.20582

McKelvey, K. S., Skinner, C. N., Chang, C., Erman, D. C., Husari, S. J., Parsons, D. J., Wagtendonk, J. W. van, & Weatherspoon, C. P. (1996). An overview of fire in the Sierra Nevada. *Pages 1033-1040 in: Sierra Nevada Ecosystem Project, Final Report to Congress, Vol. II, Assessments and Scientific Basis for Management Options. Davis, CA: University of California, Centers for Water and Wildland Resources. Report No. 37.* https://research.fs.usda.gov/treesearch/3539

Miller, C., & Urban, D. L. (1999). A model of surface fire, climate and forest pattern in the Sierra Nevada, California. *Ecological Modelling*, *114*(2–3), 113–135. https://doi.org/10.1016/S0304-3800(98)00119-7

Miller, R. O., & Kissel, D. E. (2010). Comparison of soil ph methods on soils of north america. *Soil Science Society of America Journal*, *74*(1), 310–316. https://doi.org/10.2136/sssaj2008.0047

Murphy, J. D., Johnson, D. W., Miller, W. W., Walker, R. F., Carroll, E. F., & Blank, R. R. (2006). Wildfire effects on soil nutrients and leaching in a tahoe basin watershed. *Journal of Environmental Quality*, *35*(2), 479–489. https://doi.org/10.2134/jeq2005.0144

Nave, L. E., DeLyser, K., Domke, G. M., Holub, S. M., Janowiak, M. K., Kittler, B., Ontl, T. A., Sprague, E., Sucre, E. B., Walters, B. F., & Swanston, C. W. (2022). Disturbance and management effects on forest soil organic carbon stocks in the Pacific Northwest. *Ecological Applications*, *32*(6), e2611. https://doi.org/10.1002/eap.2611

Nave, L. E., Vance, E. D., Swanston, C. W., & Curtis, P. S. (2011). Fire effects on temperate forest soil C and N storage. *Ecological Applications*, *21*(4), 1189–1201. https://doi.org/10.1890/10-0660.1

Nelson, A. R., Narrowe, A. B., Rhoades, C. C., Fegel, T. S., Daly, R. A., Roth, H. K., Chu, R. K., Amundson, K. K., Young, R. B., Steindorff, A. S., Mondo, S. J., Grigoriev, I. V., Salamov, A., Borch, T., & Wilkins, M. J. (2022). Wildfire-dependent changes in soil microbiome diversity and function. *Nature Microbiology*, *7*(9), 1419–1430. https://doi.org/10.1038/s41564-022-01203-y

Nocentini, C., Certini, G., Knicker, H., Francioso, O., & Rumpel, C. (2010). Nature and reactivity of charcoal produced and added to soil during wildfire are particle-size dependent. *Organic Geochemistry*, *41*(7), 682–689. https://doi.org/10.1016/j.orggeochem.2010.03.010

Norris, C. E., Swallow, M. J. B., Liptzin, D., Cope, M., Bean, G. M., Cappellazzi, S. B., Greub, K. L. H., Rieke, E. L., Tracy, P. W., Morgan, C. L. S., & Honeycutt, C. W. (2023). Use of phospholipid fatty acid analysis as phenotypic biomarkers for soil health and the influence of management practices. *Applied Soil Ecology*, *185*, 104793. https://doi.org/10.1016/j.apsoil.2022.104793

Ogwayo, E. (2023). Ecological succession in post-fire forests. *European Journal of Natural Sciences*, *1*(1), 13–24. https://forthworthjournals.org/journals/index.php/EJNS/article/view/87

Porter, T. M., Smenderovac, E., Morris, D., & Venier, L. (2023). All boreal forest successional stages needed to maintain the full suite of soil biodiversity, community composition, and function following wildfire. *Scientific Reports*, *13*(1), 7978. https://doi.org/10.1038/s41598-023-30732-7

Povak, N. A., Hessburg, P. F., & Salter, R. B. (2018). Evidence for scale-dependent topographic controls on wildfire spread. *Ecosphere*, *9*(10), e02443. https://doi.org/10.1002/ecs2.2443

Prendergast-Miller, M. T., De Menezes, A. B., Macdonald, L. M., Toscas, P., Bissett, A., Baker, G., Farrell, M., Richardson, A. E., Wark, T., & Thrall, P. H. (2017). Wildfire impact: Natural experiment reveals differential short-term changes in soil microbial communities. *Soil Biology and Biochemistry*, *109*, 1–13. https://doi.org/10.1016/j.soilbio.2017.01.027

Quist, C. W., Van Der Putten, W. H., & Thakur, M. P. (2020). Soil predator loss alters aboveground stoichiometry in a native but not in a related range-expanding plant when exposed to periodic heat waves. *Soil Biology and Biochemistry*, *150*, 107999. https://doi.org/10.1016/j.soilbio.2020.107999

Reiner, A. L., Ewell, C., Greenburg, J., Hancock, S., Hou, Z., Wade, L. (2018). 2018 Ferguson Fire, Sierra National Forest: Fire Behavior Assessment Team (FBAT) Report. USDA Forest Service Fire Behavior Assessment Team. 8 p.

Rhoades, J. D. (2018). Salinity: Electrical conductivity and total dissolved solids. In D. L. Sparks, A. L. Page, P. A. Helmke, R. H. Loeppert, P. N. Soltanpour, M. A. Tabatabai, C. T. Johnston, & M. E. Sumner (Eds.), *SSSA Book Series* (pp. 417–435). Soil Science Society of America, American Society of Agronomy. https://doi.org/10.2136/sssabookser5.3.c14

Rodríguez, J., González-Pérez, J. A., Turmero, A., Hernández, M., Ball, A. S., González-Vila, F. J., & Enriqueta Arias, M. (2017). Wildfire effects on the microbial activity and diversity in a Mediterranean forest soil. *CATENA*, *158*, 82–88. https://doi.org/10.1016/j.catena.2017.06.018

Sáenz De Miera, L. E., Pinto, R., Gutierrez-Gonzalez, J. J., Calvo, L., & Ansola, G. (2020). Wildfire effects on diversity and composition in soil bacterial communities. *Science of The Total Environment*, *726*, 138636. https://doi.org/10.1016/j.scitotenv.2020.138636

Savage, S. M. (1974). Mechanism of fire-induced water repellency in soil. *Soil Science Society of America Journal*, *38*(4), 652–657. https://doi.org/10.2136/sssaj1974.03615995003800040033x

Schoeneberger, P.J., Wysocki, D.A., Benham, E.C., & Soil Survey Staff. (2012). *Field book for describing and sampling soils, Version 3.0.* U.S. Department of Agriculture, Natural Resources Conservation Service

Seidl, R., & Turner, M. G. (2022). Post-disturbance reorganization of forest ecosystems in a changing world. *Proceedings of the National Academy of Sciences*, *119*(28), e2202190119. https://doi.org/10.1073/pnas.2202190119

Seiwa, K., Kunii, D., Masaka, K., Hayashi, S., & Tada, C. (2021). Hardwood mixture enhances soil water infiltration in a conifer plantation. *Forest Ecology and Management*, *498*, 119508. https://doi.org/10.1016/j.foreco.2021.119508

Sheldrick, B. H. & Wang, C. (1993). Particle-size Distribution. In: Carter, M. R. (Ed), *Soil Sampling and Methods of Analysis*, 499-511. Canadian Society of Soil Science, Lewis Publishers

Sims, J.T. (2000) Soil Test Phosphorus: Olsen P. In: Pierzynski, G.M., Ed., Methods for Phosphorus Analysis for Soils, Sediments, Residuals and Water, Kansas State University, Manhttan, 20-21

Slakes: A free smartphone app to measure aggregate stability. (2023, December 1). https://soilhealthinstitute.org/our-work/initiatives/slakes/

Slessarev, E. W., Lin, Y., Jiménez, B. Y., Homyak, P. M., Chadwick, O. A., D'Antonio, C. M., & Schimel, J. P. (2020). Cellular and extracellular C contributions to respiration after wetting dry soil. *Biogeochemistry*, *147*(3), 307–324. https://doi.org/10.1007/s10533-020-00645-y

Smith, J.L., and J.W. Doran. 1996. Measurement and Use of pH and Electrical Conductivity for Soil Quality Analysis. In: Methods for Assessing Soil Quality. Soil Science Society of America Special Publication 49. Madison WI. p. 169-185.

Smith, N. R., Kishchuk, B. E., & Mohn, W. W. (2008). Effects of wildfire and harvest disturbances on forest soil bacterial communities. *Applied and Environmental Microbiology*, *74*(1), 216–224. https://doi.org/10.1128/AEM.01355-07

Soil properties | california soil resource lab. (n.d.). Retrieved July 20, 2025, from https://casoilresource.lawr.ucdavis.edu/soil-properties/

Soil Survey Staff (1996) Soil Survey Laboratory Method Manuals. Soil Survey Investigation Reports No. 4. Version 3.

Soil Survey Staff. (2012). Field book for describing and sampling soils, version 3.0. USDA, Natural Resources Conservation Service. U.S. Government Printing Office.

Soong, J. L., & Cotrufo, M. F. (2015). Annual burning of a tallgrass prairie inhibits C and N cycling in soil, increasing recalcitrant pyrogenic organic matter storage while reducing N availability. *Global Change Biology*, *21*(6), 2321–2333. https://doi.org/10.1111/gcb.12832

Špela, Ž., Damjana, D., Matej, H., Matic, N., & Marina, P. (2025). Soil water repellency of two disturbed soils contaminated with different agricultural microplastics tested under controlled laboratory conditions. *Geoderma*, *453*, 117124. https://doi.org/10.1016/j.geoderma.2024.117124

Štursová, M., Šnajdr, J., Koukol, O., Tláskal, V., Cajthaml, T., & Baldrian, P. (2020). Long-term decomposition of litter in the montane forest and the definition of fungal traits in the successional space. *Fungal Ecology*, *46*, 100913. https://doi.org/10.1016/j.funeco.2020.100913

Thakur, M. P., Herrmann, M., Steinauer, K., Rennoch, S., Cesarz, S., & Eisenhauer, N. (2015). Cascading effects of belowground predators on plant communities are density-dependent. *Ecology and Evolution*, *5*(19), 4300–4314. https://doi.org/10.1002/ece3.1597

Thomas, G.W., 1996. Soil pH and soil activity. *In:* D.L. Sparks (ed.) Methods of Soil Analysis. Part 3. Chemical Methods. American Society of Agronomy Inc., Soil Science Society of America, Inc. Madison WI. p. 475-489.

Turner, M. G. (2010). Disturbance and landscape dynamics in a changing world. *Ecology*, *91*(10), 2833–2849. https://doi.org/10.1890/10-0097.1

Ulery, A. L., & Graham, R. C. (1993). Forest fire effects on soil color and texture. *Soil Science Society of America Journal*, *57*(1), 135–140. https://doi.org/10.2136/sssaj1993.03615995005700010026x

U.S. Department of Agriculture. (2014). *Rim Fire Recovery (43033) Draft Environmental Impact Statement* [Draft environmental impact statement]. USDA Forest Service. www.hcd.ca.gov

U.S. Forest Service. (2001). *Sierra Nevada Framework* (Vol. 2).

U.S. Geological Survey. (2000). *Chapter 1: Sierra Nevada Ecosystems*.

Usda plants database. (n.d.). Retrieved July 9, 2025, from https://plants.usda.gov/

Vahedifard, F., Abdollahi, M., Leshchinsky, B. A., Stark, T. D., Sadegh, M., & AghaKouchak, A. (2024). Interdependencies between wildfire-induced alterations in soil properties, near-surface processes, and geohazards. *Earth and Space Science*, *11*(2), e2023EA003498. https://doi.org/10.1029/2023EA003498

Van De Water, K., & North, M. (2010). Fire history of coniferous riparian forests in the Sierra Nevada. *Forest Ecology and Management*, *260*(3), 384–395. https://doi.org/10.1016/j.foreco.2010.04.032

Van Wagtendonk, J. W., Moore, P. E., Yee, J. L., & Lutz, J. A. (2020). The distribution of woody species in relation to climate and fire in Yosemite National Park, California, USA. *Fire Ecology*, *16*(1), 22. https://doi.org/10.1186/s42408-020-00079-9

Vázquez, F. J., Acea, M. J., & Carballas, T. (1993). Soil microbial populations after wildfire. *FEMS Microbiology Ecology*, *13*(2), 93–103. https://doi.org/10.1111/j.1574-6941.1993.tb00055.x

Verma, S., & Jayakumar, S. (2012). Impact of forest fire on physical, chemical and biological properties of soil: A review. *Proceedings of the International Academy of Ecology and Environmental Sciences*, *2*(3), 168–176.

Wahl, N. A. (2008). Variability of water repellency in sandy forest soils under broadleaves and conifers in north-western Jutland/Denmark. *Soil and Water Research*, *3*(Special Issue 1), S155–S164. https://doi.org/10.17221/1407-SWR

Wang, C., Wang, G., Wang, Y., Rafique, R., Ma, L., Hu, L., & Luo, Y. (2016). Fire alters vegetation and soil microbial community in alpine meadow. *Land Degradation & Development*, *27*(5), 1379–1390. https://doi.org/10.1002/ldr.2367

Web Soil Survey Home. (n.d.). Retrieved July 9, 2025, from https://websoilsurvey.sc.egov.usda.gov/app/

Whiteleaf manzanita(U. S. National park service). (n.d.). Retrieved July 9, 2025, from https://www.nps.gov/articles/manzanita.htm

Whitman, E., Parisien, M.-A., Thompson, D. K., & Flannigan, M. D. (2019). Short-interval wildfire and drought overwhelm boreal forest resilience. *Scientific Reports*, *9*(1), 18796. https://doi.org/10.1038/s41598-019-55036-7

Wieting, C., Ebel, B. A., & Singha, K. (2017). Quantifying the effects of wildfire on changes in soil properties by surface burning of soils from the Boulder Creek Critical Zone Observatory. *Journal of Hydrology: Regional Studies*, *13*, 43–57. https://doi.org/10.1016/j.ejrh.2017.07.006

Wixon, D. L., & Balser, T. C. (2013). Toward conceptual clarity: PLFA in warmed soils. *Soil Biology and Biochemistry*, *57*, 769–774. https://doi.org/10.1016/j.soilbio.2012.08.016

Wu, Z., He, H. S., Liang, Y., Cai, L., & Lewis, B. J. (2013). Determining relative contributions of vegetation and topography to burn severity from landsat imagery. *Environmental Management*, *52*(4), 821–836. https://doi.org/10.1007/s00267-013-0128-3

Xue, L., Li, Q., & Chen, H. (2014). Effects of a wildfire on selected physical, chemical and biochemical soil properties in a pinus massoniana forest in south china. *Forests*, *5*(12), 2947–2966. https://doi.org/10.3390/f5122947

Xue, P.-P., Carrillo, Y., Pino, V., Minasny, B., & McBratney, Alex. B. (2018). Soil properties drive microbial community structure in a large scale transect in south eastern australia. *Scientific Reports*, *8*(1), 11725. https://doi.org/10.1038/s41598-018-30005-8

Zajícová, K., & Chuman, T. (2021). Spatial variability of forest floor and topsoil thicknesses and their relation to topography and forest stand characteristics in managed forests of Norway spruce and European beech. *European Journal of Forest Research*, *140*(1), 77–90. https://doi.org/10.1007/s10342-020-01316-1

Zhang, P., Tian, X., He, X., Song, F., Ren, L., & Jiang, P. (2008). Effect of litter quality on its decomposition in broadleaf and coniferous forest. *European Journal of Soil Biology*, *44*(4), 392–399. https://doi.org/10.1016/j.ejsobi.2008.04.005

Near Surface and Deep Soil Organic Carbon Dynamics During Post-Wildfire Recovery in the Sierra Nevada, USA

2.1. Introduction

Forests are the largest terrestrial carbon (C) sink, containing nearly 70% of global soil organic carbon (SOC) (Lal, 2005; Jandl et al., 2007; North & Hurteau, 2011). In the continental United States, temperate forests alone store an estimated 17-37 Pg of carbon, accounting for roughly 53% of terrestrial C in these ecosystems (Pan et al., 2024). However, this substantial C reservoir is increasingly at risk from catastrophic wildfires (McCool et al., 2023). Climate change is intensifying weather extremes, including prolonged drought and rising global temperatures, which heighten wildfire frequency and severity (Nave et al., 2011; Earls et al., 2014; Abatzoglou & Williams, 2016). Additionally, decades of fire suppression and conventional forest management practices in the United States have led to dense, homogenous, and fire intolerant canopy structures that promote high intensity burns (McKelvey et al., 1996; Certini, 2005; Collins et al., 2007; Beaty & Taylor, 2008). This has facilitated an emerging regime of extreme fire behavior that poses a significant threat to forest C stocks and may further reduce ecosystem productivity through alteration of cycling.

SOC loss has cascading effects on ecosystem productivity, primarily through the reduction of microbial activity and alteration of nutrient stocks and cycling including cation exchange capacity (CEC) (Powlson et al., 2015). Immediately following catastrophic wildfire, SOC pools are depleted due to their relatively low volatilization temperature, removing C as an available microbial energy source (Baird et al., 1999; Chen & Xu, 2010; Sahu et al., 2017). This disrupts the soil microbial carbon pump (MCP), which is a conceptual framework that outlines the role of microbial anabolism in C stabilization (Liang et al., 2017; Liang, 2020; Moukanni et al., 2022). Disruption of this crucial C input pathway reduces CEC due to the substantial proportion that SOC contributes (~50%) to nutrient retention and soil fertility (Powlson et al., 2015; Solly et al., 2020).

Despite initial fire induced SOC losses, ecological succession is a major contributor of post-disturbance regeneration and cycling (Badalamenti et al., 2019; Duan et al., 2020; Xing et al., 2023). The establishment of graminoids and shrubs in disturbed areas, and their subsequent overtaking by competition from conifer stands, may alter allocation of C to SOC pools. In the context of post-wildfire recovery and ecological succession, particulate organic matter (POM) and mineral-associated organic matter (MAOM) formation depends on the amount and quality of litter from vegetation input, as well as physio-chemical interactions of microbially processed SOC with mineral surfaces (Lavellee et al. 2020; Moukanni et al., 2022; Peter-Contesse et al., 2024; Zhu et al., 2024). POM is primarily comprised of fractionated and depolymerized plant and fungal material (Lavallee et al., 2020; Moukanni et al., 2022; Leuthold et al., 2024). The MAOM fraction forms as a byproduct of microbial decomposition. Stabilization of MAOM occurs via physio-chemical protection from microbial uptake through sorption to soil mineral surfaces and occlusion in microaggregates (Lavallee et al., 2020; Cotrufo & Lavallee, 2022; Moukanni et al., 2022; Angst et al., 2023; Leuthold et al., 2024). The POM fraction has been observed to increase in post-disturbance secondary succession compared to climax forest communities, whereas MAOM continued to increase with forest regeneration (Zhu et al., 2024). This is likely the result of a compositional shift in leaf litter from low to high C:N ratio with forest succession, as pioneer species generally produce higher quality, more readily decomposable litter (low C:N ratio) relative to mature conifer stands (Zhang et al., 2008; Morffi-Mestre et al., 2023). Furthermore, belowground regeneration of complex root systems contributes to SOC inputs as root exudates, stimulating microbial activity and further facilitating fractionation (Lavallee et al., 2020; Xing et al., 2023). Black carbon (BC) may persist in soil after wildfire as POM, dissolved organic C, and possibly MAOM.

The objective of this study was to evaluate SOC stocks and fractions in soils recovering from wildfire relative to sites with no documented history of fire (termed herein unburned sites) in mixed conifer forests of the central Sierra Nevada. The approach leverages systematic variation in soil (Inceptisols vs Alfisols) as documented by high and low montane elevations to evaluate deep soil and near surface C stocks and fractions.

2.2. Materials and Methods

2.2.1. Site Description

The study area was located in the Stanislaus and Sierra National Forests of California's central Sierra Nevada mountains. Burned and unburned sites were identified within and around perimeters of the Rim fire (summer of 2013) and Ferguson fire (summer of 2018) . Together, these catastrophic wildfires impacted approximately 354,215 acres of land across Tuolumne and Mariposa counties (CalFire FRAP). Adjacent land within the Stanislaus and Sierra National Forests that has not been affected by fire within the past 50 years were considered unburned as no fires had been documented by CalFire and USFS.

Study sites were stratified by high (5,000-7,000 ft) and low (2,700-4,900 ft) elevations to reflect systematic differences in soil and C cycling. Mean annual precipitation (MAP) is 800 to 1000 mm in the low elevation band and 1,000 to 1,250 mm in the high elevation band. Mean annual air temperature (MAAT) is 11 ºC at low elevation sites and 9 ºC at high elevation sites (WSS, 2024). The Köppen-Geiger climate classification system identifies this area as affected by hot, dry summers and cool, moist winters (California Soil Resource Lab, n.d.). Soil temperature and moisture regimes are mesic and xeric, respectively.

Overstory vegetation (when present) in the study site is dominated by incense cedar (*Libocedrus decurrens*), ponderosa pine (*Pinus ponderosa*), white fir (*Abies concolor*), sugar pine (*Pinus lambertiana*), black oak (*Quercus kelloggii*), canyon live oak (*Quercus chrysolepis*), and leather oak (Quercus durata). Distribution of oak species is more common at low elevation sites, with canyon live oak only present. Understory vegetation across both elevations consists primarily of perennial shrubs, graminoids, and forbs (U.S. Department of Agriculture, 2023; U.S. Department of Agriculture, 2024; CalScape, 2024).

Soils in the study area were derived from granitic colluvium, residuum, and till (Hill, 2006; WSS, 2024). High elevation sites were represented by the Gerle soil series, Coarse-loamy, mixed, superactive, frigid Humic Dystroxerepts. Soils sampled from the low elevation represented the Holland soil series, Fine-loamy, mixed, active, mesic Ultic Haploxeralfs (WSS, 2024). Sampling occurred in 2023 and 2024.

2.2.2. Soil Sampling

A total of eighteen sites were selected in the study area, stratified by high and low elevations. Of the nine sample sites in each elevation band, six sites were selected from within fire affected areas and three sites from unburned areas. Each sample site consisted of one central soil profile excavation to approximately 1-m depth, and four adjacent satellite sites at 15 cm depths. From the soil profiles, genetic horizons were identified, described, and sampled using standard soil survey techniques (Soil Survey Staff, 2012). The four satellite sites were located approximately 10-m away from the central soil profile in each cardinal direction. Samples collected at the satellite sites were divided into 0-5 cm and 5-15 cm depths. Bulk density cores were collected from each genetic horizon of the central soil profile and both sampling depths of the satellite sites.

2.2.3. Laboratory Analysis

Bulk soil samples from the central profile and satellite sites were air-dried in the lab until the total mass stabilized, then were passed through a 2-mm mesh. Soil ≤ 2-mm was analyzed for SOC as total C concentration (TC) in the bulk soil. Here we use the terminology total C, however, TC can be assumed to equal total SOC given the low pH (< 6.0) at all sites. Particulate organic carbon (POM-C), and mineral-associated organic carbon (MAOM-C) fractions were measured following the particle size fractionation procedure modified from Cotrufo et al. (2019). 5 g of 2-mm air-dried soil was dispersed in 30 mL of 0.5% $Na(PO_3)_6$ by shaking for 18 hours. The resulting slurry was wet-sieved through a 53-µm mesh to separate the fine and coarse soil fractions, then oven-dried at 60 ºC until completely dry. SOC in the bulk soil and in POM/MAOM fractions was assessed by the dry combustion method using the ECS 8024 Soil Special Costech elemental analyzer. Bulk density and rock fragment volume were determined from volumetric cores collected at the field sites. Missing bulk density samples that could not be collected in the field were supplemented with data from Web Soil Survey (WSS, 2025).

2.2.4. Calculations

SOC inventories were calculated as the sum of SOC stocks to a depth of 1-m in the central soil profile. SOC stocks were determined by multiplying the TC concentration (g C/g soil) by bulk density (g/cm^3), horizon thickness (cm), and (1-fraction of rock). The result was converted from units of g/cm^2 to kg/m^2. Satellite sites were also aggregated as a depth weighted average, where both sampling depths (0-5 cm and 5-15 cm) were analyzed as one depth (0-15 cm).

$SOC\ inventory =$

$$\Sigma\left(total\ carbon\ \left(\frac{g}{g}\right) x\ bulk\ density\ \left(\frac{g}{cm^3}\right) x\ horizon\ thickness\ (cm)\ x\ (1 - fraction\ of\ rock)\right)$$

2.2.5. Statistical Analysis

All data was analyzed using RStudio. Differences in surface SOC (0-15 cm) between burned and unburned sites at high and low elevations was assessed with two-way analysis of variance (ANOVA). When significance was detected, Tukey's HSD was utilized to identify pairwise differences between treatments effects. SOC in the central soil profile was assessed with the slice-wise aggregation algorithm by 15-cm depth increments, analyzed with two-way ANOVA and Levene's test (Beaudette et al., 2013). Depth plots were visualized with the Algorithms for Quantitative Pedology (AQP) package depicting the median, 25th percentile, and 75th percentile. Sample sizes were smaller for whole soil compared to the near surface investigation.

2.3. Results

2.3.1. Post-wildfire surface SOC recovery trends

Results from near surface soil horizons (0-15 cm) demonstrated that the soil C content and its fractions either increased or were statistically indistinguishable within the first decade of post-wildfire recovery (Table 2.1; Fig. 2.1). SOC was consistently higher at high elevation sites compared to low elevation sites regardless of burn status, with the exception of burned low elevation MAOM-C (Table 2.1; Fig. 2.1). Furthermore, a divergence in SOC trends was detected between burned and unburned sites by elevation. High elevation sites were statistically indistinguishable by burn status. At low elevation, TC concentration and MAOM-C of post-wildfire recovery sites were statistically higher than unburned sites (Fig. 2.1).

Table 2.1. Comparison of changes in soil C fractions by burn status, elevation, and the interaction effect of burn and elevation using two-way ANOVA.

Measurement	ANOVA term	Df	F-value	p-value
Carbon Stock (kg/m^2)	Burn	1	9.32	**0.0032****
	Elevation	1	15.8	**0.00017*****
	Burn x Elevation	1	0.238	0.63
TC concentration (%)	Burn	1	3.25	0.076
	Elevation	1	28.4	**0.0000011*****
	Burn x Elevation	1	4.14	**0.046***
POM-C (mg C/g soil)	Burn	1	0.392	0.53
	Elevation	1	18.9	**0.000064*****
	Burn x Elevation	1	2.26	0.14
MAOM-C (mg C/g soil)	Burn	1	9.36	**0.0035****
	Elevation	1	14.7	**0.00033*****
	Burn x Elevation	1	1.47	0.23

TC concentration was 53.8% higher in soils recovering from wildfire (mean = 3.42%; $p = 0.029$) compared to unburned sites (mean = 2.23%) (Fig. 2.2). Similarly, MAOM-C was 73.3% higher (mean = 18.7 mg C/g soil; $p = 0.015$) compared to unburned sites (mean = 10.8 mg C/g soil) (Fig. 2.2). No significant differences by burn status were detected at high elevation sites, or for low elevation C-stock and POM-C (Fig. 2.2).

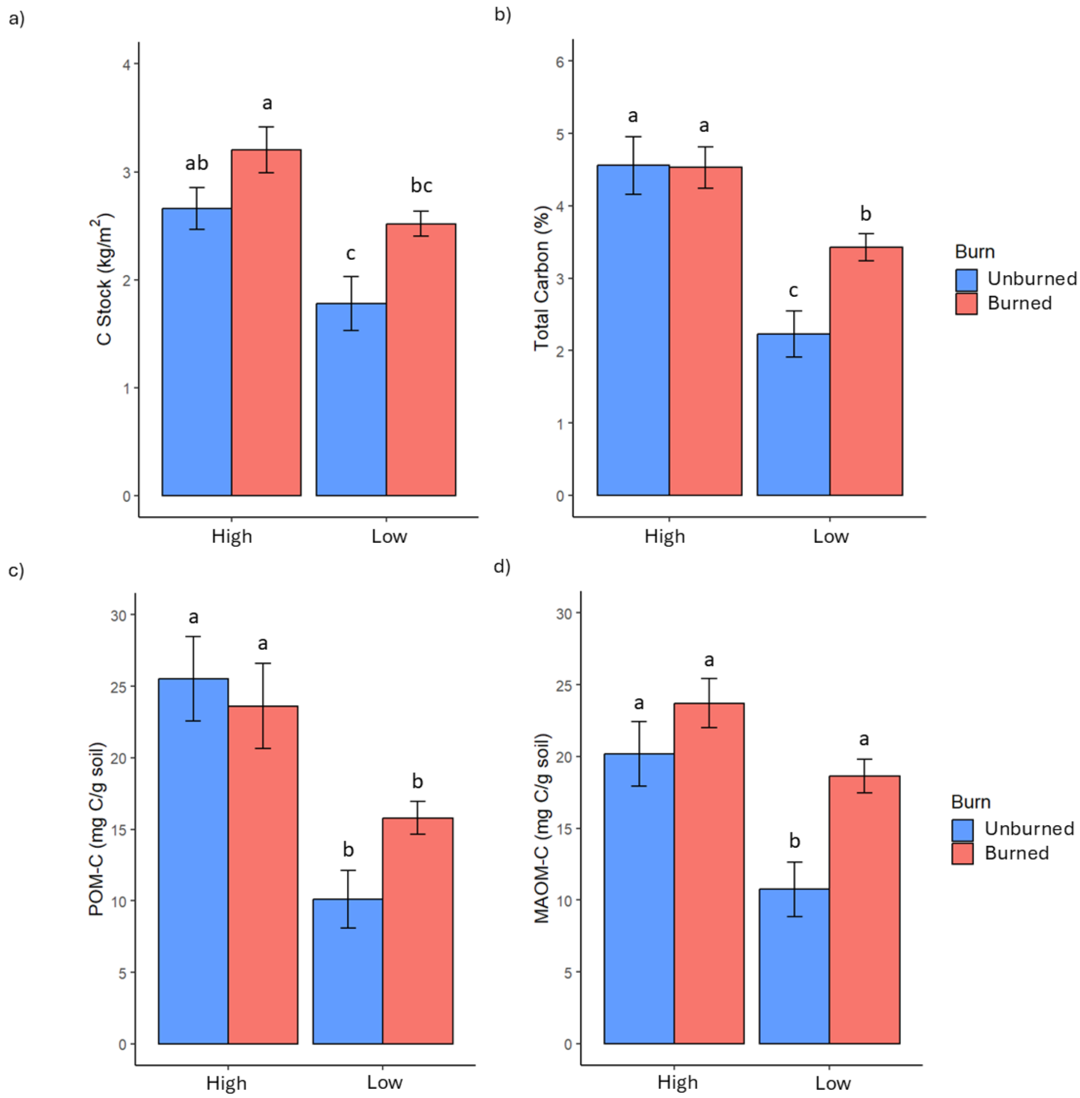

Figure 2.1. Soil carbon from (0-15 cm) at high and low elevations for unburned and sites recovering from wildfire (burned) a) carbon stocks, b) total carbon concentration, c) particulate organic carbon, and d) mineral-associated organic carbon. Bars represent mean values, whiskers depict standard error, and letters denote significant differences between mean values at $\alpha = 0.05$ by Tukey's HSD.

2.3.2. SOC distribution to 1 meter depth

SOC inventories were statistically indistinguishable relative to burn status and elevation when considering 1-m as a whole soil (termed herein whole soil) (Table 2.2; Fig. 2.2). Whole soil SOC inventories were numerically elevated in soils recovering from wildfire, and marginally higher in high elevation sites compared to low elevation sites (Fig. 2.2).

Table 2.2. Two-way ANOVA of SOC inventories between unburned and burned sites, at high and low elevations, and the interaction effect of burn status and elevation.

ANOVA term	Df	F-value	p-value
Burn	1	1.21	0.29
Elevation	1	3.85	0.069
Burn x Elevation	1	0.415	0.53

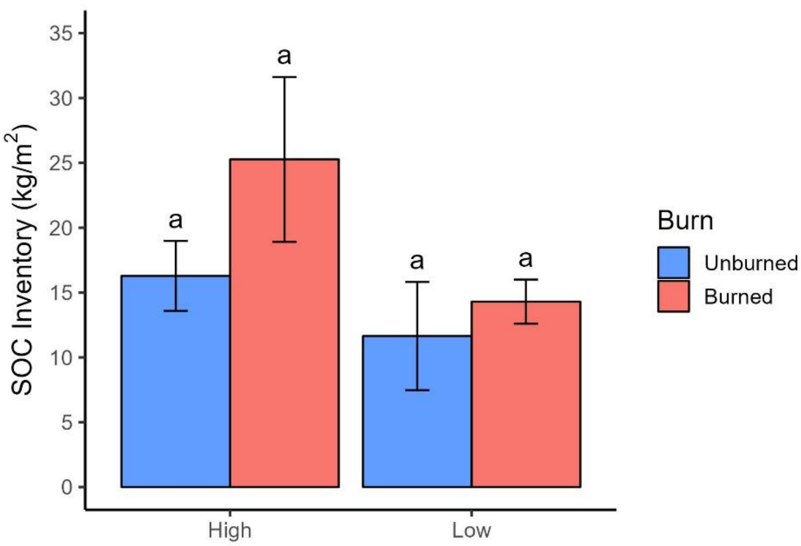

Figure 2.2. Soil carbon inventories (cumulative SOC stocks from soil profiles to 1 m) from unburned and sites recovering from wildfire (burned) at high and low elevations. Bars represent mean values, whiskers depict standard error, and letters denote significant differences between mean values at $\alpha = 0.05$ by Tukey's HSD.

Depth trends in TC concentration show subtle differences in C allocation both by elevation and as a result of burn status, but most depth intervals were not statistically different. At high elevation, median TC and MAOM-C in subsoils recovering from wildfire (20-65 cm depths) were higher than unburned soils (Fig 2.3a). Variability was also much higher in these profiles. Median values of surface horizons (0-20 cm) and deep horizons (>65 cm) were similar as a result of burn status. At low elevation, differences in TC and C fractions were evident in surface horizons (0-15 cm), where soils recovering from wildfire had higher median values (Fig. 2.3b). MAOM-C showed the most notable difference between burned and unburned soils. At depth (> 15 cm), no observable differences in TC or POM were evident. Median MAOM values in sites recovering from fire were slightly higher than unburned sites at depths below 15 cm.

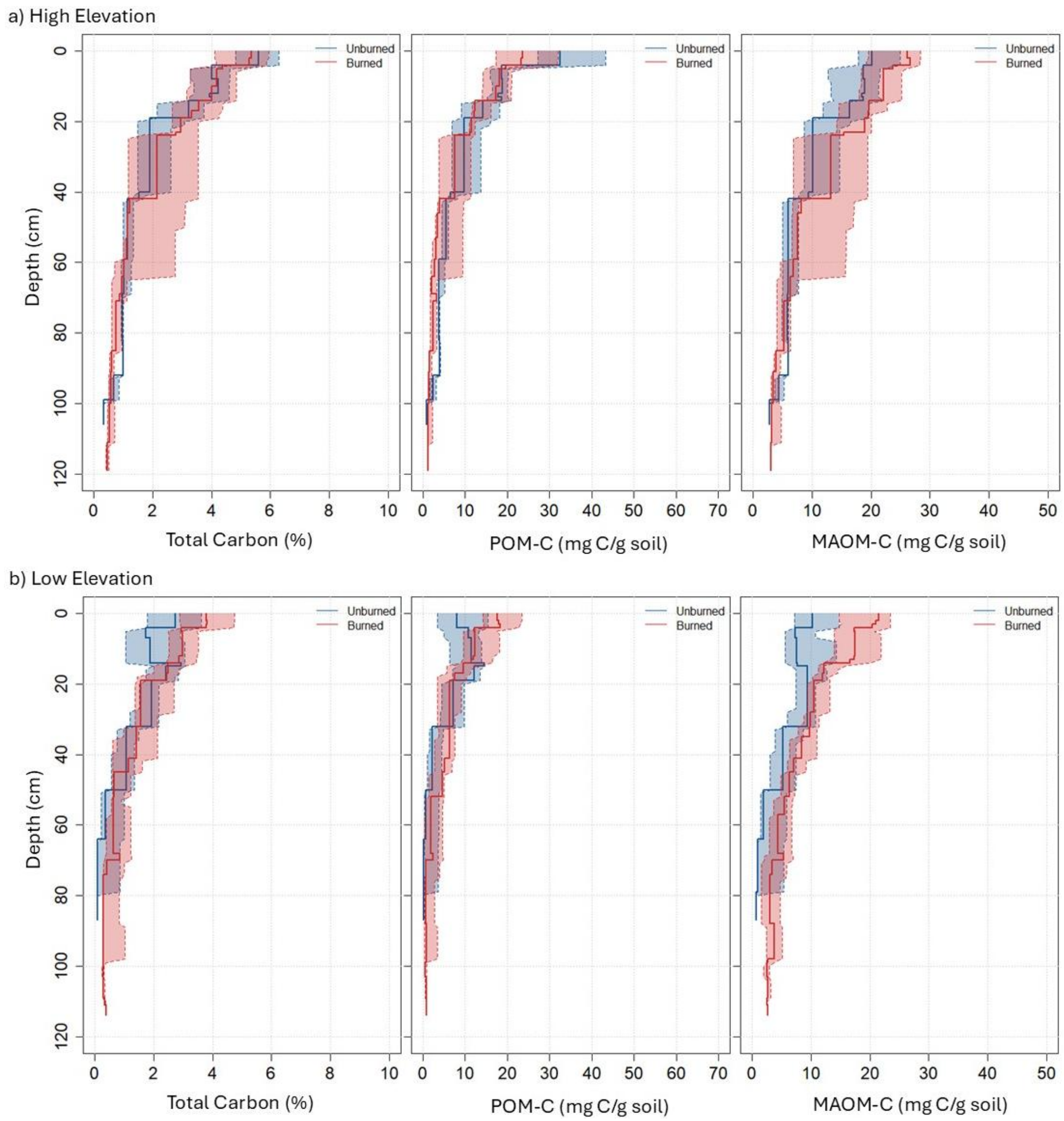

Figure 2.3. Depth plots from burned and unburned sites of total carbon concentration (%), particulate organic carbon, and mineral-associated organic carbon at a) high elevation sites, and b) low elevation sites. The median (solid lines) is bound by the 25th and 75th percentiles (highlighted with dashed lines). Note that fractions have different x-axis scales. Data was aggregated at 1-cm increments across the y-axis for visualization.

2.4. Discussion

Post-wildfire SOC recovery occurred at both high and low elevation sites. In some cases, SOC in sites recovering from fire exceeded unburned levels, with the most evident differences occurring near the soil surface. Based on our findings, MAOM appears to be the greatest contributor to SOC recovery. The conceptual diagram in Fig. 2.4 outlines recovery pathways of SOC at both elevations after initial losses from wildfire, where SOC increases can be attributed to persistence of coarse BC, preferential BC sorption to the soil mineral surface, new C additions from low C:N litter, and root rhizodeposition from secondary succession species. Although high elevation sites have elevated SOC compared to low elevation sites, the mechanisms of post-wildfire SOC recovery are similar at both elevations.

2.4.1. Litter and SOC loss from fire

Litter layers are essential to forest soil health, protecting the soil surface in many ways (Hatten et al., 2005; Mataix-Solera et al., 2011; Verma & Jayakumar, 2012). SOC accumulation in the topsoil occurs through physical fragmentation of litter or leaching of dissolved organic carbon (DOC) (Lavallee et al., 2020; Moukanni et al., 2022). Although this SOC mixes into the soil profile over time via abiotic processes or bioturbation, the most C-rich layer is generally the uppermost horizon (Shrestha et al., 2010; Gross & Harrison, 2019; Duan et al., 2020).

The soil environment immediately after wildfire, depending on severity, is characterized by losses of the litter layer and SOC. SOC loss depends on the duration and intensity of wildfire, which together determine the depth at which extreme heating occurs (Caldwell et al., 2002; Certini, 2005). High severity wildfire combusts the litter layer, which functions both as a direct SOC source and as a layer of topsoil protection against erosion (Hatten et al., 2005). Longer duration and high intensity wildfire penetrate deeper into the soil profile, which can induce microbial mortality and volatilize organic material (Baird et al., 1999; Certini, 2005; Bárcenas-Moreno & Bååth, 2009; Fontúrbel et al., 2012). Unanchored soil material may be lost to wind or water erosion following wildfire, removing remaining organic material from the soil environment (Hatten et al., 2005; Bormann et al., 2008; Mataix-Solera et al., 2011; Verma & Jayakumar, 2012; Pierson et al., 2019).

2.4.2. Transformations of material to black carbon

Regardless of initial SOC losses, elevated SOC in the recovery period following wildfire (Fig. 2.2 & 2.3) may be in part attributed to formation of black carbon (BC), which can contribute to both POM and organo-mineral associations (López-Martín et al., 2018; Burgeon et al., 2021). Incomplete combustion of organic material produces BC, which is characterized by its contributions to C sequestration and soil fertility (Liang et al., 2006; Czimczik & Masiello, 2007; Cheng et al., 2014; Qu et al., 2016; Lian & Xing, 2017). It has been estimated that as much as 3% of the preexisting ecosystem C remains in soil as BC (Forbes et al., 2006). Formation of BC also increases SOC content through its enhanced recalicitrance, and physical protection by occlusion in aggregates and sorption to the soil mineral surface (Knicker, 2007; Cheng et al., 2014; López-Martín et al., 2018; Burgeon et al., 2021). BC recalcitrance is derived from combustion-induced molecular transformations. This phenomenon is referred to as the "combustion continuum", where a gradient of increasing combustion temperatures correlates to greater aromaticity. At high enough temperatures, these aromatic structures condence to form clusters (Masiello, 2004; Keiluweit et al., 2010; Wagner et al., 2021). BC is therefore highly stable, resistant to microbial degradation with a mean residence time estimated at thousands of years (Kuzyakov et al., 2009; Posada-Baquero & Ortega-Calvo, 2011; Llorente et al., 2018). While BC surface functionality is heterogeneous and depends heavily on the material it was derived from, it is commonly comprised of carboxylic and phenolic species (Cheng et al., 2014; Qu et al., 2016; Burke et al., 2024). These functional groups preferentially sorb to iron oxyhydroxides, which have been established as important facilitators of C sequestration (Luo et al., 2019; Klaes et al., 2023). This may be one mechanism of BC persistence in our study site due to the prevalence of granitic parent material. One common mineral found in Sierra Nevada granitic rock is hornblende, a type of amphibole that weathers to iron oxyhydroxides (Perkins, n.d.; Feth et al., 1964; Cheng et al., 2008; Klaes et al., 2023). Alongside chemical recalcitrance, BC can be physically protected from biodegradation by occlusion in soil aggregates. Brodowski et al. (2006) found that BC is preferentially occluded within soil aggregates over other SOC materials due to its sorption capacity to both SOM and mineral surfaces, highlighting its role in SOC stabilization. Free and occluded BC is mixed into the soil profile over time since wildfire, further contributing to long-term C stabilization (Shrestha et al., 2010).

2.4.3. Plant succession and additions of new C

SOC generally undergoes rapid increases in the early to intermediate stages of ecological succession, largely in response to elevated plant and microbial productivity that characterizes these regimes and decomposition of dead root tissue (Swanson et al., 2011; Gundale et al., 2024). Odum's theory of ecological succession establishes that plant productivity increases with recovery time following disturbance, but declines once forest communities reach maturity. This reflects a strategic ecosystem dynamic where early to intermediate successional communities prioritize productivity, while mature stands have achieved a steady state of C cycling (Odum, 1969; Stoy et al., 2008; Gundale et al., 2024).

Sites recovering from wildfire were dominated by secondary succession species, consisting of drought- and full-sun tolerant perennial shrubs in an open canopy environment. These perennial shrubs provide new SOC additions to near surface and subsurface horizons. Commonly observed post-wildfire vegetation in the study area consisted of greenleaf manzanita (*Arctostaphylos patula*), and nitrogen fixers buckbrush (*Ceanothus cuneatus*), deerbrush

(*Ceanothus intergerrimus*), and whitethorn ceanothus (*Ceanothus cordulatus*), which are characterized by high quality (low C:N) litter and complex root systems that extend at least 50 cm into the soil profile (USDA PLANTS database, n.d.). Atmospheric C is sequestered as root biomass, further facilitating SOC cycling via subsurface root litter additions and rhizodeposition (Lei et al., 2023). DOC is a product of rhizodeposition, the formation and translocation of which promotes microbial activity and SOM stabilization as MAOM (Sanderman et al., 2008; Kaiser & Kalbitz, 2012; Srivastava & Yetgin, 2024). DOC undergoes physio-chemical alterations and microbial processing during translocation, leading to stabilization of hydrophobic and high molecular weight compounds and domains through organo-mineral interactions (Kaiser & Zech, 2000; Jagadamma et al., 2012; Kaiser & Kalbitz, 2012).

Litter quality also influences SOC accumulation and its fractionation. Yang & Luo (2011) found that forest litter quality decreases with stand age, where leaf C:N ratio is low in early successional stages and increases as forests mature. Low C:N litter is more readily decomposed by soil microbes, which may explain why MAOM appears to be the dominant fraction leading to recovery after wildfire. Conversely, unburned study sites consisted of mature mixed conifer stands, where secondary succession species had been outcompeted by conifers and the litter layer was dominated by low quality coniferous detritus (Zhang et al., 2008).

2.4.4. Depth

Within the whole soil profile, there appears to be limitations in the depth at which fire-induced changes occur (Fig. 2.3). Our results suggest that the most dynamic changes may have occurred in the top 15 cm of soil. The literature documents inconsistencies in effects of wildfire on SOC (Badía et al., 2014), including soil recovery (Prieto-Fernández et al., 1998). Differences in SOC loss are mainly a result of heat transfer, which decreases with depth depending on fire intensity and water content (Santiesteban-Serrano et al., 2025). Elevated temperatures associated with wildfire rarely transfer deeper than 20-30 cm in the soil profile, which constrains immediate effects of wildfire (Certini, 2005; Caon et al., 2014). Some have suggested that these inconsistencies are partially due to the dilution of soil measurements when sampling layers with a thickness that exceeds the effect of fire (Badía et al., 2014). This may be why our whole soil stocks were similar but near surface changes were statistically different. However, wildfire effects on SOC was detected to a depth of 65 cm in the recovery period of this study (Fig. 2.3). Therefore, post-wildfire translocation of SOC and microbial productivity gradients may be mechanisms that constrain differences in SOC between burned and unburned sites deeper than 65 cm. Rhizodeposition from perennial root systems extending approximately 50 cm and mixing of SOC throughout the soil profile from increased net primary productivity may have a priming effect on deep soil microbial activity (USDA PLANTS database, n.d.; Sanderman et al., 2008; Kaiser & Kalbitz, 2012; Xu et al., 2022; Gundale et al., 2024). While microbial biomass generally declines with depth, elevated resource availability could have induced the deep SOC processing observed in Fig. 2.4 (Fierer et al., 2003; Eilers et al., 2012).

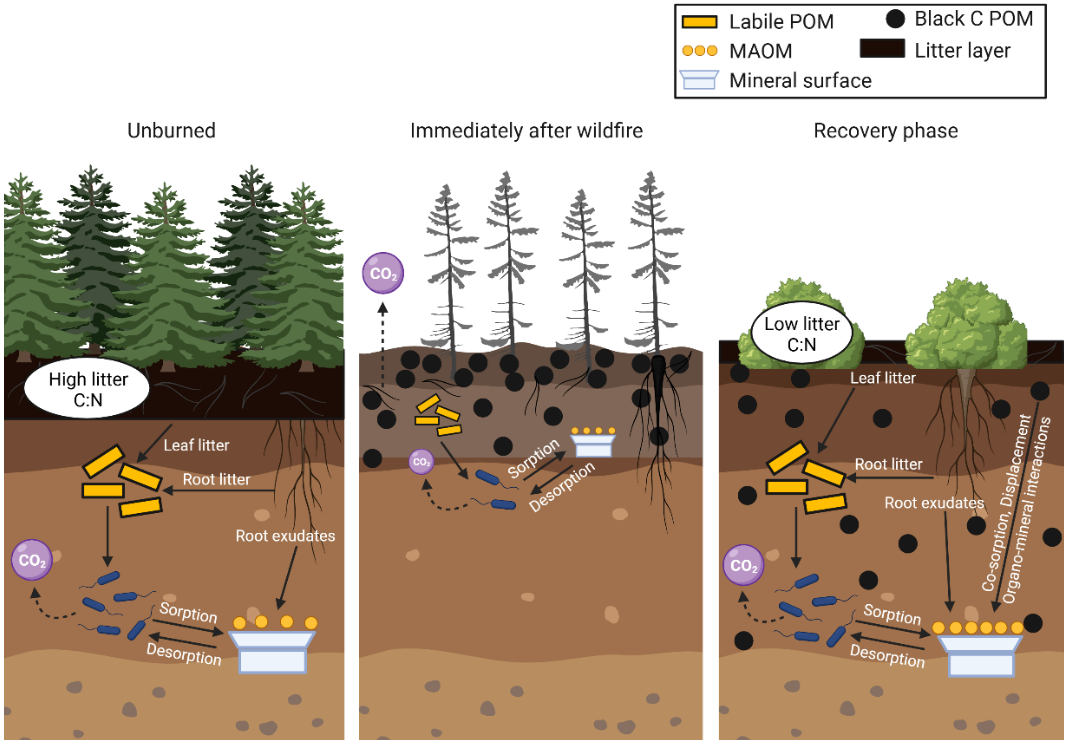

Figure 2.4. Conceptual diagram of SOC across successional stages following wildfire. Darker soil profiles represent greater overall carbon content compared to the lighter soil profile in the upper two horizons immediately after wildfire. Carbon loss from combustion is also depicted immediately after wildfire. Lower quality litter (high C:N ratio) limit microbial uptake, leading to thicker litter layers and greater accumulation of POM in the unburned state. During the recovery phase, elevated SOC results from inputs of higher quality litter (low C:N ratio) and persistence of black carbon. Coarse material contributes to the POM fraction, while co-sorption, competitive displacement, and organo-mineral interactions contributes to the MAOM fraction.

The effects of wildfire on SOC inventories and cycling, particularly in deeper soil layers, are currently not well documented. Much of existing literature focuses on the upper 30 cm of the soil profile (Yost & Hartemink, 2020), which Gross & Harrison (2019) suggest in their review leads to an overall underestimation of changes in SOC across the whole soil. While not as dynamic as the soil surface, deep soil layers are influenced by SOC inputs via root exudates, downward movement of DOC, SOC sorption, and microbial activity (Kaiser & Zech, 2000; Kaiser & Kalbitz, 2012; Schrumpf et al., 2013; Moreland et al., 2022). Deeper soil horizons may be protected from the effects of some fires. As a result, we advocate for the measurement of near surface SOC inventories to document fire effects on forest soil health and whole soil inventories to understand how C sequestration has been affected.

2.5. Conclusion

SOC recovery trends in the first decade of post-wildfire recovery were detectable when considering the soil surface (0-15 cm), but not when considering the full 1-m inventories. At low elevation, burned sites had significantly higher TC concentration and MAOM-C in the surface layer compared to unburned sites. This increase may be attributed to the combined effects of new plant productivity associated with secondary ecological succession, black carbon persistence, and differences in litter quality of perennial shrubs relative to mature conifers. In contrast, cumulative SOC inventories, total C concentration, POM-C, and MAOM-C across the whole 1-m profile showed no significant differences between burned and unburned sites at either elevation. Results demonstrate that systematic variation within soils must be constrained when conducting soil health assessments in forest soils. Consideration of near surface horizons and the whole soil profile, including deeper horizons, are needed for different reasons. Near surface measurements best evaluate soil recovery and the impact of disturbance on dynamic soil properties. From a carbon sequestration perspective, whole profile soil inventories are important to assess the effects of wildfire and/or recovery.

References

Abatzoglou, J. T., & Williams, A. P. (2016). Impact of anthropogenic climate change on wildfire across western US forests. *Proceedings of the National Academy of Sciences*, *113*(42), 11770–11775. https://doi.org/10.1073/pnas.1607171113

Badalamenti, E., Battipaglia, G., Gristina, L., Novara, A., Rühl, J., Sala, G., Sapienza, L.,Valentini, R., & La Mantia, T. (2019). Carbon stock increases up to old growth forest along a secondary succession in Mediterranean island ecosystems. *PLOS ONE*, *14*(7), e0220194. https://doi.org/10.1371/journal.pone.0220194

Badía, D., Martí, C., Aguirre, A. J., Aznar, J. M., González-Pérez, J. A., De La Rosa, J. M., León, J., Ibarra, P., & Echeverría, T. (2014). Wildfire effects on nutrients and organic carbon of a Rendzic Phaeozem in NE Spain: Changes at cm-scale topsoil. *CATENA*, *113*, 267–275. https://doi.org/10.1016/j.catena.2013.08.002

Baird, M., Zabowski, D., & Everett, R. L. (1999). Wildfire effects on carbon and nitrogen in inland coniferous forests. *Plant and Soil*, *209*(2), 233–243. https://doi.org/10.1023/A:1004602408717

Bárcenas-Moreno, G., & Bååth, E. (2009). Bacterial and fungal growth in soil heated at different temperatures to simulate a range of fire intensities. *Soil Biology and Biochemistry*, *41*(12), 2517–2526. https://doi.org/10.1016/j.soilbio.2009.09.010

Beaty, R. M., & Taylor, A. H. (2008). Fire history and the structure and dynamics of a mixed conifer forest landscape in the northern Sierra Nevada, Lake Tahoe Basin, California, USA. *Forest Ecology and Management*, *255*(3–4), 707–719. https://doi.org/10.1016/j.foreco.2007.09.044

Beaudette, D. E., Roudier, P., & O'Geen, A. T. (2013). Algorithms for quantitative pedology: A toolkit for soil scientists. *Computers & Geosciences*, *52*, 258–268. https://doi.org/10.1016/j.cageo.2012.10.020

Bormann, B. T., Homann, P. S., Darbyshire, R. L., & Morrissette, B. A. (2008). Intense forest wildfire sharply reduces mineral soil C and N: The first direct evidence. *Canadian Journal of Forest Research*, *38*(11), 2771–2783. https://doi.org/10.1139/X08-136

Brodowski, S., John, B., Flessa, H., & Amelung, W. (2006). Aggregate-occluded black carbon in soil. *European Journal of Soil Science*, *57*(4), 539–546. https://doi.org/10.1111/j.1365-2389.2006.00807.x

Burgeon, V., Fouché, J., Leifeld, J., Chenu, C., & Cornélis, J.-T. (2021). Organo-mineral associations largely contribute to the stabilization of century-old pyrogenic organic matter in cropland soils. *Geoderma*, *388*, 114841. https://doi.org/10.1016/j.geoderma.2020.114841

Burke, M., Marín-Spiotta, E., & Ponette-González, A. G. (2024). Black carbon in urban soils: Land use and climate drive variation at the surface. *Carbon Balance and Management*, *19*(1), 9. https://doi.org/10.1186/s13021-024-00255-3

Caldwell, T. G., Johnson, D. W., Miller, W. W., & Qualls, R. G. (2002). Forest floor carbon and nitrogen losses due to prescription fire. *Soil Science Society of America Journal*, *66*(1), 262–267. https://doi.org/10.2136/sssaj2002.2620

California Native Plant Society. (n.d.). Calscape. https://calscape.org/

California Department of Forestry and Fire Protection. (n.d.). https://www.fire.ca.gov/

Caon, L., Vallejo, V. R., Ritsema, C. J., & Geissen, V. (2014). Effects of wildfire on soil nutrients in Mediterranean ecosystems. *Earth-Science Reviews*, *139*, 47–58. https://doi.org/10.1016/j.earscirev.2014.09.001

Certini, G. (2005). Effects of fire on properties of forest soils: A review. *Oecologia*, *143*(1), 1–10. https://doi.org/10.1007/s00442-004-1788-8

Chen, C., & Xu, Z. (2010). Forest ecosystem responses to environmental changes: The key regulatory role of biogeochemical cycling. *Journal of Soils and Sediments*, *10*(2), 210–214. https://doi.org/10.1007/s11368-009-0164-z

Cheng, C.-H., Lehmann, J., & Engelhard, M. H. (2008). Natural oxidation of black carbon in soils: Changes in molecular form and surface charge along a climosequence. *Geochimica et Cosmochimica Acta*, *72*(6), 1598–1610. https://doi.org/10.1016/j.gca.2008.01.010

Cheng, C.-H., Lin, T.-P., Lehmann, J., Fang, L.-J., Yang, Y.-W., Menyailo, O. V., Chang, K.-H., & Lai, J.-S. (2014). Sorption properties for black carbon (Wood char) after long term exposure in soils. *Organic Geochemistry*, *70*, 53–61. https://doi.org/10.1016/j.orggeochem.2014.02.013

Collins, B. M., Kelly, M., Van Wagtendonk, J. W., & Stephens, S. L. (2007). Spatial patterns of large natural fires in Sierra Nevada wilderness areas. *Landscape Ecology*, *22*(4), 545–557. https://doi.org/10.1007/s10980-006-9047-5

Cotrufo, M. F., Ranalli, M. G., Haddix, M. L., Six, J., & Lugato, E. (2019). Soil carbon storage informed by particulate and mineral-associated organic matter. *Nature Geoscience*, *12*(12), 989–994. https://doi.org/10.1038/s41561-019-0484-6

Cotrufo, M. F., & Lavallee, J. M. (2022). Chapter One - Soil organic matter formation, persistence, and functioning: A synthesis of current understanding to inform its conservation and regeneration. In D. L. Sparks (Ed.), *Advances in Agronomy* (Vol. 172, pp. 1–66). Academic Press. https://doi.org/10.1016/bs.agron.2021.11.002

Czimczik, C. I., & Masiello, C. A. (2007). Controls on black carbon storage in soils. *Global Biogeochemical Cycles*, *21*(3), 2006GB002798. https://doi.org/10.1029/2006GB002798

Duan, B., Man, X., Cai, T., Xiao, R., & Ge, Z. (2020). Increasing soil organic carbon and nitrogen stocks along with secondary forest succession in permafrost region of the Daxing'an mountains, northeast China. *Global Ecology and Conservation*, *24*, e01258. https://doi.org/10.1016/j.gecco.2020.e01258

Earles, J. M., North, M. P., & Hurteau, M. D. (2014). Wildfire and drought dynamics destabilize carbon stores of fire-suppressed forests. *Ecological Applications*, *24*(4), 732–740. https://doi.org/10.1890/13-1860.1

Eilers, K. G., Debenport, S., Anderson, S., & Fierer, N. (2012). Digging deeper to find unique microbial communities: The strong effect of depth on the structure of bacterial and archaeal communities in soil. *Soil Biology and Biochemistry*, *50*, 58–65. https://doi.org/10.1016/j.soilbio.2012.03.011

Feth, J. H., Roberson, C. E., Polzer, W. L. (1964). *Sources of mineral constituents in water from granitic rocks, Sierra Nevada, California and Nevada*. (1964). https://doi.org/10.3133/wsp1535I

Fierer, N., Schimel, J. P., & Holden, P. A. (2003). Variations in microbial community composition through two soil depth profiles. *Soil Biology and Biochemistry*, *35*(1), 167–176. https://doi.org/10.1016/S0038-0717(02)00251-1

Fontúrbel, M. T., Barreiro, A., Vega, J. A., Martín, A., Jiménez, E., Carballas, T., Fernández, C., & Díaz-Raviña, M. (2012). Effects of an experimental fire and post-fire stabilization treatments on soil microbial communities. *Geoderma*, *191*, 51–60. https://doi.org/10.1016/j.geoderma.2012.01.037

Forbes, M. S., Raison, R. J., & Skjemstad, J. O. (2006). Formation, transformation and transport of black carbon (Charcoal) in terrestrial and aquatic ecosystems. *Science of The Total Environment*, *370*(1), 190–206. https://doi.org/10.1016/j.scitotenv.2006.06.007

Gross, C. D., & Harrison, R. B. (2019). The case for digging deeper: Soil organic carbon storage, dynamics, and controls in our changing world. *Soil Systems*, *3*(2), 28. https://doi.org/10.3390/soilsystems3020028

Gundale, M. J., Axelsson, E. P., Buness, V., Callebaut, T., DeLuca, T. H., Hupperts, S. F., Ibáñez, T. S., Metcalfe, D. B., Nilsson, M., Peichl, M., Spitzer, C. M., Stangl, Z. R., Strengbom, J., Sundqvist, M. K., Wardle, D. A., & Lindahl, B. D. (2024). The biological controls of soil carbon accumulation following wildfire and harvest in boreal forests: A review. *Global Change Biology*, *30*(5), e17276. https://doi.org/10.1111/gcb.17276

Hatten, J., Zabowski, D., Scherer, G., & Dolan, E. (2005). A comparison of soil properties after contemporary wildfire and fire suppression. *Forest Ecology and Management*, *220*(1–3), 227–241. https://doi.org/10.1016/j.foreco.2005.08.014

Hill, M. (2006). 6. Great is granite. In *Geology of the Sierra Nevada* (pp. 177–210). University of California Press. https://www.degruyterbrill.com/document/doi/10.1525/9780520936942-009/html

Jagadamma, S., Mayes, M. A., & Phillips, J. R. (2012). Selective sorption of dissolved organic carbon compounds by temperate soils. *PLoS ONE*, *7*(11), e50434. https://doi.org/10.1371/journal.pone.0050434

Jandl, R., Lindner, M., Vesterdal, L., Bauwens, B., Baritz, R., Hagedorn, F., Johnson, D. W., Minkkinen, K., & Byrne, K. A. (2007). How strongly can forest management influence soil carbon sequestration? *Geoderma*, *137*(3–4), 253–268. https://doi.org/10.1016/j.geoderma.2006.09.003

Kaiser, K., & Kalbitz, K. (2012). Cycling downwards – dissolved organic matter in soils. *Soil Biology and Biochemistry*, *52*, 29–32. https://doi.org/10.1016/j.soilbio.2012.04.002

Kaiser, K., & Zech, W. (2000). Dissolved organic matter sorption by mineral constituents of subsoil clay fractions. *Journal of Plant Nutrition and Soil Science*, *163*(5), 531–535. https://doi.org/10.1002/1522-2624(200010)163:5<531::AID-JPLN531>3.0.CO;2-N

Keiluweit, M., Nico, P. S., Johnson, M. G., & Kleber, M. (2010). Dynamic molecular structure of plant biomass-derived black carbon(Biochar). *Environmental Science & Technology*, *44*(4), 1247–1253. https://doi.org/10.1021/es9031419

Klaes, B., Thiele-Bruhn, S., Wörner, G., Höschen, C., Mueller, C. W., Marx, P., Arz, H. W., Breuer, S., & Kilian, R. (2023). Iron (Hydr)oxide formation in Andosols under extreme climate conditions. *Scientific Reports*, *13*(1), 2818. https://doi.org/10.1038/s41598-023-29727-1

Knicker, H. (2007). How does fire affect the nature and stability of soil organic nitrogen and carbon? A review. *Biogeochemistry*, *85*(1), 91–118. https://doi.org/10.1007/s10533-007-9104-4

Kuzyakov, Y., Subbotina, I., Chen, H., Bogomolova, I., & Xu, X. (2009). Black carbon decomposition and incorporation into soil microbial biomass estimated by 14C labeling. *Soil Biology and Biochemistry*, *41*(2), 210–219. https://doi.org/10.1016/j.soilbio.2008.10.016

Lal, R. (2005). Forest soils and carbon sequestration. *Forest Ecology and Management*, *220*(1–3), 242–258. https://doi.org/10.1016/j.foreco.2005.08.015

Lavallee, J. M., Soong, J. L., & Cotrufo, M. F. (2020). Conceptualizing soil organic matter into particulate and mineral-associated forms to address global change in the 21st century. *Global Change Biology*, *26*(1), 261–273. https://doi.org/10.1111/gcb.14859

Lei, X., Shen, Y., Zhao, J., Huang, J., Wang, H., Yu, Y., & Xiao, C. (2023). Root exudates mediate the processes of soil organic carbon input and efflux. *Plants*, *12*(3), 630. https://doi.org/10.3390/plants12030630

Leuthold, S., Lavallee, J. M., Haddix, M. L., & Cotrufo, M. F. (2024). Contrasting properties of soil organic matter fractions isolated by different physical separation methodologies. *Geoderma*, *445*, 116870. https://doi.org/10.1016/j.geoderma.2024.116870

Lian, F., & Xing, B. (2017). Black carbon (Biochar) in water/soil environments: Molecular structure, sorption, stability, and potential risk. *Environmental Science & Technology*, *51*(23), 13517–13532. https://doi.org/10.1021/acs.est.7b02528

Liang, B., Lehmann, J., Solomon, D., Kinyangi, J., Grossman, J., O'Neill, B., Skjemstad, J. O., Thies, J., Luizão, F. J., Petersen, J., & Neves, E. G. (2006). Black carbon increases cation exchange capacity in soils. *Soil Science Society of America Journal*, *70*(5), 1719–1730. https://doi.org/10.2136/sssaj2005.0383

Liang, C., Schimel, J. P., & Jastrow, J. D. (2017). The importance of anabolism in microbial control over soil carbon storage. *Nature Microbiology*, *2*(8), 17105. https://doi.org/10.1038/nmicrobiol.2017.105

Liang, C. (2020). Soil microbial carbon pump: Mechanism and appraisal. *Soil Ecology Letters*, *2*(4), 241–254. https://doi.org/10.1007/s42832-020-0052-4

Llorente, M., Turrión, M.-B., & Glaser, B. (2018). Rapid and economical quantification of black carbon in soils using a modified benzene polycarboxylic acids (Bpca) method. *Organic Geochemistry*, *115*, 197–204. https://doi.org/10.1016/j.orggeochem.2017.11.005

López-Martín, M., González-Vila, F. J., & Knicker, H. (2018). Distribution of black carbon and black nitrogen in physical soil fractions from soils seven years after an intense forest fire and their role as C sink. *Science of The Total Environment*, *637–638*, 1187–1196. https://doi.org/10.1016/j.scitotenv.2018.05.084

Luo, L., Chen, Z., Lv, J., Cheng, Y., Wu, T., & Huang, R. (2019). Molecular understanding of dissolved black carbon sorption in soil-water environment. *Water Research*, *154*, 210–216. https://doi.org/10.1016/j.watres.2019.01.060

Masiello, C. A. (2004). New directions in black carbon organic geochemistry. *Marine Chemistry*, *92*(1–4), 201–213. https://doi.org/10.1016/j.marchem.2004.06.043

Mataix-Solera, J., Cerdà, A., Arcenegui, V., Jordán, A., & Zavala, L. M. (2011). Fire effects on soil aggregation: A review. *Earth-Science Reviews*, *109*(1–2), 44–60. https://doi.org/10.1016/j.earscirev.2011.08.002

McCool, K. D., Holub, S. M., Gao, S., Morrissette, B. A., Blunn, J. E., Gallo, A. C., & Hatten, J. A. (2023). Quantifying impacts of forest fire on soil carbon in a young, intensively managed tree farm in the western Oregon Cascades. *Soil Science Society of America Journal*, *87*(6), 1458–1473. https://doi.org/10.1002/saj2.20582

McKelvey, K. S., Skinner, C. N., Chang, C., Erman, D. C., Husari, S. J., Parsons, D. J., Wagtendonk, J. W. van, & Weatherspoon, C. P. (1996). An overview of fire in the Sierra Nevada. *Pages 1033-1040 in: Sierra Nevada Ecosystem Project, Final Report to Congress, Vol. II, Assessments and Scientific Basis for Management Options. Davis, CA: University of California, Centers for Water and Wildland Resources. Report No. 37.* https://research.fs.usda.gov/treesearch/3539

Moreland, K., Tian, Z., Berhe, A. A., McFarlane, K. J., Hartsough, P., Hart, S. C., Bales, R., & O'Geen, A. T. (2021). Deep in the Sierra Nevada critical zone: Saprock represents a large terrestrial organic carbon stock. *Environmental Research Letters*, *16*(12), 124059. https://doi.org/10.1088/1748-9326/ac3bfe

Morffi-Mestre, H., Ángeles-Pérez, G., Powers, J. S., Andrade, J. L., Feldman, R. E., May-Pat, F., Chi-May, F., & Dupuy-Rada, J. M. (2023). Leaf litter decomposition rates: Influence of successional age, topography and microenvironment on six dominant tree species in a tropical dry forest. *Frontiers in Forests and Global Change*, *6*, 1082233. https://doi.org/10.3389/ffgc.2023.1082233

Moukanni, N., Brewer, K. M., Gaudin, A. C. M., & O'Geen, A. T. (2022). Optimizing carbon sequestration through cover cropping in mediterranean agroecosystems: Synthesis of mechanisms and implications for management. *Frontiers in Agronomy*, *4*, 844166. https://doi.org/10.3389/fagro.2022.844166

Nave, L. E., Vance, E. D., Swanston, C. W., & Curtis, P. S. (2011). Fire effects on temperate forest soil C and N storage. *Ecological Applications*, *21*(4), 1189–1201. https://doi.org/10.1890/10-0660.1

North, M. P., & Hurteau, M. D. (2011). High-severity wildfire effects on carbon stocks and emissions in fuels treated and untreated forest. *Forest Ecology and Management*, *261*(6), 1115–1120. https://doi.org/10.1016/j.foreco.2010.12.039

Pan, Y., Birdsey, R. A., Phillips, O. L., Houghton, R. A., Fang, J., Kauppi, P. E., Keith, H., Kurz, W. A., Ito, A., Lewis, S. L., Nabuurs, G.-J., Shvidenko, A., Hashimoto, S., Lerink, B., Schepaschenko, D., Castanho, A., & Murdiyarso, D. (2024). The enduring world forest carbon sink. *Nature*, *631*(8021), 563–569. https://doi.org/10.1038/s41586-024-07602-x

Pierson, D. N., Robichaud, P. R., Rhoades, C. C., & Brown, R. E. (2019). Soil carbon and nitrogen eroded after severe wildfire and erosion mitigation treatments. *International Journal of Wildland Fire*, *28*(10), 814. https://doi.org/10.1071/WF18193

Posada-Baquero, R., & Ortega-Calvo, J.-J. (2011). Recalcitrance of polycyclic aromatic hydrocarbons in soil contributes to background pollution. *Environmental Pollution*, *159*(12), 3692–3699. https://doi.org/10.1016/j.envpol.2011.07.012

Prieto-Fernández, A., Acea, M. J., & Carballas, T. (1998). Soil microbial and extractable C and N after wildfire. *Biology and Fertility of Soils*, *27*(2), 132–142. https://doi.org/10.1007/s003740050411

Odum, E. P. (1969). The Strategy of Ecosystem Development: An understanding of ecological succession provides a basis for resolving man's conflict with nature. *Science*, *164*(3877), 262–270. https://doi.org/10.1126/science.164.3877.262

Perkins, D. (n.d.). *Hornblende-actinolite*. (n.d.). Retrieved August 21, 2025, from https://sites.und.edu/dexter.perkins/opticalmin/hornblende.htm

Peter-Contesse, H., Lajtha, K., Boettcher, A., O'Kelley, R., & Mayedo, A. (2024). Unearthing the legacy of wildfires: Post fire pyrogenic carbon and soil carbon persistence across complex Pacific Northwest watersheds. *Biogeochemistry*, *167*(7), 927–944. https://doi.org/10.1007/s10533-024-01151-1

Powlson, D., Cai ZuCong, C. Z., & Lemanceau, P. (2015). Soil carbon dynamics and nutrient cycling. In S. A. Banwart, E. Noellemeyer, & E. Milne (Eds.), *Soil carbon: Science, management and policy for multiple benefits* (1st ed., pp. 98–107). CABI. https://doi.org/10.1079/9781780645322.0098

Qu, X., Fu, H., Mao, J., Ran, Y., Zhang, D., & Zhu, D. (2016). Chemical and structural properties of dissolved black carbon released from biochars. *Carbon*, *96*, 759–767. https://doi.org/10.1016/j.carbon.2015.09.106

Sahu, N., Vasu, D., Sahu, A., Lal, N., & Singh, S. K. (2017). Strength of microbes in nutrient cycling: A key to soil health. In V. S. Meena, P. K. Mishra, J. K. Bisht, & A. Pattanayak (Eds.), *Agriculturally Important Microbes for Sustainable Agriculture: Volume I: Plant-soil-microbe nexus* (pp. 69–86). Springer. https://doi.org/10.1007/978-981-10-5589-8_4

Sanderman, J., Baldock, J. A., & Amundson, R. (2008). Dissolved organic carbon chemistry and dynamics in contrasting forest and grassland soils. *Biogeochemistry*, *89*(2), 181–198. https://doi.org/10.1007/s10533-008-9211-x

Santiesteban-Serrano, A., Rincón, A., & Aponte, C. (2025). Does wildfire severity reduce soil multifunctionality in the short-term? A matter of depth. *Ecological Indicators*, *175*, 113500. https://doi.org/10.1016/j.ecolind.2025.113500

Savage, S. M. (1974). Mechanism of fire-induced water repellency in soil. *Soil Science Society of America Journal*, *38*(4), 652–657. https://doi.org/10.2136/sssaj1974.03615995003800040033x

Schrumpf, M., Kaiser, K., Guggenberger, G., Persson, T., Kögel-Knabner, I., & Schulze, E.-D. (2013). Storage and stability of organic carbon in soils as related to depth, occlusion within aggregates, and attachment to minerals. *Biogeosciences*, *10*(3), 1675–1691. https://doi.org/10.5194/bg-10-1675-2013

Shrestha, G., Traina, S. J., & Swanston, C. W. (2010). Black carbon's properties and role in the environment: A comprehensive review. Sustainability, 2(1), 294–320. https://doi.org/10.3390/su2010294

Soil properties | california soil resource lab. (n.d.). Retrieved July 20, 2025, from https://casoilresource.lawr.ucdavis.edu/soil-properties/

Soil Survey Staff. (2012). Field book for describing and sampling soils, version 3.0. USDA, Natural Resources Conservation Service. U.S. Government Printing Office.

Solly, E. F., Weber, V., Zimmermann, S., Walthert, L., Hagedorn, F., & Schmidt, M. W. I. (2020). A critical evaluation of the relationship between the effective cation exchange capacity and soil organic carbon content in swiss forest soils. *Frontiers in Forests and Global Change*, *3*, 98. https://doi.org/10.3389/ffgc.2020.00098

Srivastava, R. K., & Yetgin, A. (2024). An overall review on influence of root architecture on soil carbon sequestration potential. *Theoretical and Experimental Plant Physiology*, *36*(2), 165–178. https://doi.org/10.1007/s40626-024-00323-6

Stoy, P. C., Katul, G. G., Siqueira, M. B. S., Juang, J., Novick, K. A., McCARTHY, H. R., Oishi, A. C., & Oren, R. (2008). Role of vegetation in determining carbon sequestration along ecological succession in the southeastern United States. *Global Change Biology*, *14*(6), 1409–1427. https://doi.org/10.1111/j.1365-2486.2008.01587.x

Swanson, M. E., Franklin, J. F., Beschta, R. L., Crisafulli, C. M., DellaSala, D. A., Hutto, R. L., Lindenmayer, D. B., & Swanson, F. J. (2011). The forgotten stage of forest succession: Early-successional ecosystems on forest sites. *Frontiers in Ecology and the Environment*, *9*(2), 117–125. https://doi.org/10.1890/090157

United States Department of Agriculture, Natural Resources Conservation Service. (n.d.). *PLANTS database*. https://plants.usda.gov/.

United States Department of Agriculture, Natural Resources Conservation Service. (n.d.). *Web soil survey*. U.S. Department of Agriculture. https://websoilsurvey.sc.egov.usda.gov/.

Verma, S., & Jayakumar, S. (2012). Impact of forest fire on physical, chemical and biological properties of soil: A review. *Proceedings of the International Academy of Ecology and Environmental Sciences*, *2*(3), 168–176.

Wagner, S., Coppola, A. I., Stubbins, A., Dittmar, T., Niggemann, J., Drake, T. W., Seidel, M., Spencer, R. G. M., & Bao, H. (2021). Questions remain about the biolability of dissolved black carbon along the combustion continuum. Nature Communications, 12(1), 4281. https://doi.org/10.1038/s41467-021-24477-y

Web soil survey—Home. (n.d.). Retrieved July 9, 2025, from https://websoilsurvey.sc.egov.usda.gov/app/

Xing, G., Wang, X., Jiang, Y., Yang, H., Mai, S., Xu, W., Hou, E., Huang, X., Yang, Q., Liu, W., & Long, W. (2023). Variations and influencing factors of soil organic carbon during the tropical forest succession from plantation to secondary and old–growth forest. *Frontiers in Ecology and Evolution*, *10*, 1104369. https://doi.org/10.3389/fevo.2022.1104369

Xu, S., Eisenhauer, N., Pellegrini, A. F. A., Wang, J., Certini, G., Guerra, C. A., & Lai, D. Y. F. (2022). Fire frequency and type regulate the response of soil carbon cycling and storage to fire across soil depths and ecosystems: A meta-analysis. *Science of The Total Environment*, *825*, 153921. https://doi.org/10.1016/j.scitotenv.2022.153921

Yang, Y., & Luo, Y. (2011). Carbon: Nitrogen stoichiometry in forest ecosystems during stand development: C : N stoichiometry over age sequence. *Global Ecology and Biogeography*, *20*(2), 354–361. https://doi.org/10.1111/j.1466-8238.2010.00602.x

Yost, J. L., & Hartemink, A. E. (2020). How deep is the soil studied – an analysis of four soil science journals. *Plant and Soil*, *452*(1–2), 5–18. https://doi.org/10.1007/s11104-020-04550-z

Zhang, P., Tian, X., He, X., Song, F., Ren, L., & Jiang, P. (2008). Effect of litter quality on its decomposition in broadleaf and coniferous forest. *European Journal of Soil Biology*, *44*(4), 392–399. https://doi.org/10.1016/j.ejsobi.2008.04.005

Zhu, Y., Hu, M., Hui, D., Niu, G., Li, J., Yao, X., Hu, Y., Huang, X., Li, Y., Zhang, D., & Deng, Q. (2024). Plants and microorganisms both contribute to soil organic matter formation through mineral interactions: Evidence from a subtropical forest succession. *Geoderma*, *452*, 117099. https://doi.org/10.1016/j.geoderma.2024.11709

Supplemental Data

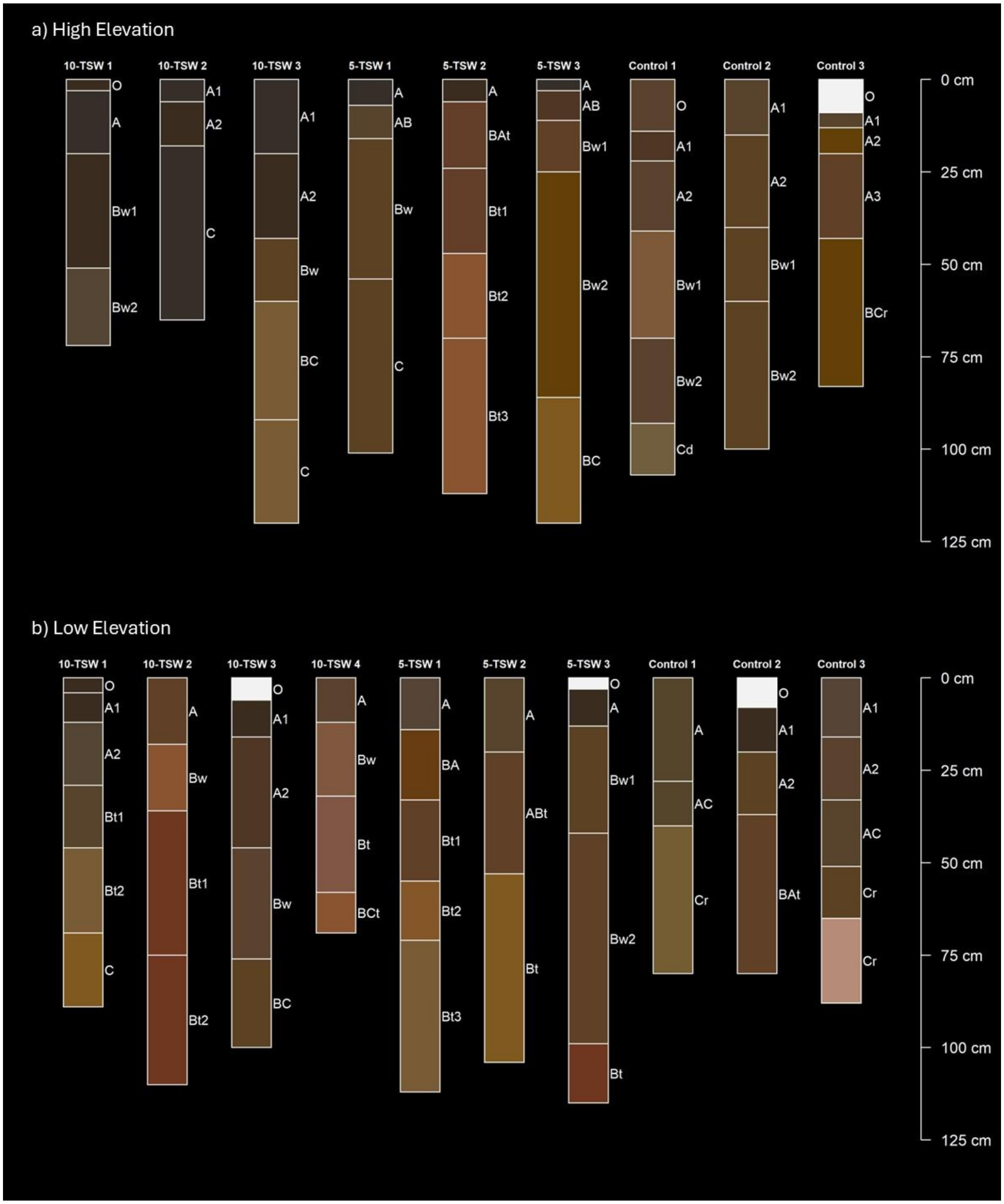

Figure S1. Soil profiles from each time-since-wildfire replicate (10-TSW, 5-TSW, and control), differentiated by a) high elevation sites, and b) low elevation sites. Soil profile sketches were generated in Rstudio using the aqp package. Some horizon data was supplemented by Soil Web (California Soil Resource Lab, n.d.).

Table S1. Summary of soil profile characteristics from each time-since-wildfire replicate differentiated by high and low elevation sites.

Profile ID	Depth (cm)	Horizon	Texture	Color	Depth (cm)	Horizon	Texture	Color
	High Elevation				Low Elevation			
10-TSW 1	0-3	O	-	10 YR 2/2	0-4	O	-	10 YR 2/2
	3-20	A	Sand	10 YR 2/1	4-12	A1	Sandy loam	10 YR 2/2
	20-51	Bw1	Sand	10 YR 2/2	12-29	A2	Sandy loam	10 YR 3/2
	51-72	Bw2	Sand	10 YR 3/2	29-46	Bt1	Sandy loam	10 YR 3/3
	-	-	-	-	46-69	Bt2	Sandy loam	10 YR 4/4
	-	-	-	-	69-89	C	Sandy loam	10 YR 4/6
10-TSW 2	0-6	A1	Loamy sand	10 YR 2/1	0-18	A	Loam	7.5 YR 3/4
	6-18	A2	Loamy sand	10 YR 2/2	18-36	Bw	Loam	5 YR 4/6
	18-65	C	Loamy sand	10 YR 2/1	36-75	Bt1	Clay	2.5 YR 3/6
	-	-	-		74-110	Bt2	Clay	2.5 YR 3/6
10-TSW 3	0-20	A1	Loamy sand	10 YR 2/1	0-6	O	-	-
	20-43	A2	Loamy sand	10 YR 2/2	6-16	A1	Loamy sand	10 YR 2/2
	43-60	Bw	Loamy sand	10 YR 3/4	16-46	A2	Loamy sand	7.5 YR 2.5/3
	60-92	BC	Sandy loam	10 YR 4/4	46-76	Bw	Loamy sand	7. YR 3/3
	92-120	C	Sandy loam	10 YR 4/4	76-100	BC	Loamy sand	10 YR3/4
10-TSW 4	-	-	-	-	0-12	A	Loam	7.5 YR 3/3
	-	-	-	-	12-32	Bw	Loam	5 YR 4/4
	-	-	-	-	32-58	Bt	Clay loam	2.5 YR 4/4
	-	-	-	-	58-69	BCt	Sandy loam	5 YR 4/6
5-TSW 1	0-7	A	Loamy sand	10 YR 2/1	0-14	A	Sandy loam	7.5 YR 3/2
	7-16	AB	Loamy sand	10 YR 3/3	14-33	BA	Sandy loam	7.5 YR 3/6
	16-54	Bw	Loamy sand	10 YR 3/4	33-55	Bt1	Sandy loam	7.5 YR 3/4
	54-101	C	Sandy loam	10 YR 3/4	55-71	Bt2	Sandy loam	7.5 YR 4/6
	-	-	-	-	71-112	Bt3	Sandy loam	10 YR 4/4
5-TSW 2	0-6	A	Sandy loam	10 YR 2/2	0-20	A	Sandy loam	10 YR 3/3
	6-24	BAt	Sandy loam	5 YR 3/4	20-53	ABt	Sandy loam	7.5 YR 3/4
	24-47	Bt1	Sandy loam	5 YR 3/4	53-104	Bt	Sandy loam	10 YR 4/6
	47-70	Bt2	Sandy loam	5 YR 4/6	-	-	-	-

	70-112	Bt3	Sandy clay loam	5YR 4/6	-	-	-	-
5-TSW 3	0-3	A	Loamy sand	10 YR 2/1	0-3	O	-	-
	3-11	AB	Loamy sand	7.5 YR 2.5/3	3-13	A	Sandy loam	10 YR 2/2
	11-25	Bw1	Loamy sand	7.5 YR 3/4	13-42	Bw1	Sandy loam	10 YR 3/4
	25-86	Bw2	Loamy sand	10 YR 3/6	42-99	Bw2	Sandy loam	7.5 YR 3/4
	86-120	BC	Sandy loam	10 YR 4/6	99-115	Bt	Sandy loam	2.5 YR 3/6
Control 1	0-14	O	-	7.5 YR 3/3	0-28	A	Loamy sand	2.5 Y 3/3
	14-22	A1	Sandy loam	7.5 YR 2.5/3	28-40	AC	Loamy sand	2.5 Y 3/3
	22-41	A2	Silt loam	7.5 YR 3/3	40-80	Cr	Sand	2.5 Y 4/4
	41-70	Bw1	Loam	7.5 YR 4/4	-	-	-	-
	70-93	Bw2	Loam	7.5 YR 3/3	-	-	-	-
	93-107	Cd	Sandy loam	2.5 Y 4/3	-	-	-	-
Control 2	0-15	A1	Loamy sand	10 YR 3/3	0-8	O	-	-
	15-40	A2	Loamy sand	10 YR 3/4	8-20	A1	Sandy clay loam	10 YR 2/2
	40-60	Bw1	Loamy sand	10 YR 3/4	20-37	A2	Sandy clay loam	10 YR 3/4
	60-100	Bw2	Sandy loam	10 YR 3/4	37-80	BAt	Sandy clay loam	7.5 YR 3/4
Control 3	0-9	O	-	-	0-16	A1	Sandy loam	7.5 YR 3/2
	9-13	A1	Sandy loam	10 YR 3/3	16-33	A2	Sandy loam	7.5 YR 3/3
	13-20	A2	Sandy clay loam	10 YR 3/6	33-51	AC	Sandy loam	10 YR 3/3
	20-43	A3	Sandy clay loam	7.5 YR 3/4	51-65	Cr	Sandy loam	10 YR 3/4
	43-83	BCr	Sandy loam	10 YR 3/6	65-88	Cr	Loamy sand	2.5 YR 6/4

Table S2. Relative abundance (%) of PLFA taxa in each TSW group at high and low elevations.

Time Since Wildfire	Actinomycetes	AM Fungi	Gram Negative Bacteria	Eukaryotes	Other Fungi	Gram Positive Bacteria
High Elevation						
50+ yr	12.2%	4.01%	53.6%	2.51%	6.02%	21.7%
10 yr	12.5%	4.83%	47.9%	2.30%	7.48%	25.0%
5 yr	11.1%	3.77%	54.7%	2.33%	5.47%	22.7%
Low Elevation						
50+ yr	12.5%	5.10%	49.9%	2.78%	5.72%	24.0%
10 yr	13.3%	4.54%	48.6%	1.74%	6.22%	25.6%
5 yr	14.4%	4.74%	50.1%	1.93%	3.46%	25.7%

Table S3. Summary of PLFA taxa (nmol/g soil) at high and low elevation sites since wildfire (mean ± standard error; n = 9 replicates & n = 12 replicates for low elevation 10-TSW sites) at 0-5 cm and 5-15 cm in depth. Within a sampling depth for each soil health indicator, means with the same letter are statistically indistinguishable at $\alpha = 0.05$ by Tukey's HSD.

Depth	Time Since Wildfire	Actinomycetes	AM Fungi	Gram Negative Bacteria	Eukaryote	Fungi	Gram Positive Bacteria
High Elevation							
0-5 cm	50+ yr	8.82 ^{a} ± 0.6	3.34 ^{a} ± 0.316	43.3 ± 4.11	2.13 ± 0.252	5.75 ± 1.30	16.7 ± 1.22
	10 yr	8.07 ^{a} ± 1.54	3.34 ^{a} ± 0.746	32.1 ± 7.29	1.89 ± 0.658	7.72 ± 3.96	16.9 ± 3.43
	5 yr	5.38 ^{a} ± 0.81	2.84 ^{a} ± 0.597	32.9 ± 5.02	1.56 ± 0.215	4.79 ± 0.901	13.9 ± 2.70
5-15 cm	50+ yr	8.13 ^{a} ± 0.554	2.42 ^{ab} ± 0.215	34.2 ± 3.60	1.43 ± 0.115	2.92 ± 0.398	13.8 ± 0.806
	10 yr	8.33 ^{a} ± 1.64	3.26 ^{b} ± 0.697	32.8 ± 6.61	1.57 ± 0.384	6.17 ± 2.04	16.4 ± 3.16
	5 yr	4.27 ^{a} ± 0.34	1.07 ^{a} ± 0.167	18.1 ± 1.60	0.684 ± 0.103	1.22 ± 0.323	7.80 ± 0.764
Low Elevation							
0-5 cm	50+ yr	6.62 ^{a} ± 0.748	2.98 ^{a} ± 0.326	29.6 ± 3.66	1.70 ± 0.186	4.05 ± 0.635	13.2 ± 1.35
	10 yr	6.03 ^{a} ± 0.398	2.55 ^{a} ± 0.199	26.2 ± 1.77	0.934 ± 0.092	3.70 ± 0.599	13.1 ± 0.747
	5 yr	6.21 ^{a} ± 0.455	2.27 ^{a} ± 0.182	23.3 ± 1.65	0.918 ± 0.089	1.84 ± 0.234	12.1 ± 0.828
5-15 cm	50+ yr	5.92 ^{a} ± 0.728	2.22 ^{a} ± 0.311	22.6 ± 3.90	1.16 ± 0.173	2.04 ± 0.332	10.9 ± 1.41
	10 yr	5.29 ^{a} ± 0.582	1.56 ^{a} ± 0.242	16.6 ± 1.78	0.636 ± 0.099	2.25 ± 0.630	9.28 ± 1.10
	5 yr	6.79 ^{a} ± 0.603	2.12 ^{a} ± 0.214	22.9 ± 1.61	0.845 ± 0.058	1.37 ± 0.179	11.7 ± 0.984

Table S4. Summary of PLFA ratios at high elevation sites over time since burn (mean ± standard error; n = 9 replicates & n = 12 replicates for low elevation 10-TSW sites) at 0-5 cm and 5-15 cm in depth. Within a sampling depth for each soil health indicator, means with the same letter are statistically indistinguishable at $\alpha = 0.05$ by Tukey's HSD

Depth	Time Since Wildfire	Fungi: Bacteria	$Gram^{-}:Gram^{+}$ Bacteria	Predator: Prey	Saturated: Unsaturated PLFA	Monosaturated: Polysaturated PLFA	$Gram^{-}$ Metabolic Stress
High Elevation							
0-5 cm	50+ yr	0.152 ± 0.0196	0.603 ^{a} ± 0.0216	0.0372 ^{a} ± 0.00539	0.950 ^{a} ± 0.0519	6.83 ± 1.30	2.08 ± 0.125
	10 yr	0.183 ± 0.0288	0.807 ^{b} ± 0.0290	0.0342 ^{a} ± 0.00391	1.13 ^{ab} ± 0.0796	6.20 ± 0.783	1.93 ± 0.113
	5 yr	0.161 ± 0.0226	0.570 ^{a} ± 0.0198	0.0350 ^{a} ± 0.00240	1.20 ^{b} ± 0.116	5.46 ± 0.493	2.40 ± 0.375
5-15 cm	50+ yr	0.120 ± 0.0135	0.669 ^{a} ± 0.0365	0.0309 ^{a} ± 0.00199	1.12 ^{a} ± 0.0785	7.89 ± 1.08	1.69 ± 0.113
	10 yr	0.164 ± 0.0214	0.766 ^{a} ± 0.0256	0.0304 ^{a} ± 0.00369	1.22 ^{ab} ± 0.112	7.40 ± 1.48	1.68 ± 0.137
	5 yr	0.0856 ± 0.0107	0.670 ^{a} ± 0.0267	0.0263 ^{a} ± 0.00263	1.66 ^{b} ± 0.109	8.55 ± 0.608	1.39 ± 0.234
Low Elevation							
0-5 cm	50+ yr	0.167 ± 0.00882	0.697 ^{a} ± 0.0405	0.0407 ^{b} ± 0.00146	1.04 ^{a} ± 0.0423	5.96 ± 0.441	2.55 ± 0.127
	10 yr	0.161 ± 0.0155	0.735 ^{a} ± 0.0148	0.0238 ^{a} ± 0.00143	1.15 ^{a} ± 0.0510	6.81 ± 0.462	2.75 ± 0.167
	5 yr	0.118 ± 0.00662	0.791 ^{a} ± 0.0257	0.0266 ^{a} ± 0.00276	1.11 ^{a} ± 0.0643	9.77 ± 0.870	2.25 ± 0.166
5-15 cm	50+ yr	0.131 ± 0.00655	0.782 ^{a} ± 0.0401	0.0357 ^{b} ± 0.00255	1.19 ^{a} ± 0.0725	7.28 ± 0.499	2.02 ± 0.113
	10 yr	0.138 ± 0.0163	0.882 ^{a} ± 0.0275	0.0241 ^{a} ± 0.00239	1.50 ^{a} ± 0.0837	7.40 ± 0.834	1.61 ± 0.0723
	5 yr	0.102 ± 0.00722	0.806 ^{a} ± 0.0354	0.0248 ^{b} ± 0.000909	1.16 ^{a} ± 0.0734	10.7 ± 0.541	1.91 ± 0.252

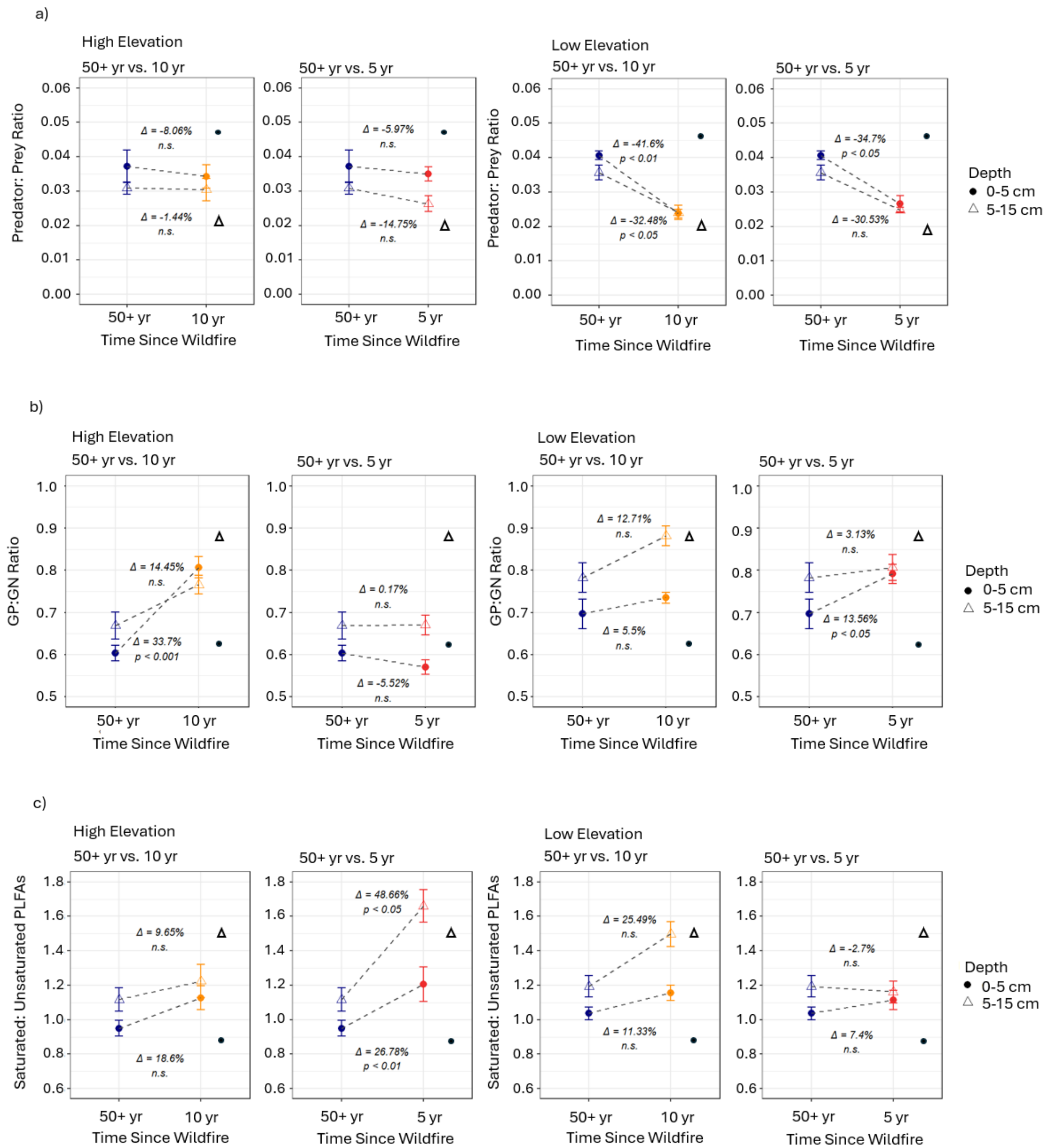

Figure S2. Comparison of microbial stress ratios sensitive to change for: a) Predator: Prey ratio, b) Gram Positive: Gram Negative (GP:GN) Bacteria ratio, and c) Saturated: Unsaturated PLFA ratio, determined by ANOVA, between the 50+ year (control) and 10- or 5- year since burn treatments at high and low elevations. Points on the plot are mean values, whiskers show standard error, and dashed lines with Δ indicate the percent-difference between means. The filled circle and clear triangle on the plot indicate the sampling depth of each percent-difference and significance value.

Table S5. Summary of soil health indicators at high and low elevation sites over time since burn (mean ± standard error; *n* = 12 replicates for pH, EC, TC, TN, and C:N; *n* = 9 replicates for Extractable P) at 0-5 cm and 5-15 cm in depth.

Depth	Time Since Wildfire	pH $CaCl_2$	EC (dS/m)	Extractable P (ppm)	TC (%)	TN (%)	C:N Ratio
High Elevation							
0-5 cm	50+ yr	5.06 ^{a} ± 0.09	0.0916 ^{a} ± 0.0107	67.58 ± 24.77	6.11 ± 0.67	0.223 ± 0.0217	27.33 ^{b} ± 0.859
	10 yr	4.78 ^{a} ± 0.14	0.0601 ^{a} ± 0.0109	99.78 ± 23.32	5.86 ± 0.45	0.210 ± 0.0761	30.16 ^{b} ± 2.84
	5 yr	5.81 ^{b} ± 0.13	0.1338 ^{a} ± 0.0208	29.43 ± 9.13	4.66 ± 0.47	0.265 ± 0.0262	18.03 ^{a} ± 1.02
5-15 cm	50+ yr	4.99 ^{ab} ± 0.08	0.0659 ^{b} ± 0.0079	49.51 ± 18.64	3.78 ± 0.32	0.144 ± 0.0117	26.30 ^{a} ± 1.074
	10 yr	4.73 ^{a} ± 0.15	0.0325 ^{a} ± 0.0050	66.41 ± 17.76	4.73 ± 0.39	0.172 ± 0.0217	29.88 ^{a} ± 2.971
	5 yr	5.62 ^{b} ± 0.11	0.0691 ^{b} ± 0.0120	18.28 ± 5.08	3.60 ± 0.34	0.173 ± 0.0154	20.98 ^{a} ± 0.748
Low Elevation							
0-5 cm	50+ yr	4.93 ^{a} ± 0.09	0.0875 ^{a} ± 0.0118	66.64 ± 15.06	2.67 ± 0.37	0.124 ± 0.0144	21.43 ± 1.34
	10 yr	5.72 ^{b} ± 0.09	0.1684 ^{a} ± 0.0208	24.04 ± 6.71	4.09 ± 0.37	0.199 ± 0.0237	21.40 ± 0.858
	5 yr	5.28 ^{ab} ± 0.09	0.0917 ^{a} ± 0.0205	70.21 ± 14.50	4.08 ± 0.28	0.200 ± 0.0219	21.92 ± 1.703
5-15 cm	50+ yr	4.84 ^{a} ± 0.08	0.0531 ^{a} ± 0.0088	71.49 ± 19.90	1.9 ± 0.29	0.087 ± 0.0086	20.88 ± 1.48
	10 yr	5.64 ^{b} ± 0.09	0.0957 ^{b} ± 0.0092	13.69 ± 3.31	2.85 ± 0.24	0.133 ± 0.0146	22.74 ± 1.26
	5 yr	5.30 ^{ab} ± 0.10	0.0627 ^{ab} ± 0.0088	48.76 ± 13.52	3.41 ± 0.24	0.159 ± 0.0144	21.96 ± 0.737

Table S6. Summary of the POM and MAOM fractions at high and low elevation sites over time since burn (mean ± standard error; *n* = 9 replicates & n = 12 replicates at low elevation 10-TSW) at 0-5 cm and 5-15 cm in depth. Sites sharing the same letter are indistinguishable by Tukey's HDS (α = 0.05)

Depth	Time Since Wildfire	POM-C (mg C/g soil)	MAOM-C (mg C/g soil)	POM-N (mg N/g soil)	MAOM-N (mg N/g soil)	POM C:N Ratio	MAOM C:N Ratio
High Elevation							
0-5 cm	50+ yr	39.48 ^{a} ± 6.15	23.62 ± 2.71	1.057 ± 0.194	1.060 ^{a} ± 0.123	39.69 ± 2.24	22.64 ^{b} ± 1.18
	10 yr	35.68 ^{a} ± 7.12	29.17 ± 2.02	1.165 ± 0.275	1.458 ^{a} ± 0.0884	32.66 ± 1.95	20.04 ^{ab} ± 0.822
	5 yr	22.82 ^{a} ± 2.59	22.35 ± 2.05	0.940 ± 0.130	1.449 ^{a} ± 0.152	25.83 ± 2.20	15.89 ^{a} ± 0.918
5-15 cm	50+ yr	18.57 ^{a} ± 1.59	18.47 ± 2.23	0.446 ± 0.0498	0.816 ^{a} ± 0.124	43.52 ± 2.67	23.89 ^{a} ± 1.699
	10 yr	24.72 ^{a} ± 4.55	27.07 ± 2.48	0.678 ± 0.133	1.293 ^{a} ± 0.116	37.68 ± 1.79	21.08 ^{a} ± 0.868
	5 yr	16.8 ^{a} ± 6.15	23.62 ± 2.71	0.501 ± 0.0576	0.985 ^{a} ± 0.105	39.69 ± 2.24	22.64 ^{a} ± 1.18
Low Elevation							
0-5 cm	50+ yr	11.48 ^{a} ± 3.60	12.40 ± 1.90	0.365 ± 0.0802	0.655 ^{a} ± 0.707	26.82 ± 5.10	18.34 ^{a} ± 1.026
	10 yr	21.06 ^{a} ± 2.45	20.66 ± 1.70	0.825 ± 0.124	1.205 ^{a} ± 0.0853	26.64 ± 1.66	17.03 ^{a} ± 0.461
	5 yr	20.88 ^{a} ± 1.82	20.72 ± 2.01	0.761 ± 0.110	1.274 ^{a} ± 0.163	29.76 ± 2.43	16.90 ^{a} ± 0.687
5-15 cm	50+ yr	9.44 ^{a} ± 1.52	9.95 ± 1.92	0.289 ± 0.0384	0.529 ^{a} ± 0.0653	32.45 ± 5.048	17.72 ^{a} ± 1.201
	10 yr	13.09 ^{a} ± 1.57	16.56 ± 1.34	0.426 ± 0.0577	0.869 ^{a} ± 0.0567	31.47 ± 2.42	19.05 ^{a} ± 0.835
	5 yr	13.38 ^{a} ± 1.43	19.08 ± 2.06	0.403 ± 0.0568	1.081 ^{a} ± 0.138	26.82 ± 5.10	18.34 ^{a} ± 1.026

Table S7. Summary of physical soil health indicators at high and low elevation sites over time since burn (mean ± standard error) at 0-5 cm and 5-15 cm in depth. Within a sampling depth for each soil health indicator, means with the same letter are statistically indistinguishable at $\alpha = 0.05$ by Tukey's HSD.

Depth	Time Since Wildfire	Aggregate Stability Index	Bulk Density (g/cm^3)	Rock Fragment Volume (cm^3)
High Elevation				
0-5 cm	50+ yr	0.873 ± 0.0176	0.721 ± 0.0571	0.625^{a} ± 0.0312
	10 yr	0.886 ± 0.0223	0.776 ± 0.0296	0.943^{b} ± 0.0284
	5 yr	0.824 ± 0.0460	0.860 ± 0.0258	0.810^{b} ± 0.00864
5-15 cm	50+ yr	0.873 ± 0.0176	0.721 ± 0.0571	0.625^{a} ± 0.0312
	10 yr	0.886 ± 0.0223	0.776 ± 0.0296	0.943^{b} ± 0.0284
	5 yr	0.824 ± 0.0460	0.860 ± 0.0258	0.810^{b} ± 0.00864
Low Elevation				
0-5 cm	50+ yr	0.865 ± 0.0386	0.707 ± 0.0499	0.777^{a} ± 0.0153
	10 yr	0.918 ± 0.0299	0.856 ± 0.0338	0.935^{b} ± 0.0340
	5 yr	0.921 ± 0.0183	0.892 ± 0.0223	0.804^{ab} ± 0.0118
5-15 cm	50+ yr	0.865 ± 0.0386	0.707 ± 0.0499	0.777^{a} ± 0.0153
	10 yr	0.918 ± 0.0299	0.856 ± 0.0338	0.935^{b} ± 0.0340
	5 yr	0.921 ± 0.0183	0.892 ± 0.0223	0.804^{ab} ± 0.0118

Table S8. Summary particle size at high and low elevation sites over time since burn (mean ± standard error) at 0-5 cm and 5-15 cm in depth.

Depth	Time Since Wildfire	Sand (%)	Silt (%)	Clay (%)
High Elevation				
0-5 cm	50+ yr	63.3 ± 10.5	26.7 ± 9.8	10.0 ± 4.0
	10 yr	84.0 ± 5.2	14.7 ± 4.8	1.67 ± 0.33
	5 yr	72.7 ± 1.8	23.3 ± 2.3	4.00 ± 1.2
5-15 cm	50+ yr	63.3 ± 10.5	26.7 ± 9.8	10.0 ± 4.0
	10 yr	84.0 ± 5.2	14.7 ± 4.8	1.67 ± 0.33
	5 yr	72.7 ± 1.8	23.3 ± 2.3	4.00 ± 1.2
Low Elevation				
0-5 cm	50+ yr	63.3 ± 8.5	30.0 ± 7.6	6.67 ± 1.8
	10 yr	77.3 ± 4.2	19.3 ± 4.7	3.33 ± 0.67
	5 yr	76.7 ± 2.4	20.0 ± 1.2	3.33 ± 1.3
5-15 cm	50+ yr	63.3 ± 8.5	30.0 ± 7.6	6.67 ± 1.8
	10 yr	77.3 ± 4.2	19.3 ± 4.7	3.33 ± 0.67
	5 yr	76.7 ± 2.4	20.0 ± 1.2	3.33 ± 1.3

Table S9. Summary of soil carbon (0-15 cm; 0-1 m only for C Inventory) at high and low elevations for unburned sites and sites recovering from wildfire (burned) (mean ± standard error). For each soil carbon measurement, means with the same letter are statistically indistinguishable at $\alpha = 0.05$ by Tukey's HSD.

Burn Status	C Stock (kg/m^2)	TC (%)	POM-C (mg C/g soil)	MAOM-C (mg C/g soil)	C Inventory (kg/m^2)
High Elevation					
Unburned	$2.66^{ac} \pm 0.20$	$4.56^{a} \pm 0.40$	$25.5^{a} \pm 2.9$	$20.2^{a} \pm 2.3$	$16.3^{a} \pm 2.7$
Burned	$3.20^{a} \pm 0.21$	$4.53^{a} \pm 0.29$	$23.6^{a} \pm 3.0$	$23.7^{a} \pm 1.7$	$25.3^{a} \pm 6.4$
Low Elevation					
Unburned	$1.78^{b} \pm 0.25$	$2.23^{b} \pm 0.32$	$10.1^{b} \pm 2.0$	$10.8^{b} \pm 1.9$	$11.6^{a} \pm 4.2$
Burned	$2.52^{bc} \pm 0.11$	$3.42^{c} \pm 0.19$	$15.8^{b} \pm 1.2$	$18.7^{a} \pm 1.2$	$14.3^{a} \pm 1.7$